WET ETCHING OF P-GAN FOR CRYSTALLOGRAPHICALLY SMOOTH VERTICAL SIDEWALLS

A Thesis

Presented to the Faculty of the Graduate School

of Cornell University

In Partial Fulfillment of the Requirements for the Degree of

Master of Science

by

Jui-Yuan (Steven) Hsu

Aug 2019

© 2019 Jui-Yaun Hsu

ABSTRACT

GaN vertical power devices have gained increased attention in recent years due to the advantages over lateral transistors in high breakdown voltage/high current applications as well as thermal performance. Trench etching is a key technology to achieve high-voltage trench-based vertical GaN devices; rough surfaces or sharp corners can lead to device preliminary breakdown due to the electric field crowding. The combination of inductively couple plasma and tetramethylammonium hydroxide (TMAH) etching is commonly utilized in fabrication of smooth and vertical gate planes to minimize surface state charge and achieve high channel mobility. Several groups have reported that TMAH can smooth the n-GaN or UID GaN etched surfaces to reveal $(1\bar{1}00)$ planes, while negligible etching occurs for p-GaN due to the lack of holes at the surface. In this work, the etch process was found to be diffusion limited for GaN in TMAH. A reaction mechanism for the etch process is proposed. In addition, crystallographically smooth vertical p-GaN sidewalls were achieved by a novel wet etching technique: "hydrogen-passivation-assisted wet etching". The vertical trench sidewall is preferable for the realization of damage-free high mobility normally-off channel in trench-based vertical GaN devices for high-voltage applications.

BIOGRAPHICAL SKETCH

Jui-Yuan Hsu was born in Taiwan. He earned a B.S. in Materials Science from National Taiwan University of Science and Technology, where he studied the effects of Zr-based thin film metallic glass coatings on surgical appliances. Since 2017, he has been working on advanced GaN power device technologies. In summer 2018, he worked as a R&D intern at Applied Materials, mainly working on selective area deposition and photoresist bridge defect removal. During his Master of Science program in Materials Science and Engineering program at Cornell University, he devoted his graduate work into developing novel wet etching techniques for GaN UMOS applications under the guidance of Professors Huili Grace Xing and Debdeep Jena.

Dedicated to my parents.

ACKNOWLEDGMENTS

I would like to express my gratitude to all those who helped me during my M.S. program. My deepest gratitude goes first to my advisors, Professors Huili Grace Xing and Debdeep Jena, for their constant encouragements and valuable suggestions on my study. I would also like to thank Wenshen Li and Dr. Zongyang Hu for mentoring me in these two years.

I am also thankful to Dr. Kazuki Nomoto and the staff members in CNF at Cornell: Amrita Banerjee, Alan R. Bleier, Garry Boordonaro, Phil Infante, Tom Pennell, Michael Skvarla, Aaron Windsor, Jerry Drumheller. In addition, I would like to thank my collaborators from Yale University. Prof. Jun Han and Bingjun Li helped me with NH_3 annealing. I would not be able to complete the experiments without all their help.

Special thanks to all the group members in Jena-Xing group for giving their help and care in the past year: Dr. Vladimir Protasenko, Dr. Kazuki Nomoto, Dr. Yongjin Cho, Dr. Zongyang Hu, Austin Hickman, Hyunjea Lee, Jashan Singhal, Jeffrey Miller, Jimy Encomendero, John Wright, Jonathan McCandless, Joseph Casamento, Kevin Lee, Nicholas Tanen, Philip Dang, Reet Chaudhuri, Ryan Page, Sam Bader, Shyam Bharadwaj, Xiang Li, Zexuan Zhang, Vasanth Balakrishnan, Ren Zhong, Anni Wu, Shuyao Chen, Shao-Ting Ho, Derek Rowen, Yuxin Ren. It is a great honor and pleasure to be one of the members of this group.

The last but not least, my gratitude also extended to my beloved family who have been supporting and caring me all of my life.

TABLE OF CONTENTS

CHAPTER 3

Experimental Section

CHAPTER 4

Results and discussion

LIST OF FIGURES

Chapter 3

3.6 (a) Preparation of UV-assisted TMAH etching. The handheld lamp and intensity detector are shown. (b) TMAH etching with UV illumination. The lamp is directly placed on the top of beaker to illuminate the GaN wafer.

3.7 (a) Carbon Nanotube/Graphene furnace in CNF at Cornell, (b) Commercial MOCVD system (Aixtron 200/4 RF) at Yale University.

Chapter 4

4.1 Sample ID: JH-GaN on Sapphire-Control01. Scanning electron microscope (SEM) images of the Mg-activated dry-etched fins along <1$\bar{2}$10> direction after Cl2-based dry etching. Slanted rough sidewalls and uneven etched surface due to ion bombardments and redeposition of nickel under high energy plasma. Widths of fins were (a) 2 μm and (b) 1.6 μm.

4.2 Sample ID: JH-GaN on Sapphire-Control01. SEM images of the Mg-activated dry-etched-then-wet-etched fins with p-n structure after etching in hot TMAH at 85 oC for 30 mins. (a), (b), and (c): The fins along <1$\bar{2}$10> direction. Pillars were removed after TMAH treatment. Besides, staircase-shaped m-plane sidewalls and semi-polar planes were formed. (d): The fins along <1 0$\bar{1}$ 0> direction with the formation nano-prism structures due to the surface bonding configuration.

4.3 Sample ID: JH-GaN on Sapphire-Control01. Cross-sectional SEM images of the cleaved-then-TMAH-etched fins along <1$\bar{2}$10> direction after etching in hot TMAH at 85 oC for 30 mins. (a) Vertical sidewalls achieved. (b) Semi-polar and non-polar facet exposed on the surface. M-plane sidewalls were formed near the fin edges but not toward to the bottom of sidewalls.

4.4 (Top view) Schematic of fin pattern and cleavage plane. The designed striped patterns are ranging from 0.5 to 20.0 μm, which arrayed along the <1$\bar{2}$10> and <10$\bar{1}$0> directions.

4.5 Sample ID: JH-GaN on Sapphire-Control01. SEM images of the Mg-activated dry/wet etched-then-cleaved fins along <1$\bar{2}$10> direction after etching in hot TMAH at 85 oC for 1 hr. A slanted sidewall with three-stage slope were formed at the interior fin.

4.6 Sample ID: JH-GaN on Sapphire-Control01. SEM images of the Mg-activated cleaved-then-wet-etched fins along <11$\bar{2}$0> direction after etching in hot TMAH at 85 oC for 15 mins. Vertical sidewall of p-Gan was formed near the fin edge by TMAH etching for 15 mins. Hexagonal prism-like features were exposed on the cleavage plane after wet etching.

4.7 (Top view) The developing velocity profile of a TMAH fluid entering fins during the wet etching process, experiencing from hydrodynamic entrance region to full developed region between the fins. Interior sidewalls between the fins were difficult to be wet etched due boundary layer increases as the distance from fin edge increases.

4.8 SEM images of GaN micro truncated-pyramids immerged into KOH solution for (a) 0 min, (b) 10 min, (c) 30 min and (d) 40 min, respectively (reported by Chen et al.). (e) shows the schematic of etch process (reported by Sandia National Lab). High etch rate at convex point.

4.9 Schematic and cross-sectional SEM images illustrating the etch sequence of a slanted sidewall toward a vertical sidewall in TMAH. (1) Staircase-shaped sidewall first appeared after TMAH etching for 30 mins. (2) Slanted sidewall with semi-polar facets then formed with increased etching time of 60 mins. (3) and (4) vertical sidewalls were achieved near the fin edge. The semi-polar facets of the GaN were removed gradually accompanied with the exposure of the m-plane facets.

4.10 Process of UV-assisted TMAH etching: (a) Electron-hole pairs are generated by UV energy. (b) Carriers are separated along the potential gradient in the depleted layer. (c) Holes react with the oxidant at the semiconductor/chemicals interface. (d) An oxide film is formed on the semiconductor surface, and the surface is etched if this oxide is soluble in the chemicals.

4.11 Sample ID: JH-GaN on Sapphire-UV01. SEM images of the Mg-activated fins along $<1\bar{2}10>$ direction. (a) and (b): rough slanted sidewalls after dry etch. (c) and (d): after UV-assisted wet etching for 30 mins. Smooth semi-polar sidewalls without staircases was formed by UV-assisted wet etching.

4.12 Schematic of sidewalls of the fins along $<11\bar{2}0>$ direction after etching in hot TMAH at 85 oC for 30 mins. (a) Staircase-shaped sidewall after conventional wet etching and (b) smooth sidewalls with two-step slope sidewall after UV-assisted wet etching for 30 mins.

4.13 SEM images of the Mg-activated dry-etched-then-wet-etched fins along $<11\bar{2}0>$ direction after etching in hot TMAH at 85 oC for 1 hr. (a), (b), and (c): Sample ID: JH-GaN on Sapphire-UV02. Smooth semi-polar planes sidewalls were exposed after UV-assisted TMAH etching (d) Sample ID: JH-GaN on Sapphire-C02. Without applying UV source after an hour TMAH etching. Staircase-shaped sidewalls were formed after conventional TMAH etching, while smooth semi-polar planes sidewalls were exposed after UV-assisted TMAH etching.

4.14 Sample ID: JH-GaN on Sapphire-Control02. SEM images of the fins along $<10\bar{1}0>$ direction after etching in hot TMAH at 85 oC for 1 hr. (a) Rough sidewalls after dry etching due to non-

uniform distribution of photoresist cover the surface before dry etching; (b) Formation of hexagonal holes after TMAH etch initialize by defective dry-etched surface.

4.15 Sample ID: JH-GaN on sapphire-H01. SEM images of the H-passivated dry-etched-then-wet-etched fins along <1$\bar{2}$10> direction after etching in hot TMAH at 85 oC for 1 hr. Vertical and smooth sidewalls achieved. (a) Cross-sectional and (b) 45° view.

4.16 SEM images of the dry-etched-then-wet-etched fins along <10$\bar{1}$0> direction after etching in hot TMAH at 85 oC for 1 hr. (a) and (b): Sample ID: JH-GaN on sapphire-H01. Straight sidewalls on H-passivated GaN wafer. (c) and (d): Sample ID: JH-GaN on Sapphire-Control02. Staircase-shaped sidewalls on Mg-activation wafer.

4.17 Sample ID: JH-GaN on sapphire-H01. (Top view) SEM images of the H-passivated dry-etched-then-wet-etched samples after etching in hot TMAH at 85 oC for 1 hr. Hexagonal-shape holes were appeared on the etched c-plane with m-plane sidewalls. The left image is a zoom-in view of the right.

4.18 Sample ID: JH-GaN on sapphire-H01. SEM images of the H-passivated dry-etched-then-wet-etched fins along <1$\bar{2}$10> direction after etching in hot TMAH at 85 oC for 1 hr. Cuboids on the m-plane sidewalls viewed at (a) a-plane cross-section and (b) 45° from the cleavage plane (i.e. a-plane).

4.19 Sample ID: JH-GaN on sapphire-H02. SEM images of the H-passivated dry-etched-then-wet-etched fins along <1$\bar{2}$10> direction after etching in hot TMAH at 85 oC for 1 hr. Mg acceptors were not successfully activated by N thermal annealing, therefore, the vertical sidewall was formed after TMAH etching.

4.20 Pictures of (a) GaN wafer before and after H annealing and (b) Copper residue in the tube of annealing furnace. This annealing furnace was typical for the growth of graphene, the particles on the sample may be diffused copper molecules.

4.21 Schematic of hole compensation and Mg activation. (a) Hydrogen atoms diffuse into GaN to form Mg-H bonds. The fermi level is raised due to the hole compensation. (b) Hydrogen atoms are driven out from GaN. The fermi level is lowered due to the Mg activation.

4.22 Sample ID: JH-GaN on GaN-C01. SEM images of Mg-activated dry-etched samples (a) and (b): slanted sidewalls. (c) and (d): rough defective sidewall.

4.23 Sample ID: JH-GaN on GaN-C01. SEM images of the Mg-activated dry-etched samples, showing the cones caused by micro-masking effect due to the Ni residue.

4.24 Sample ID: JH-GaN on GaN-C01. SEM images of the Mg-activated dry-etched samples, showing hexagonal truncated cones with well-defined six-fold sidewalls after dry etch due to the combination of chemical reaction and the radical-assisted bond breaking.

4.25 Sample ID: JH-GaN on GaN-C01. SEM images of the Mg-activated dry-etched-then-wet-etched fins along $<1\bar{2}10>$ direction (a, b, c, and, d figures) and along $<10\bar{1}0>$ direction (e and f figures) after etching in hot TMAH at 85 oC for 30 mins. Hexagonal nano-prism on a-plane sidewalls, while lateral texture on m-plane sidewalls.

4.26 Sample ID: JH-GaN on GaN-C01. SEM images of the Mg-activated dry-etched-then-wet-etched fins along $<1\bar{2}10>$ direction after etching in hot TMAH at 85 oC for 1 hr. Smooth vertical sidewall near the fin edge, staircase-shaped sidewall at interior.

4.27 Sample ID: JH-GaN on GaN-C01. SEM images of the Mg-activated dry-etched-then-wet-etched fins along $<1\bar{2}10>$ direction after etching in hot TMAH at 85 oC for 1 hr (after removing Ni mask). Smooth vertical outer sidewalls, while staircase-shaped interior sidewalls.

4.28 Sample ID: JH-GaN on GaN-C01. SEM images of the Mg-activated dry-etched-then-wet-etched fins along $<1\bar{2}10>$ direction after etching in hot TMAH at 85 oC for 1 hr, FIB-ed from the middle section of a 800 um fin. The Pt film around the fin was deposited to protect the fin surface from incurring FIB induced damage. The slanted sidewalls indicate even the n-GaN was not smoothened in the hot TMAH etch due to limited diffusion of etchants and dissolution of the etch reaction by-product.

4.29 Sample ID: JH-GaN on GaN-NH301. SEM images of the H-passivated dry-etched-then-wet-etched fins along $<1\bar{2}10>$ direction after etching in hot TMAH at 85 oC for 1 hr, FIB-ed from the middle section of a 800 um fin. The Pt film around the fin was deposited to protect the fin surface from incurring FIB induced damage. The vertical sidewalls indicate the etch rate of p-GaN was increased due to the hole compensation.

4.30 Sample ID: JH-GaN on GaN-NH301. SEM images of the H-passivated dry-etched-then-wet-etched fins after etching in hot TMAH at 85 oC for 1 hr. (a) and (b): formation of Ultra-smooth m-plane sidewalls. (c) and (d): a-plane straight sidewalls textured by adjacent m-planes.

LIST OF TABLES

CHAPTER 1

INTRODUCTION AND MOTIVATION OF STUDY

1.1 Vertical GaN power MOSFET Technologies

1.1.1 GaN vs. Si: Power electronics is the application of solid-state electronics to the control and conversion of electric power.[1] The first power MOSFETs appeared in late 1970s as alternatives to bipolar transistors. These majority carrier devices were faster, more rugged, and had higher current gain than the minority-carrier counterpart.[2] Si has been the dominant semiconductor material in power management for over 60 years because it is abundant in the earth, mechanically strong, relatively easy to purify, and has decent electrical properties.[3] However, Si technology is reaching its performance limits in high-power switching electronics. Wide-bandgap semiconductors such as GaN are emerging as attractive alternatives due to their superior physical and electrical properties. In high-power switching devices, it is desirable to achieve low on-resistance (R_{on}) and high breakdown voltage (BV). Comparing to the well-established silicon MOSFET power devices, GaN-based switches offer a better capability in efficiency and power handling due to its high breakdown field, mobility, saturation velocity, and lower capacitance, as shown in Figure 1.1.[4-6] These properties allow GaN power devices have a lower R_{on} and switching losses than Si devices for the same BV.

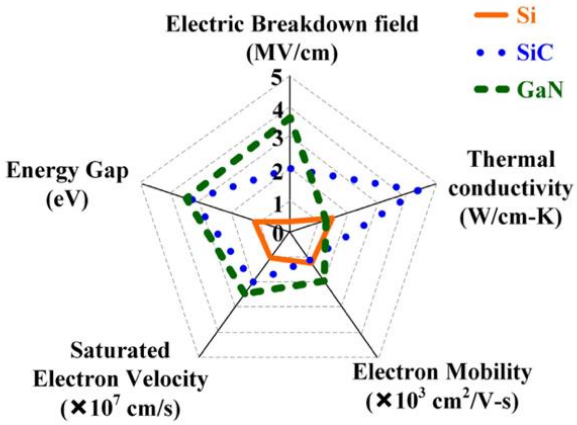

Figure 1.1. Comparison of Si, SiC, and GaN for power semiconductor applications.[4]

1.1.2 Lateral vs. Vertical power devices: Currently, two types of GaN device structures are considered: lateral AlGaN/GaN high-electron-mobility transistors (HEMTs) and vertical GaN MOSFETs. For lateral structures, it can induce high-density and high-mobility two-dimensional electron gas (2DEG) thus effectively reduce on-state resistance. Also, lateral HEMTs have been demonstrated to achieve a record combination of low on-resistance (R_{on}) and high breakdown voltage.[7] However, the limitations are less area efficient for high voltages and low threshold voltage for high-power automotive applications. In lateral HEMTs, substantial gate/drain spacing defines the break down voltage, as shown in Figure 1.2.[8] The device size will sacrifice for achieving a high-current and high-voltage rating. In contrast, vertical GaN MOSFETs have gained increasing attention in high voltage/current levels due to: (1) chip area utilization is more efficient; (2) device operation is less sensitive to surface trapping; (2) superior thermal performance than lateral devices. Therefore, these properties make vertical MOSFETs superior to HEMTs in the high voltage/current applications such as electric vehicles and renewable energy processing.[5-9]

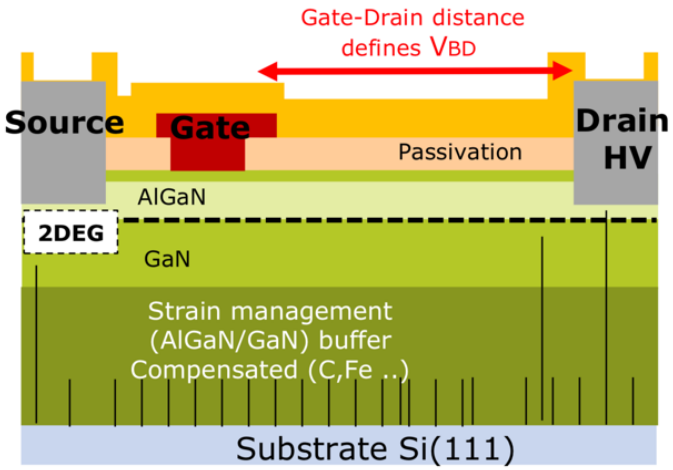

Figure 1.2. Schematic of lateral GaN HEMT. The gate/drain spacing defines the break down voltage. [8]

Vertical GaN power devices: A variety of GaN vertical structures have been developed. To date, two major device structures have been reported. One has the gate placed on the epitaxial surface including a current aperture vertical electron transistor (CAVET) proposed by UCSB and polarization doped MOSFET (PolarMOS) proposed by our group at Cornell, i.e. VDMOS-like devices.[10-12] The other one is the vertical trench MOSFET, which has the gate placed on the sidewall.[7,13,14] The CAVET or PolarMOS embodies a high electron mobility channel at the AlGaN/GaN heterojunction merged with the voltage most dropped over a vertical bulk drift region, as shown in Figure 1.3 (a). The CAVET can also incorporate a trench semi-polar gate, as shown in Figure 1.3 (b). Even though CAVET can utilize high mobility AlGaN/GaN to achieve low R_{on}, channel regrowth posts severe challenges in achieving low off-state leakage in un-gated regrowth interfaces. Compared to CAVET, vertical MOSFETs do not need the regrowth of AlGaN/GaN channels and are intrinsically normally off, as shown in Figure 1.3 (c).[5,14,15] Among the numerous vertical device designs, the trench MOSFET is a favorable device structure for reducing on-resistance due to its capability of high cell density and the absence of a JFET region.

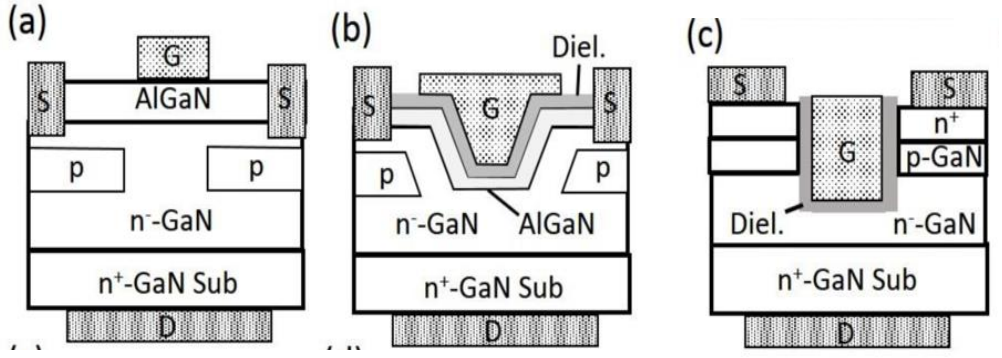

Figure. 1.3. Schematic of vertical GaN transistors: (a) CAVET; (b) Trench CAVET; (c) Trench MOSFET.[5]

1.1.3 Device fabrication of vertical GaN trench MOSFETs: The major process steps for the fabrication of GaN vertical trench MOSFET was shown in Figure. 1.4 reported by Ray et al.[13] First of all, 8-μm-thick n−-GaN drift layer and 800-nm-p-GaN base layer were grown on bulk GaN substrate by metal-organic-chemical-vapor-deposition (MOCVD). The drift and base layer have a Si doping concentration of $1\sim2\times10^{16}$ cm^{-3} and a Mg concentration of $\sim2\times10^{18}$ cm^{-3}, respectively, as determined by secondary-ion-mass-spectroscopy (SIMS). Second, a n+-GaN layer with the Si concentration of ~5x10^{18} cm-3 was selective grown on top of the base layer. Afterwards, 2-μm-wide gate trenches were formed by Cl-based ICP etch, using patterned SiO2 layer as the etch mask. The wet etching was then performed on the wafer by Tetra-Methyl-Ammonium-Hydroxide (TMAH) to clean etched surface and to smooth gate trench sidewall surface. After that, 70-nm-thick AlN/SiN gate dielectric layer was grown by MOCVD. (Note: an activation annealing of p-GaN layer at 850 °C in N_2 ambient was performed after each MOCVD step. Mechanisms of hole compensation will be discussed in the next section 1.1.4. After the gate dielectric deposition, the combination of dry and Buffer-oxide-etchant (BOE) etching was performed to open contact via. The body contact to the p-GaN base layer was formed by alloying Ni/Au. After body contact metallization, the source and gate electrodes were formed by Ti/Al metal stack, and the drain electrode was formed by Ti/Ni/Au stack on the back side of wafer. Last, Ti/Au source metal interconnect was formed on the front side.[7,13]

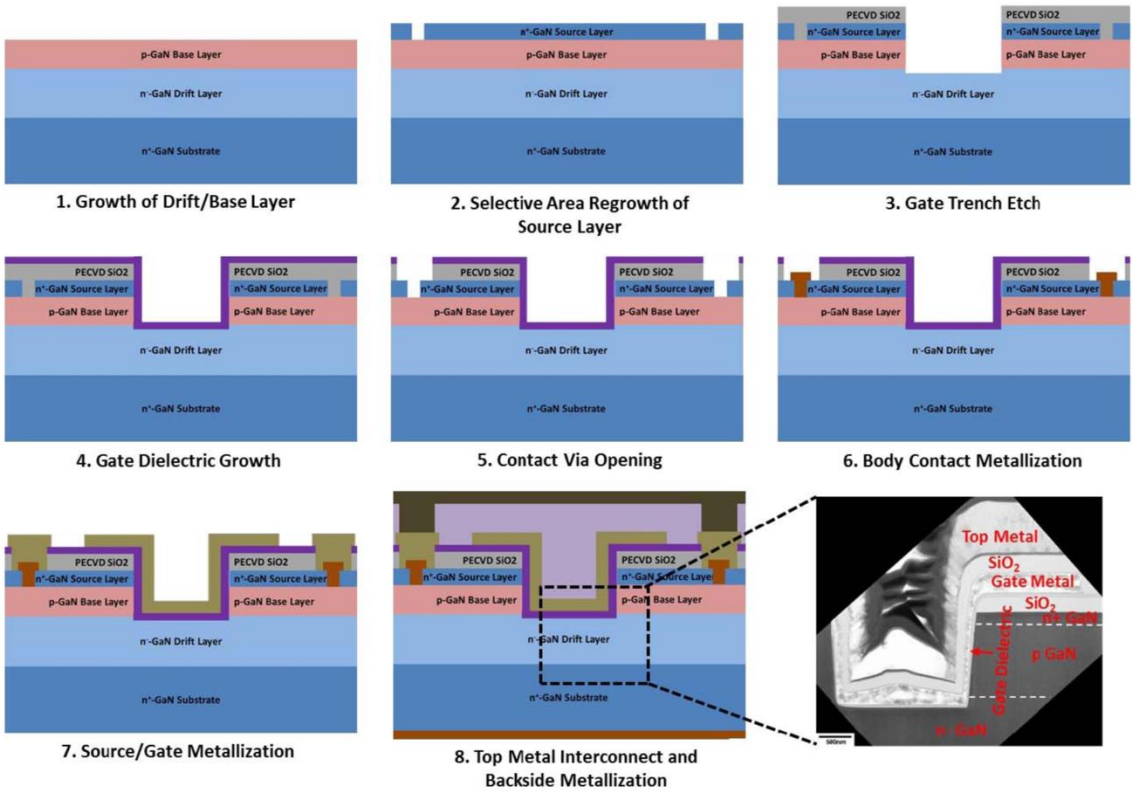

Figure 1.4. Major process steps of fabricating the GaN vertical trench MOSFET and TEM cross-sectional image of the gate region of a fabricated device.[13]

1.1.4 Hydrogen in GaN: Mg-doped GaN grown by metal-organic chemical vapor deposition (MOCVD) requires the post-growth activation of the acceptors to release mobile holes due to the hydrogen incorporation during growing process.[16-18] In 1992, Nakamura et al. reported a hole compensation mechanism of Mg-doped GaN films.[19] They found that the resistivity of low-resistivity p-GaN films began to increase when the NH_3-ambient annealing temperature elevate to 500 ^oC, and the resistivity reached maximum of $1x10^6$ Ω-cm when the annealing temperature in the region of 600 to 1000 ^oC. The resistivity change in Mg-doped GaN films as a function of annealing temperature in NH_3-ambient is shown in Figure 1.5 (a). These results indicate that the atomic hydrogen produced by NH_3 dissociation diffuses into p-GaN film at temperature above 400 ^oC. Then the formation of Mg-H complexes caused hole compensation. As a result, Mg dopant would be passivated by hydrogen and Mg-doped films become resistive.

In the device fabrication, p-GaN layer of p-n diode is typically grown in trimethylgallium (TMG), NH_3, and bis-cyclopentadienyl by MOCVD at the temperature above 1000 ^oC. The NH_3 can dissociate and diffuse into GaN film causes hole compensation. Therefore, the activation annealing of p-GaN layer is necessary. Successful activation of p-GaN required two steps: (1) break Mg-H bonds and (2) drive the hydrogen out of the GaN. Nakamura et al. found that the hydrogen can diffuse out from exposed p-GaN surfaces at the temperature above 700 ^oC in nitrogen gas due to the broken of Mg-H bonds. The resistivity decreased from $1x10^6$ Ω cm to 5 Ω cm, indicating that low resistivity p-GaN film can be obtained by thermal annealing alone.[20]

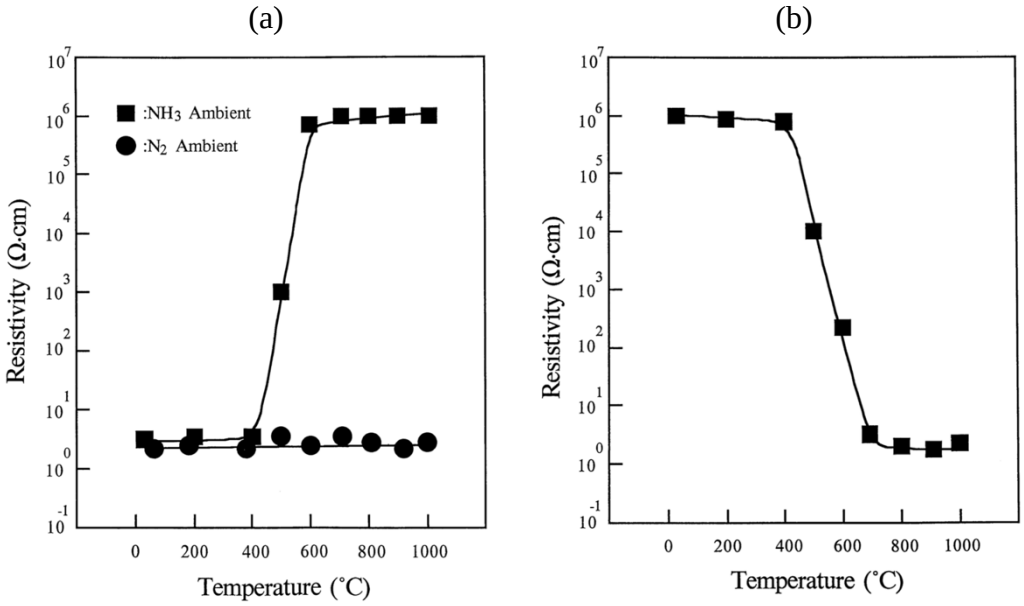

Figure 1.5. (a) The resistivity change in Mg-doped GaN films as a function of annealing temperature in NH_3 and N_2 ambient gasses; (b) Resistivity of Mg-doped GaN films as a function of annealing temperature in N_2 ambient gas.[19,20]

1.1.5 Trench MOSFET working principle: In the trench GaN MOSFET structure, the gate electrode is embedded within a trenched into the GaN surface in order to increase device density and thereby further reduce R_{on}.[21] The trench MOSFET was commonly formed by dry etching process. Depending on the precise crystal alignment, the sidewall may lie approximately along the $(1\bar{1}00)$, $(11\bar{2}0)$, or intermediate crystal planes. There are two n+ doped regions at top and down of the MOS device that form the source and drain, respectively. The n-type channel is formed on the sidewall of the trench at the surface of the p-base region, leading to the current flow parallel to the c-axis of the crystal, as shown in Figure 1.6.[8,22]

It is crucial for the MOSFET to control the interface quality between the semiconductor channel and the dielectric material in order to minimize the trap states and suppress the leakage current. The process optimization for trench formation is the key to reduce the trapping. Since the cleavage plane is relatively smooth and has the fewest broken bonds, the reduction of sidewall defects can enable a higher mobility and better material quality in the regions near etched sidewalls. In addition, the more vertical sidewall can mitigate current crowding and obtain uniformly distribution of electric field.[7,22,23]

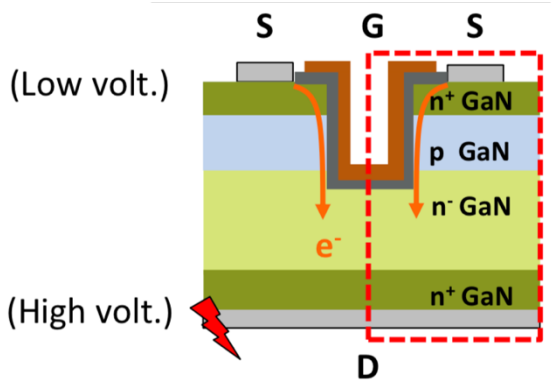

Figure 1.6. Schematic of vertical GaN UMOS. N-type channel is formed on the sidewall of the trench at the surface of the p-base region [8]

1.1.6 Trench formation: Dry plasma etch is dominant in patterning for GaN due to the limitation of wet etching. Plasma etching proceeds by either physical sputtering, chemical reaction, or a combination of the two (ion-assisted plasma etching).[24,25] To anisotropic etch GaN, energetic ions are formed in the plasma and then be accelerated toward the substrate surface at high energies. The materials are then ejected from the surface due to the transfer of energy and momentum to the substrate.[26] Reactive ion etching (RIE) is one of the common dry etching techniques. The plasma was typically generated by applying radio frequency (RF) power of 13.56 MHz between two parallel electrodes in a reactive gas at low pressures ranging from a few mTorr to 200 mTorr. The low pressure can allow less collision scattering of ions during acceleration in the sheath due to the large mean free path, therefore, achieve anisotropic etch profile.[27]

Compared to RIE, the use of high-density plasma etching systems such as inductively coupled plasma (ICP) can improve etch characteristic for the GaN owing to the bond breaking efficiency. High density ICP plasma was formed in a dielectric vessel encircled by an inductive coil into which RF power was applied. The alternating electric field between the coils induces strong alternating magnetic field trapping electrons in the center of the chamber and generating plasmas with uniform density and energy distribution. By keeping ion and electron energy low, a lower damage etching while maintaining fast etch rates can be realized in ICP system. [28,29]

For GaN electronic devices, the electrical performance is very sensitive to surface damage. Dry etching is the most common etching technique to form the trench for vertical GaN MOSFET, however, it can result in considerable problems such as etch-induced damage/defects (e.g., N vacancies) and rough surface morphology thus minimizing device performance.[30] This unsatisfactory termination lowers the inversion layer mobility and causes the leakage current. Sugimoto et al. reported that the surface of p-GaN sidewall could be changed to a depleted or an n-GaN layer by inductively coupled plasma (ICP) reactive-ion etching (RIE), inducing a large leakage under high reverse bias.[31] To mitigate the leakage current, the post-treatment by anisotropic wet etching is desirable to remove the damages and to form vertical sidewalls.[32-34] Zhang et al. reported that TMAH wet etching (25% concentration) at 85 C can preferentially etches the side slope and effectively removed the damage from etched sidewalls without increasing the etching depth. A TMAH treatment for 60 minutes reduces the sidewall leakage by more than 50 x, as shown in Figure 1.7. Besides, the reduction of sidewall defects and a reduction of current crowding with a more vertical sidewall lead to a better forward characteristics of GaN-on-Si vertical diodes.[30]

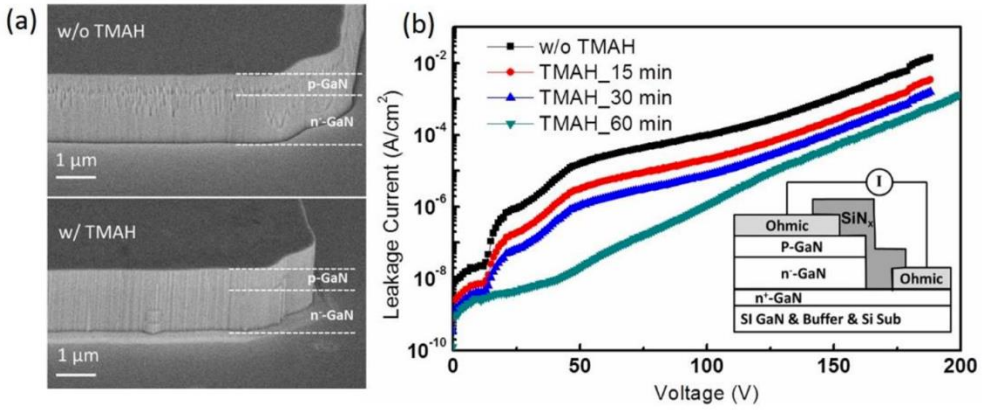

Figure 1.7. (a) SEM images of the etched GaN sidewalls before and after TMAH treatment for 60 minutes. (b) Leakage for the quasi-vertical structures after TMAH treatment with different time.[30]

Trench profile: The trench shape and bottom morphology are determining factors for device breakdown voltage because the device peak electric field is typically located near the trench corners or bottoms. Any sharp corners and surface damage will cause the high leakage current and early breakdown. Therefore, trench formation and corner rounding are the key processes to demonstrate high-voltage trench vertical GaN MOSFET. [33,35] Zhang et al. reported the importance of trench profile by the simulation of E-field distribution in the device. Three types of trench shape were simulated at a high reverse bias: a non-rounded trench, a rounded trench with a flat bottom, and a rounded trench with a tapered bottom, as shown in Figure 1.8. The non-rounded trench shows the highest peak electric fields in GaN and dielectrics located around the sharp corners, and the rounded trench with a tapered bottom has an electric field crowding at the bottom rounded corner. Among these three structures, the rounded trench with a flat bottom shows the lowest peak electric field, indicating it's an optimum trench shape for high-voltage vertical GaN power devices.

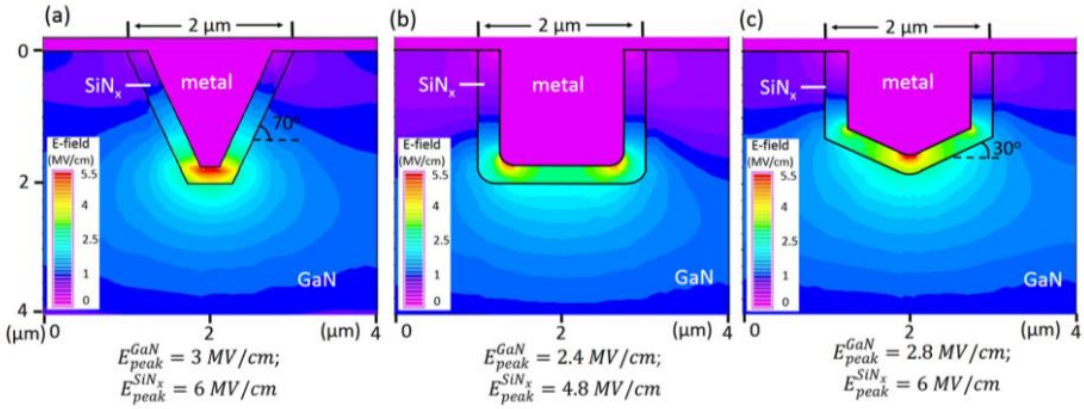

Figure 1.8. Simulated E-field distribution of a device unit-cell at a reverse bias of 600V, for three different trench shapes: (a) non-rounded trench, (b) rounded trench with a flat bottom, and (c) rounded with a tapered bottom.

1.2 Motivation of study:

GaN power electronics with a higher breakdown strength, faster switching speed, higher thermal conductivity and lower on-resistance is anticipated to play a key role in the power conversion market. In vertical trench MOSFET, the trench shape and surface roughness are determining factors for achieving high breakdown voltage and reduce leakage current. It is critical to control the interface quality between the semiconductor channel and the dielectric material in order to minimize the trap states and suppress the leakage current. However, the unsatisfactory termination structures cause GaN vertical power devices are still under development.

Since it is beneficial to place the gate on the cleavage plane of semiconductor due to the fewest broken bonds can enable a higher mobility and better material quality of the channel. In this work, the objective is to fabricate a trench with smooth and vertical non-polar sidewall on GaN sidewall with p-n structure for the applications of the vertical U-trench GaN MOSFET.

1.3 Outline of the thesis:

In Chapter 2, hydroxide-based wet etching is introduced from its mechanism to applications in the fabrication of GaN power device. The challenge of p-GaN etching is discussed in this chapter as well. In Chapter 3, the experimental methods and procedure are covered. In Chapter4, three types of wet etching methods are investigated: (1) Conventional wet etching; (2) UV-assisted wet etching; and (3) Hydrogen-passivation-assisted wet etching. Among these etching methods, the non-polar sidewall is only achieved by Hydrogen-passivation-assisted wet etching. The final chapter, Chapter 5 concludes the thesis with a summary of research work.

BIBLIOGRAPY

[1]Blaabjerg, Frede, ed. *Control of power electronic converters and systems*. Vol. 2. Academic Press, 2018.

[2]Ahmed, M. R., R. Todd, and A. J. Forsyth. "Switching performance of a SiC MOSFET body diode and SiC schottky diodes at different temperatures." *2017 IEEE Energy Conversion Congress and Exposition (ECCE)*. IEEE, 2017.

[3]Corey, D. P., and C. F. Stevens. "Science and technology of patch-recording electrodes." *Single-channel recording*. Springer, Boston, MA, 1983. 53-68.

[4]Jones, Edward A., Fei Fred Wang, and Daniel Costinett. "Review of commercial GaN power devices and GaN-based converter design challenges." *IEEE Journal of Emerging and Selected Topics in Power Electronics* 4.3 (2016): 707-719.

[5]Amano, H., et al. "The 2018 GaN power electronics roadmap." *Journal of Physics D: Applied Physics* 51.16 (2018): 163001.

[6]Ahmed, M. R., R. Todd, and A. J. Forsyth. "Switching performance of a SiC MOSFET body diode and SiC schottky diodes at different temperatures." *2017 IEEE Energy Conversion Congress and Exposition (ECCE)*. IEEE, 2017.

[7]Oka, Tohru, et al. "1.8 mΩ· cm2 vertical GaN-based trench metal–oxide–semiconductor field-effect transistors on a free-standing GaN substrate for 1.2-kV-class operation." *Applied Physics Express* 8.5 (2015): 054101.

[8]http://www1.semi.org/eu/sites/semi.org/files/events/presentations/05_Thomas%20Mikolajick_NaMlab.pdf

[9]Zhang, Yuhao, et al. "Electrothermal simulation and thermal performance study of GaN vertical and lateral power transistors." *IEEE Transactions on Electron Devices* 60.7 (2013): 2224-2230.

[10]Gao, Yan, et al. "Optimization of AlGaN/ GaN current aperture vertical electron transistor (CAVET) fabricated by photoelectrochemical wet etching." (2004): 6925-6927.

[11]Ji, Dong, et al. "Normally OFF trench CAVET with active Mg-doped GaN as current blocking layer." *IEEE Transactions on Electron Devices* 64.3 (2016): 805-808.

[12]Chowdhury, Srabanti, Brian L. Swenson, and Umesh K. Mishra. "Enhancement and depletion mode AlGaN/GaN CAVET with Mg-ion-implanted GaN as current blocking layer." *IEEE Electron Device Letters* 29.6 (2008): 543-545.

[13]Li, Ray, et al. "600 V/$1.7~\Omega $ Normally-Off GaN Vertical Trench Metal–Oxide–Semiconductor Field-Effect Transistor." *IEEE Electron Device Letters* 37.11 (2016): 1466-1469.

[14]Li, Wenshen, et al. "600 V GaN vertical V-trench MOSFET with MBE regrown channel." *2017 75th Annual Device Research Conference (DRC)*. IEEE, 2017.

[15]Zhang, Yuhao. *GaN-based vertical power devices*. Diss. Massachusetts Institute of Technology, 2017.

[16]Li, Wenshen, et al. "Activation of buried p-GaN in MOCVD-regrown vertical structures." *Applied Physics Letters* 113.6 (2018): 062105.

[17]Götz, W., et al. "Hydrogen passivation of Mg acceptors in GaN grown by metalorganic chemical vapor deposition." *Applied physics letters* 67.18 (1995): 2666-2668.

[18]Obloh, H., et al. "Self-compensation in Mg doped p-type GaN grown by MOCVD." *Journal of crystal growth* 195.1-4 (1998): 270-273.

[19]Nakamura, Shuji, et al. "Hole compensation mechanism of p-type GaN films." *Japanese Journal of Applied Physics* 31.5R (1992): 1258.

[20]Nakamura, Shuji, et al. "Thermal annealing effects on p-type Mg-doped GaN films." *Japanese Journal of Applied Physics*31.2B (1992): L139.

[21]Gupta, Chirag, et al. "A novel device design to lower the on-resistance in GaN trench MOSFETs." *2016 74th Annual Device Research Conference (DRC)*. IEEE, 2016.

[22]Tesfaye, A. "SiC Semiconductor Devices Technology, Modeling, and Simulation." *Doctor, Technical University of Vienna, Austria* (2004).

[23]Fukushima, Hayata, et al. "Vertical GaN pn diode with deeply etched mesa and capability of avalanche breakdown." *Applied Physics Express* (2019).

[24]Pearton, S. J., R. J. Shul, and Fan Ren. "A review of dry etching of GaN and related materials." *Materials Research Society Internet Journal of Nitride Semiconductor Research*5.1 (2000).

[25]Ng, Doris Keh-Ting, et al. "Sub-Micron Anisotropic InP-based III–V Semiconductor Material Deep Etching for On-Chip Laser Photonics Devices." *Advanced Engineering Materials* 20.2 (2018): 1700465.

[26]Douglas, Monte A. "Trench etch process for a single-wafer RIE dry etch reactor." U.S. Patent No. 4,855,017. 8 Aug. 1989.

[27]Nalwa, Hari Singh. *Handbook of thin film materials*. Academic Press, 2002.

[28]Shul, R. J., et al. "Inductively coupled plasma etching of GaN." *Applied physics letters* 69.8 (1996): 1119-1121.

[29]Sheu, Jinn-Kong, et al. "Inductively coupled plasma etching of GaN using Cl 2/Ar and Cl 2/N 2 gases." *Journal of applied physics* 85.3 (1999): 1970-1974.

[30]Zhang, Yuhao, et al. "Origin and control of OFF-state leakage current in GaN-on-Si vertical diodes." *IEEE Transactions on Electron Devices* 62.7 (2015): 2155-2161.

[31]Sugimoto, Masahiro, et al. "Study on leakage current of pn diode on GaN substrate at reverse bias." *physica status solidi c* 8.7-8 (2011): 2512-2514.

[32]Kodama, Masahito, et al. "GaN-based trench gate metal oxide semiconductor field-effect transistor fabricated with novel wet etching." *Applied physics express* 1.2 (2008): 021104.

[33]Zhang, Yuhao, et al. "Trench formation and corner rounding in vertical GaN power devices." *Applied Physics Letters* 110.19 (2017): 193506

[34]Uesugi, Tsutomu, and Tetsu Kachi. "GaN power switching devices for automotive applications." *Proc. Int. Conf. CS Matech*. 2009.

[35]Williams, Richard K., et al. "The trench power MOSFET: Part I—History, technology, and prospects." *IEEE Transactions on Electron Devices* 64.3 (2017): 674-691.

CHAPTER 2

Chemistry of the Etching Mechanism

2.1 Fundamentals of wet etching

2.1.1 Chemical etching mechanisms and rate-limiting step: Wet etching plays a critical role in improving the morphology and surface quality of trench MOSFET. In general, the wet etching of semiconductors involves oxidation of the semiconductor surface and subsequent dissolution of the resulting oxides. Firstly, the etchant species diffuse toward the film surface and adsorb at active sites on the surface. Second, a chemical reaction between the etch etchant and the exposed surface occurs, producing soluble byproducts. Last, the byproducts will desorb and diffuse away from the surface.[1] In chemical kinetics, the overall rate of a reaction is often approximately determined by the slowest step, known as rate-limiting step. The etching will be determined by the chemical reaction step and become reaction-rate-limited if the thickness of the diffusion boundary layer is very small. In contrast, diffusion-limited etching often occurs in viscous solutions, which consist of high concentrations of the agent for dissolving the oxides and a greater number of collisions between reactants and solvent molecules.[2]

Temperature dependence: Temperature is one of the main factors to control the etch rate. In a reaction limited etching process, the etch rate has a stronger dependence on the temperature than that of diffusion limited process. In physical chemistry, the temperature dependence of reaction rates can be described by Arrhenius equation: $R = R_0 e^{-E_A/kT}$, where R_0 is the rate constant that depends on the density and diffusivity of reactants, E_A is the activation energy, and k is the Boltzmann constant. The increasing of temperature can speed up the chemical reaction, leading to a faster etch rate. [1,3,4]

Agitation dependence: Usually reaction-rate-limited etching is easier to control than that of diffusion-limited etching. For a diffusion-limited etching condition, adequate agitations can help generate a faster and more uniform etch rate because the agitation-induced turbulence will decrease the thickness of diffusion boundary layer. Lida et al. reported the stirring effect of GaAs in H_2SO_4 wet etching.[3] The etching rate can be increase by adding ultrasonic vibration during the etching process, as shown in Figure 2.1.

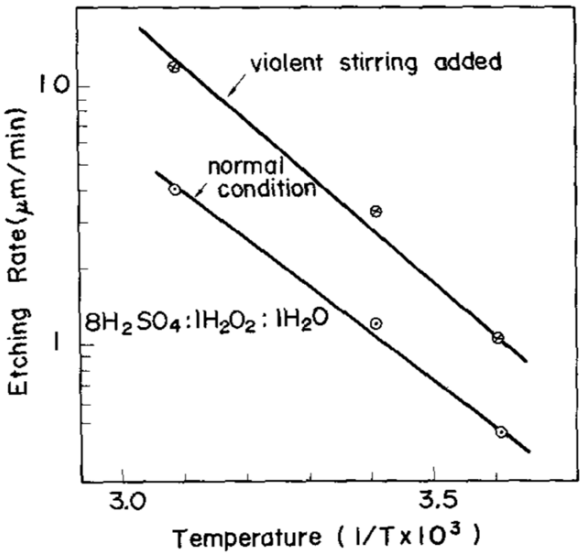

Figure 2.1. Stirring effect on the etch rate of GaAs in H_2SO_4 solution. Etching rate with violent stirring can be orders of magnitude faster than the case without stirring. [3]

2.1.2 Atomic origin of anisotropy: Etching can be seen as the reverse process as growth. Kossel and Stranski et al. proposed a Terrace Step Kink model (TSK) to describe the thermodynamics of crystal surface formation and transformation, as well as the energetics of surface defect formation.[5,6] It is based on two major concepts: (1) The energy of an atom's position on a crystal surface is determined by its bonding to neighboring atoms, and (2) Phase growth or transition involve the counting of broken and formed bonds. Figure 2.2 shows the schematic of kink, step, and terrace sites on crystal for growth and etch chemistry. It is generally not energetically favorable to attach a single molecule on the smooth surface of an ideal crystal, because it has a far smaller number of bonding molecules than those in the bulk crystal. In contrast, molecules are more likely to attach at step-edge than at terrace. In particular, a molecule at the kink effectively shifts the kink along the step but does not change the number of corner-site molecules and therefore incurs no extra energy cost. Similarly, the etching behavior on crystals is also followed a step-flow model, which can be regarded as an inverse process of bottom-up growth. Therefore, the etching process is also favorable to occur at the kink and step sites compared to terrace sites.[8]

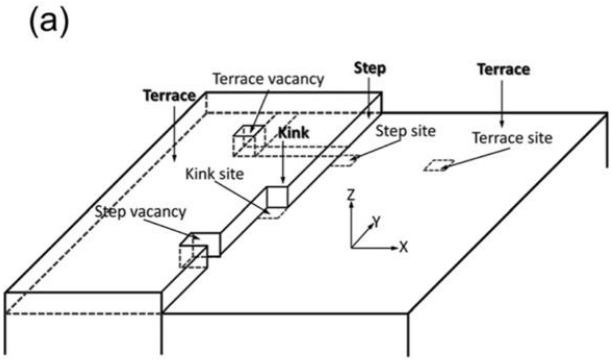

Figure 2.2. Schematic of kink, step, and terrace sites on crystal for growth and etching process. These defects are vulnerable locations on a crystal to the attack from etch solution.[7]

2.2 Chemical wet etching of GaN

2.2.1 Mechanisms of hydroxide-based wet etching: GaN with bond strength of 8.92 eV/atom is difficult to be wet etched at room temperature due to its excellent chemical stability. However, GaN is etchable by the treatment with aqueous KOH solution at elevated temperature and the etching process is strongly anisotropic. Fundamentally, etching of GaN is a combination of oxide formation and subsequent dissolution of the oxide. The wet etching of GaN in base solution can be described by $\mathrm{GaN + H_2O \xrightarrow{OH^-} Ga_2O_3 + NH_3}$.[9-11] In the reaction, OH^- is not only act as a catalytic of forming gallium oxide but also a solvent to dissolve gallium oxide. Firstly, hydroxide ions are adsorbed to the semiconductor surface and subsequently cause the formation of gallium oxide via Ga oxidation. Secondly, the gallium oxide dissolve in the hydroxide-based solution to complete the etching. In 2001, Li et al. found a clear N-H3 peak by X-ray photoelectron spectroscopy (XPS) gave evidence to the formation of ammonia (NH_3).[9] Besides, the Ga-O peak was significantly decreased after etching, indicating the gallium oxide was quick dissolved by the strong alkaline solution once it was formed. Within this context, Guo et al. reported the formation gallium hydroxide as an intermediate step, which can be described by Eq. 2. $GaN + H_2O \xrightarrow{OH^-} Ga(OH)_3 + NH_3$.[12] The Gibbs free energies of the formation reactions of $Ga(OH)_3$ and $Ga_2(OH)_3$ were 1399.9 kJ/mol and 723.5 kJ/mol, respectively. They found the dissolution rate of both compounds was strongly depended on KOH concentrations. Besides, there were several early reports indicate that the formation of insoluble gallium hydroxide will block the further etching on GaN under electrochemical solution in NaOH.[14] This made the adequate agitation necessary. Therefore, the rate-limiting step of wet etching process is not only determined by temperature but solution concentration and agitation.

2.2.2 Direction of crystallographic: Surface bonding configuration is the key factor to determine the etching stability of flat crystallographic facets. Li et al. investigated the etching of +c- and –c-plane GaN in KOH solution.[9] They found the etch rate of -c-plane surface was fast, while the etch rate of c-plane surface was highly suppressed due to the electrostatic repulsion from N dangling bonds. Figure 2.3 shows the schematic diagram of the mechanisms of the selective etching. For +c-plane, hydroxide is first adsorbed on the Ga-dangling bonds to form a Ga-OH complex by electrostatic attraction. Although the formed gallium oxide is subsequently dissolved in KOH solution, the surface is then converted into the nitrogen termination after the first layer of Ga atom on the GaN layer was removed. Therefore, hydroxide is difficult to attack Ga back bonds at the second layer due to the strong screen effect from three occupied dangling bonds of nitrogen. This prevent hydroxyl from approaching the Ga-N bonding at the second layer.[9-11]

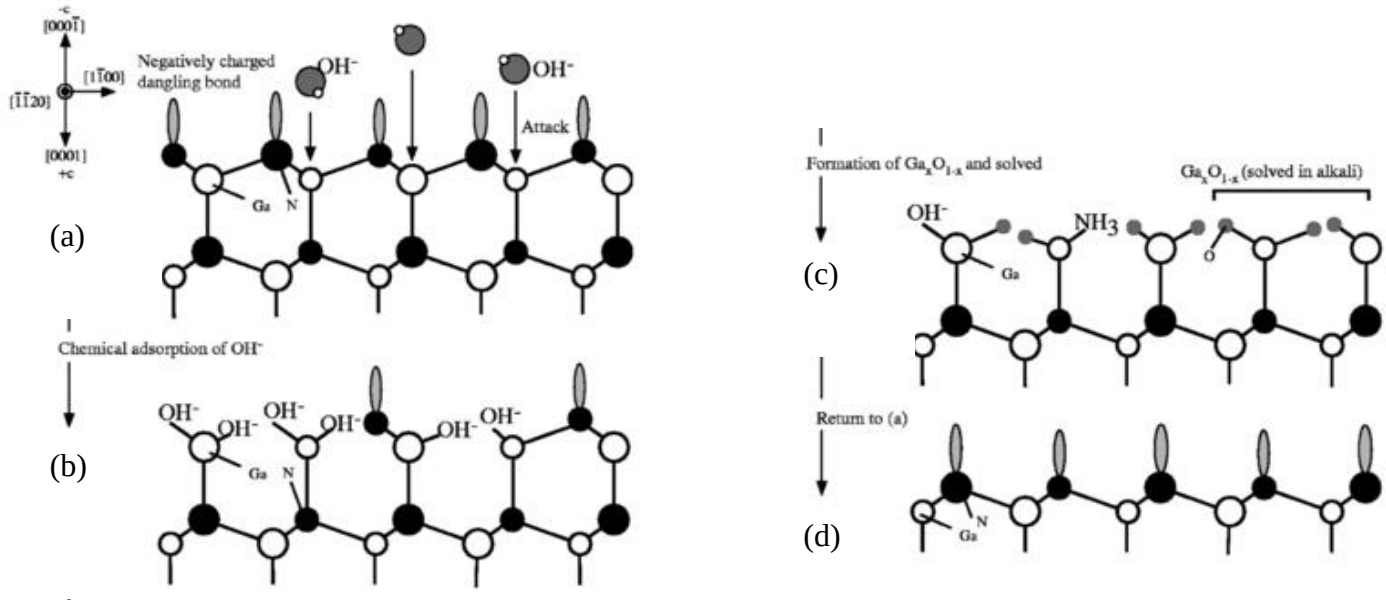

Figure 2.3. Schematic diagrams of the cross sectional GaN film viewed along the $[\bar{1}\bar{1}20]$ direction for -c GaN to explain the mechanism.[9]

Surface energy: Etching capability is affected by surface energy, which is related to planar densities and surface dangling bonds. Planar density is defined as the fraction of total crystallographic plane area that is occupied by atoms. As an example, there are 2 atoms on a m-plane of wurtzite structure GaN and the area is 16.5 $Å^2$ (lattice constant: a=3.18 nm; c=5.18 nm). Thus, the planar density of m-plane is about 0.12 numbers of atoms/ $Å^2$. Yung-Yu et al. proposed the etching barrier index (EBI) to quantitatively describe the etching ability of several common facets by multiplying the planar density and the number of dangling bonds on N atoms. The value of EBI is ranked from big to small as follows: +c-plane > a-plane > m-plane > -c-plane > (10-1-1) plane > r-plane. The etching capability performs better in the -c-plane than in the +c-plane corresponds to etching phenomena illustrated in the above-mentioned reports. The facet with high EBI is difficult to be etched, thus usually becomes an etching stop and appears in the etching process.[15,16]

Orientation of planes	(0001)	$(11\bar{2}0)$	$(1\bar{1}00)$	$(000\bar{1})$	$(10\bar{1}\bar{1})$	$(10\bar{1}2)$
	+c-plane	**a-plane**	**m-plane**	**–c-plane**		**r-plane**
	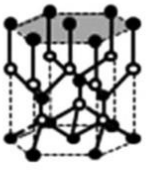	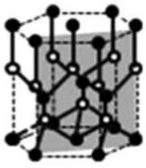		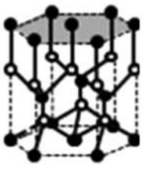	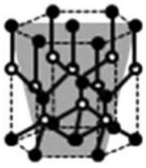	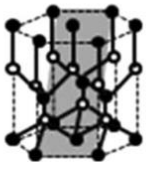
Planar density (number of atoms/$Å^2$)	0.1138	0.1398	0.1211	0.1138	0.0534	0.0414
Number of dangling bonds on N atom	3	2	1, 2	1	2	2
EBI	0.3414	0.2796	0.1211, 0.2422	0.1138	0.1068	0.0828

Table 2.1. Etching ability of each plane on GaN.[15]

2.2.3 Applications of hydroxide-based wet etching:

Light emitting diodes (LEDs): GaN is the key material for the fabrication of blue and white LEDs. Figure 2.4 shows the schematic view of photon emission pathway in LED chip. For smooth surface, most of the photons undergo total internal reflection due to the Snell's law. This phenomenon decreases the overall light efficiency because the photons either become absorbed or escape through the sidewalls. In contrast, the KOH anisotropic etching of GaN can result in a highly rough surface, which allows photons to be emitted outside of the escape cone. These photons can be redirected back into the escape cone, participating in the luminance of the device to improve the light extraction efficiency.[11,17]

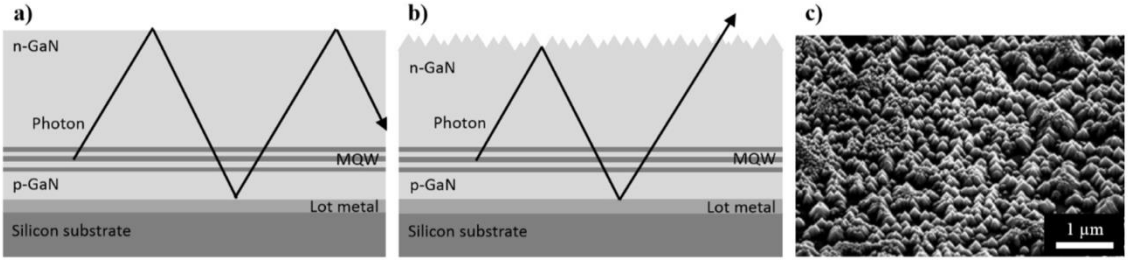

Figure 2.4. Schematic view of photon emission pathway a) without and b) with surface roughening. c) Scanning electron microscopy (SEM) image of the pyramidal morphology after roughening by KOH.[11,17]

High-frequency/power electric devices: Plasma etching is widely utilized in the fabrication of trench GaN devices. However, it can result in etch-induced damage/defects and rough surface morphology, which will affect the electric and optical performance characteristics of the devices. By KOH post treatment, a smooth and straight etched sidewall along <11$\bar{2}$0> direction correspond to (1-100) plane sidewall was formed, as shown in Figure 2.5 (b).[18] This high-quality surface is benefit for the device performance by reducing the possibility of trap states.

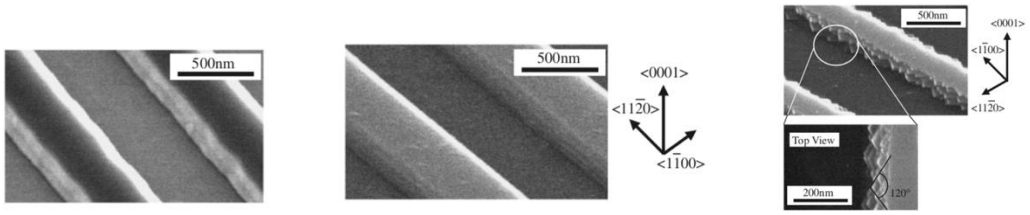

Figure 2.5. SEM images of fins: (a) along <11$\bar{2}$0> direction, as-dry-etched, (b) along <11$\bar{2}$0> direction prepared by KOH wet etching for 40 minutes after RIE, (C) along <1$\bar{1}$00> direction, etched using same procedure as (b).[18]

On the other hand, sidewall of the fins along the <1$\bar{1}$00> direction become rougher with many triangular shapes formed by two adjacent m planes. This is due to the difference of surface bonding configuration between a- and m- plane. For a-plane, (1) Ga back bonds are more stable than those in m-plane because they are connected to three N atoms, while the Ga back bonds in m-plane are only connected to two N atoms, (2) The repelling forces between OH- ions and N dangling bonds are larger because Ga atom at the top layer is connected to two N atoms, while Ga atom in m-plane is only connected to one N atom. Therefore, a smaller number of OH- ions react with the Ga back bonds as well as Ga dangling bonds in the a-plane.[9-11,18] As a result, m-plane sidewalls are revealed before the appearance of a-plane sidewalls. These crystallographic vertical smooth sidewalls are difficult to be further wet etched because it is generally not energetically favorable to create a cavity on this smooth surface to perform etching. This is probably the reason why m-planes were observed eventually instead of a-planes.

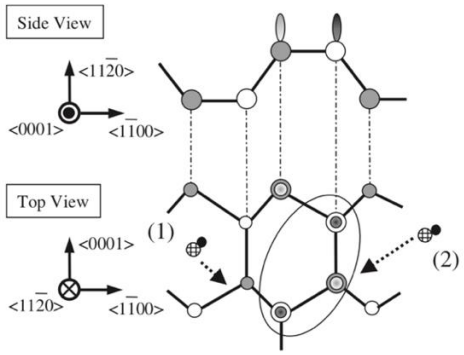

Figure 2.6. Schematic top and side views of GaN a-plane for explaining differences from m-plane.[18]

2.2.4 Tetramethylammonium hydroxide (TMAH): TMAH is a quaternary ammonium salt with the molecular formula $N(CH_3)_4+ OH^-$. In 2008, Kodama et al. reported a U-shape trench with the $(1\bar{1}00)$ plane sidewall formed by the combination of inductively coupled plasma (ICP) and subsequent tetramethylammonium hydroxide (TMAH) etching, as shown in Fig. 2.7.[19] In trench GaN MOSFET, a trench gate structure with non-polar plane is favorable not only for normally-off operation but also for low R_{on} by high integration. In addition, the main advantage of TMAH-based solution is their full compatibility with IC technologies.[20] Even though KOH solutions have been widely used in nanofabrication due to good etched surfaces and low toxicity, but compatibility with MOS processes is not good due to mobile ion (K+) contamination. Thus, TMAH is advantageous over KOH in fabrication of GaN MOSFET.

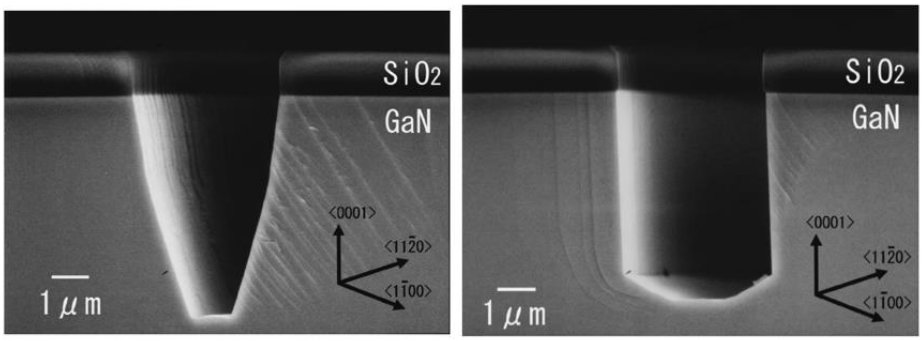

Figure 2.7. SEM images of the trench along <11$\bar{2}$0> direction on a free standing (0001) GaN substrate. (a) after dry etch. (b) after wet etch.[19]

2.2.5 Etching of n- and p-GaN: The etching rate of semiconductor surface is influenced by doping in terms of adjusting surface potential as well as band bending. In general, wet etching on p-GaN surface shows a lower rate than on n-GaN.[1,21] P-type GaN has been reported to be resistant to photoelectrochemical (PEC) etching because photogenerated holes needed for oxidation of the surface are swept away from the depletion region near the surface into the bulk, as shown in Figure 2.8 (a).[21] In contrast, a potential well exists for holes at the surface for n-type material. Reaction between holes in the valence band and oxidants in the chemicals result in oxidation of the semiconductor for the etching process. Therefore, selective etching of n-type GaN over both intrinsic and p-type GaN has been demonstrated. The undercut semiconductor layer structure has important applications in the fabrication of field effect transistors and photodetectors, as shown in Figure 2.8 (b).[18,22-25] P-GaN is not only resistant to photoelectrochemical etching but also in the case of conventional etching without using any photo- or electrically assistance. Li et al. reported the n-GaN etches more quickly than the p-GaN in AZ400k, leading to flashlight shaped nanorod LEDs, as shown in Figure 2.9.[26] The p-GaN had been reported to present a lower etch rate than n-GaN due to the depletion of holes at the electrolyte semiconductor interface. Similar features are also routinely observed in our own laboratory in GaN, e.g., nanowire FETs and tunnel FETs fabricated by Dr. Kazuki Nomoto in our group and Alex Chaney.

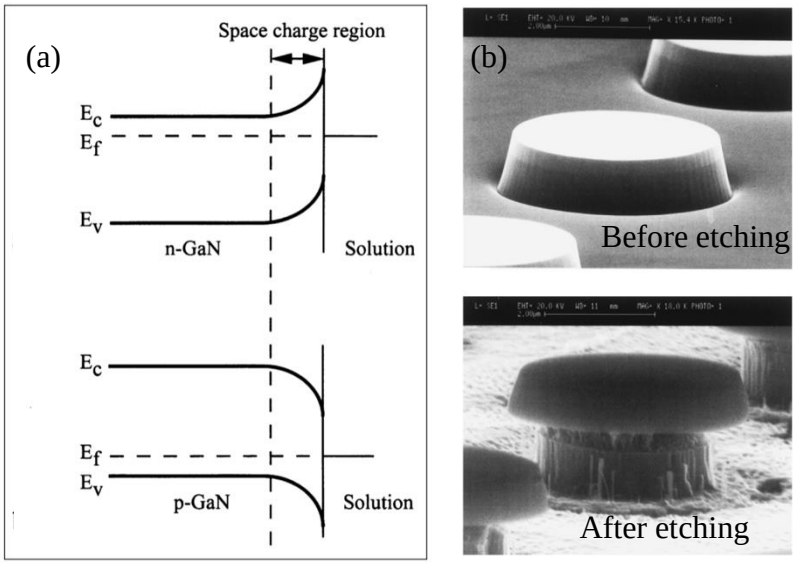

Figure 2.8. (a) Surface energy band diagram for n-type and p-type semiconductor. (b) P-on-n GaN sample before and after PEC etching. Undercutting of p-type layer formed. Ec: conduction band edge; Ef: fermi level; Ev: valence band edge. [21]

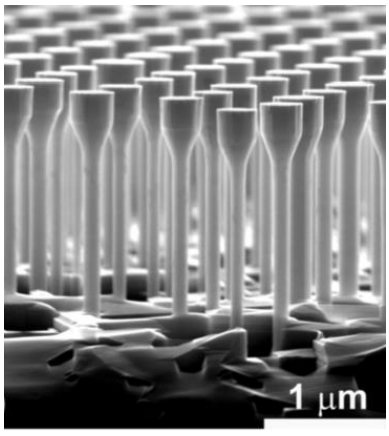

Figure 2.9. SEM images of flashlight shaped nanorod LEDs array after wet etching.[26]

Electrochemistry: From the perspective of electrochemistry, it requires the presence and transport of electrons and holes. Ga oxidation consists out of two separate electrochemical reactions: " $2GaN + 6h^+ \rightarrow 2Ga^{3+} + N_2$" and "$6H^+ + 6e^- \rightarrow 3H_2$". N and H molecules are formed instead of NH_3.

In the scenario for n-GaN without ohmic contacts, GaN only has a direct contact with the solution, therefore, forming a surface band bending as shown in Figure 2.10 (a). In equilibrium the redox couple pins the Fermi level of n-GaN, leading to a positive space charge layer depleted by electrons. The electrons must overcome this potential barrier to be injected into solution (redox system). The electron transport consists of three steps: (1) electron excitation from the Fermi level (E_f) to the conduction band, (2) electron diffusion to the GaN-solution interface, get in direct contact with the solution by overcoming the barrier in the space charge layer (SCL) by thermionic emission or tunneling, (3) some electrons recombine with holes that also reach the GaN-solution interface (see below, and these electrons/holes do not contribute to etching), and other electrons will react with the oxidizer H^+.[1,11,27] Meanwhile, photo-generated holes undergo drifting toward the GaN-solution interface due to the surface band bending. Since holes physically represent broken bonds, a hole reaching the GaN-solution interface means a Ga-N bond is broken; with the presence of solution, the Ga atom with sufficient number of broken bonds gets dissolved in the solution, i.e. etching. In this process, both electrons and holes transport to the solution through the same GaN-solution interface.

In the scenario for n-GaN with ohmic contacts, as shown in Figure 2.10 (c), can allow much easier extraction of the electrons from the n-GaN. Holes drift toward the GaN-solution interface to break Ga-N bonds on the GaN surface thus etching while electrons diffuse to the n+GaN ohmic contacts then get injected into the solution. This process closes the current loop. In PEC etching, the surface

energy barrier for n-GaN can become reasonably low under illumination. In addition, electrons in GaN have much lower effective mass than holes. Therefore, the thermionic or tunneling current of electrons injected into the solution can be sufficiently high to allow etching to proceed as long as holes are swept to the GaN surface.

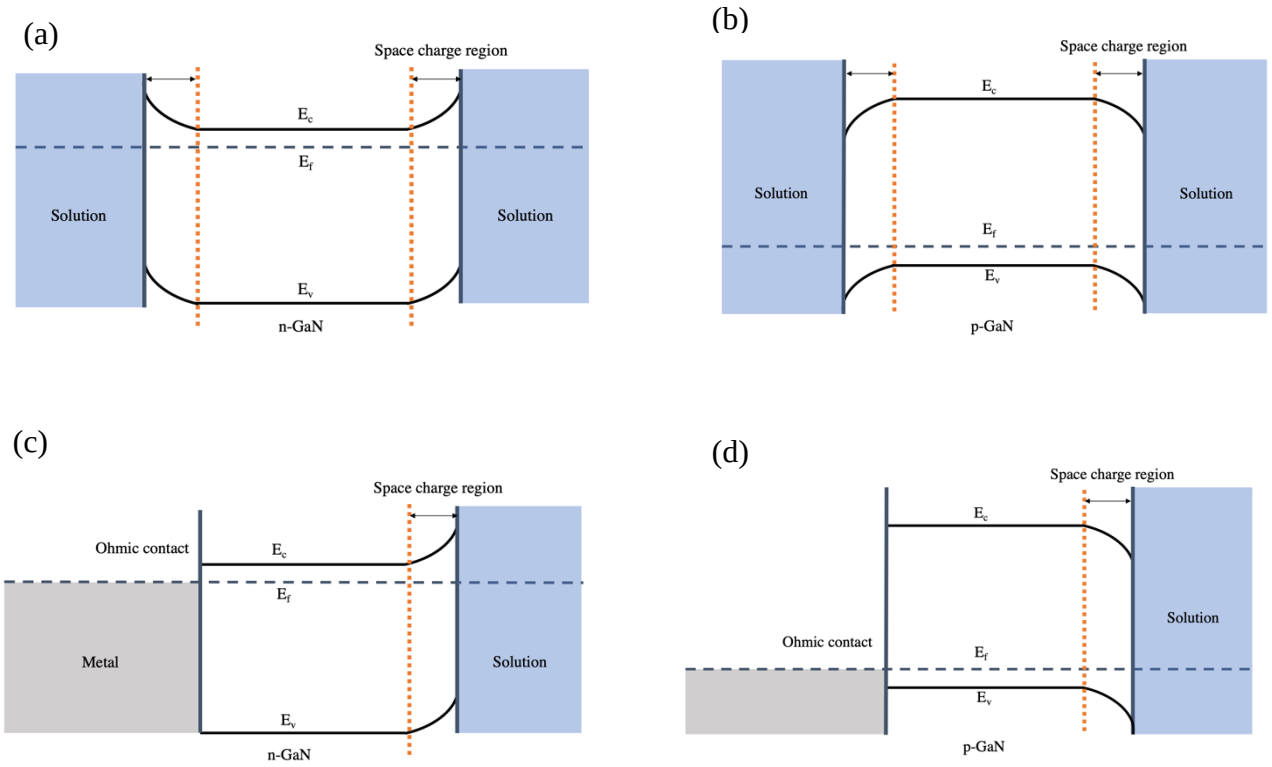

Figure 2.10. Surface energy band diagram of the GaN/etchant interface. (a) and (b) are the scenario for n-GaN and p-GaN without ohmic contacts, respectively. (c) shows a piece of n-GaN with an ohmic contact, which can allow electrons to be injected into solution and holes go to the GaN surface to be etched. (d) show a piece of p-GaN with an ohmic contact. For p-GaN, the band bending is most likely smaller due to a smaller carrier lifetime. It is very difficult to flatten the band in p-GaN.

In contrast, the Fermi level of p-GaN lies closer to the valence band than the conduction band, as shown in Figure 2.10 (b). Electrons that are excited from to the conduction band can be readily injected to the solution due to the downward surface band bending. However, it is extremely

difficult for holes to reach the GaN-solution interface to initiate etch. Under optical illumination, the band bending will reduce; if a flat band condition is reached, it is possible for both electrons and holes to diffuse to the GaN-solution interface. However, under the same optical illumination power the flattening in the surface band bending is most likely smaller for p-GaN due to a smaller minority carrier lifetime compared to that of n-GaN (there are more defects in p-GaN than n-GaN). This means it is very difficult to flatten the band in p-GaN and holes are difficult to be swept or diffuse to the surface. Therefore, the wet etch rate of n-GaN is generally faster than that of p-GaN.

Cavity etch model: Typically, dry-etched GaN nanowires (NWs) have a trapezoidal shape with rough and defective surfaces.[28] In 2018, Yu et al. found that GaN NWs with n-p structure (p-GaN was buried beneath n-GaN) can achieve a vertical sidewall after the treatment in AZ400K developer at 90 °C for 3 hours, while a tapered structure appeared at the p-n junction when p-GaN was on the top of the NWs.[29] The latter cased is in good agreement with the results in previous discussion on flashlight shaped nanorod LEDs array. However, the former cased need to be further explained by the "cavity etch model". In 1993, Elwenspoek proposed this model to explain the anisotropy etch rate of single crystallin silicon in KOH based solution.[30] The concept of the model is that isotropic etching on smooth crystallographic surfaces is initialized by the formation of atomic-scale cavities with steps at the cavity edges. Etching is basically a reverse process of island growth. Thus, the etching rate and activation energy are determined by the nucleation barrier of the cavities. In the case of NWs etching, Yu et al. proposed that the reaction rate of the step moving along the -*c*-direction ($v_s\downarrow$) is faster than the one along *c*-direction ($v_s\uparrow$) due to semi-polar facets along (11-2-2) or (10-1-1) are more stable than the ones along (11-22) or (10-11).[29] As a result, nanowires (NWs) with n-p structure can maintain a vertical sidewall because of the fast

propagation of steps from top n-region. This vertical architecture is promising for implementations in future 3D electronics.

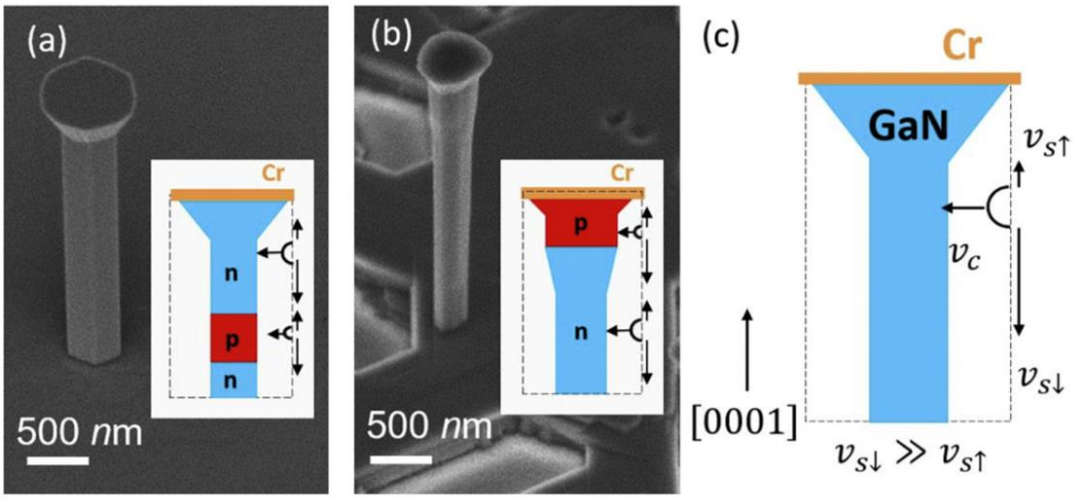

Figure 2.11. SEM images (45° tilted) of wet-etched GaN NWs with (a) n-p and (b)p-n junctions in AZ400K at 90 °C. (c) Schematic of the wet-etching kinetic on the GaN NWs with Cr masks on top. vc is the rate of creating small cavities on flat sidewalls, while $v_s \uparrow$ and $v_s \downarrow$ represent the moving velocities of cavity edges (steps) along the c- and −c-directions, respectively.[29] Similar results are also obtained in the Jena-Xing lab by Dr. Kazuki Nomoto and Alex Chaney (not shown).

BIBLIOGRAPHY

[1]Zhuang, D., and J. H. Edgar. "Wet etching of GaN, AlN, and SiC: a review." *Materials Science and Engineering: R: Reports*48.1 (2005): 1-46.

[2]Stocker, D. A., E. F. Schubert, and Joan Marie Redwing. "Crystallographic wet chemical etching of GaN." *Applied Physics Letters* 73.18 (1998): 2654-2656.

[3]Iida, Shinya, and Kazuhiro Ito. "Selective Etching of Gallium Arsenide Crystals in H 2 SO 4-H 2 O 2-H 2 O System." *Journal of The Electrochemical Society* 118.5 (1971): 768-771.

[4]Han, Seung-Cheol, et al. "Formation of hexagonal pyramids and pits on V-/VI-polar and III-/II-polar GaN/ZnO surfaces by wet etching." *Journal of the Electrochemical Society* 157.1 (2010): D60-D64.

[5]Kossel W., Nachr. Ges. Wiss. Goettingen Math. Phys., K1 11A (1927) 135.

[6] N. Stranski, Zur Theorie des Kristallwachstums, "On the theory of crystal growth", Z. phys Chem. 136, 259–278 (1928).

[7]Bahrig, Lydia, Stephen G. Hickey, and Alexander Eychmüller. "Mesocrystalline materials and the involvement of oriented attachment–a review." *CrystEngComm* 16.40 (2014): 9408-9424.

[8]Fatahilah, Muhammad Fahlesa, et al. "3D GaN nanoarchitecture for field-effect transistors." *Micro and Nano Engineering* 3 (2019): 59-81.

[9]Li, Dongsheng, et al. "Selective etching of GaN polar surface in potassium hydroxide solution studied by x-ray photoelectron spectroscopy." *Journal of Applied Physics* 90.8 (2001): 4219-4223.

[10]Ng, Hock M., Nils G. Weimann, and Aref Chowdhury. "GaN nanotip pyramids formed by anisotropic etching." *Journal of applied physics* 94.1 (2003): 650-653.

[11]Tautz, Markus, and David Diaz Diaz. "Wet-Chemical Etching of GaN: Underlying Mechanism of a Key Step in Blue and White LED Production." *ChemistrySelect* 3.5 (2018): 1480-1494.

[12]Guo, W., et al. "KOH based selective wet chemical etching of AlN, AlxGa1− xN, and GaN crystals: A way towards substrate removal in deep ultraviolet-light emitting diode." *Applied Physics Letters* 106.8 (2015): 082110.

[13]Li, Dongsheng, et al. "Selective etching of GaN polar surface in potassium hydroxide solution studied by x-ray photoelectron spectroscopy." *Journal of Applied Physics* 90.8 (2001): 4219-4223.

[14]Pankove, J. I. "Electrolytic etching of GaN." *Journal of the Electrochemical Society* 119.8 (1972): 1118-1119.

[15]Lai, Yung-Yu, et al. "The study of wet etching on GaN surface by potassium hydroxide solution." *Research on Chemical Intermediates* 43.6 (2017): 3563-3572.

[16]Yu, Feng, et al. "GaN nanowire arrays with nonpolar sidewalls for vertically integrated field-effect transistors." *Nanotechnology* 28.9 (2017): 095206.

[17]Peng, Wei Chih, and Yew Chung Sermon Wu. "Improved luminance intensity of InGaN–GaN light-emitting diode by roughening both the p-Ga N surface and the undoped-GaN surface." *Applied physics letters* 89.4 (2006): 041116.

[18]Itoh, Morimichi, et al. "Straight and smooth etching of GaN (1100) plane by combination of reactive ion etching and KOH wet etching techniques." *Japanese journal of applied physics*45.5R (2006): 3988.

[19]Kodama, Masahito, et al. "GaN-based trench gate metal oxide semiconductor field-effect transistor fabricated with novel wet etching." *Applied physics express* 1.2 (2008): 021104.

[20]Merlos, A., et al. "TMAH/IPA anisotropic etching characteristics." *Sensors and Actuators A: Physical* 37 (1993): 737-743.

[21]Youtsey, C., G. Bulman, and I. Adesida. "Dopant-selective photoenhanced wet etching of GaN." *Journal of electronic materials* 27.4 (1998): 282-287.

[22]Zhang, Yu, et al. "A conductivity-based selective etching for next generation GaN devices." *physica status solidi (b)* 247.7 (2010): 1713-1716.

[23]Park, Sung Hyun, et al. "Wide bandgap III-Nitride nanomembranes for optoelectronic applications." *Nano letters*14.8 (2014): 4293-4298.

[24]Chang, Tzu-Hsuan, et al. "Strain Balanced AlGaN/GaN/AlGaN nanomembrane HEMTs." *Scientific reports* 7.1 (2017): 6360.

[25]Park, Joonmo, et al. "Doping selective lateral electrochemical etching of GaN for chemical lift-off." *Applied Physics Letters*94.22 (2009): 221907.

[26]Li, Qiming, et al. "Optical performance of top-down fabricated InGaN/GaN nanorod light emitting diode arrays." *Optics express* 19.25 (2011): 25528-25534.

[27]Wang, Liancheng, et al. "Mechanisms in thermal stress aided electroless etching of GaN grown on sapphire and approaches to vertical devices." *RSC Advances* 3.27 (2013): 10934-10943.

[28]Li, Qiming, et al. "Single-mode GaN nanowire lasers." *Optics express* 20.16 (2012): 17873-17879.

[29]Yu, Feng, et al. "Normally Off Vertical 3-D GaN Nanowire MOSFETs With Inverted ${p} $-GaN Channel." *IEEE Transactions on Electron Devices* 65.6 (2018): 2439-2445.

[30]Elwenspoek, M. "On the mechanism of anisotropic etching of silicon." *Journal of the Electrochemical Society* 140.7 (1993): 2075-2080.

CHAPTER 3

Experimental Section

3.1 Process flow

The fabrication steps from photoresist spin coating to wet etching are shown in Figure. 3.1. Mask Layout and etching process are covered in this section in detail.

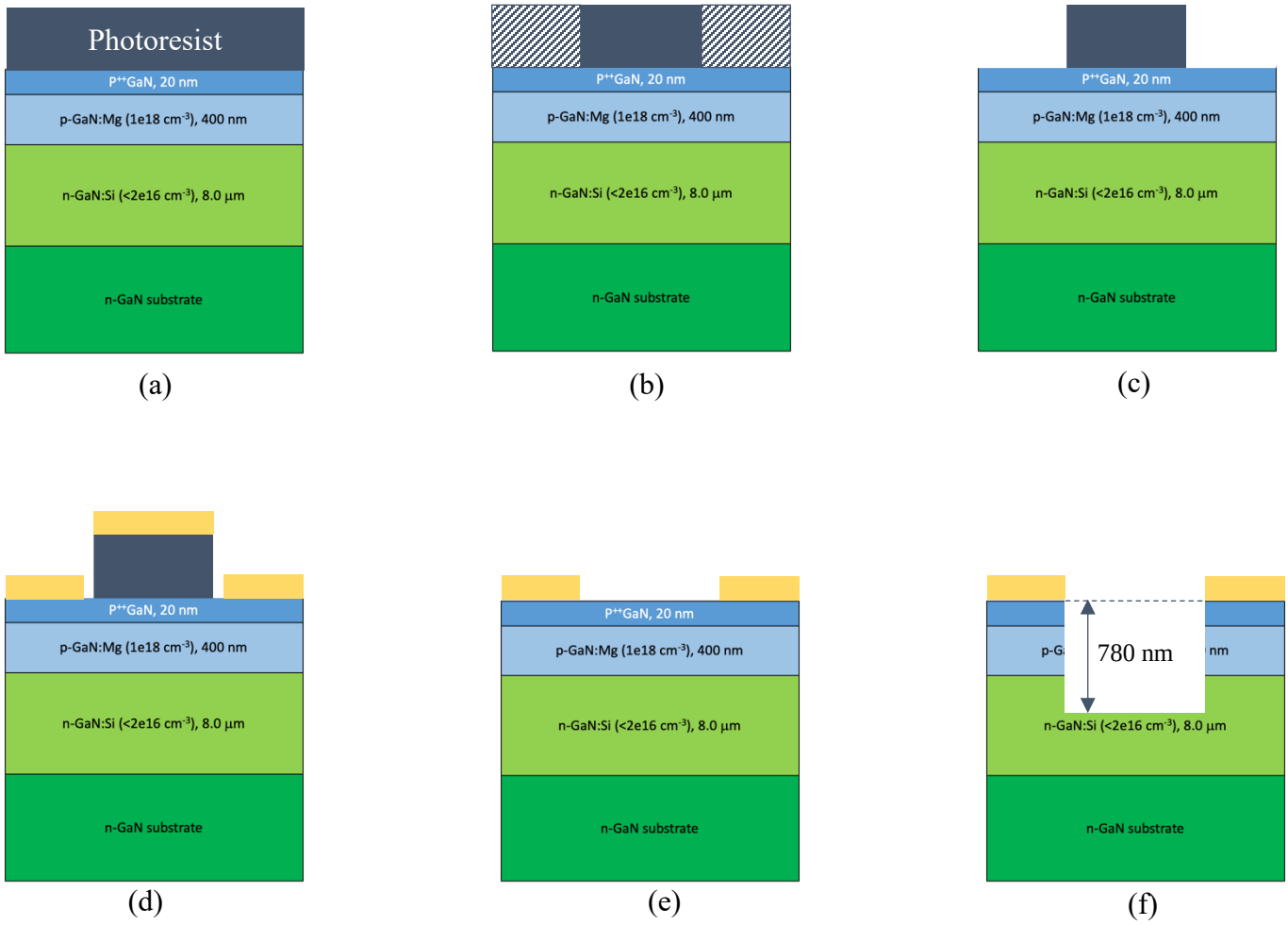

Figure 3.1. GaN trench fabrication process: (a) photoresist spin coating, (b) exposure by i-line stepper, (c) develop by AZ726 MIF, (d) Cr/Ni metal evaporation, (e) lift-off by remover 1165, and (f) combination of dry/wet etching.

3.2 Substrate preparation

The starting epitaxial structure is similar with our previous high voltage p-n diodes.[1] Figure 3.1 shows the schematic of cross-sectional wafer. The starting as-grown epitaxial wafer is a p-n diode structure grown by metalorganic chemical vapor deposition (MOCVD) on sapphire or 2-in bulk n-type GaN substrates. The wafer consists of the top 400 nm p-GaN base layer with Mg-doping concentration of $1x10^{18}$ cm^{-3} (capped with a 20 nm p^{++} layer for ohmic contact purpose) and 8 μm n-GaN drift layer with Si-doping concentration of ~$1\text{-}2x10^{16}$ cm^{-3}. Owing to the incorporation of atomic hydrogen during MOCVD growth, the GaN wafer is activated in-situ in the MOCVD chamber prior to device fabrication. To ensure the cleanness of wafers, GaN surface is ultrasonically rinsed sequentially with acetone, methanol, DI water for each 3 minutes and subsequently dried by nitrogen gas.

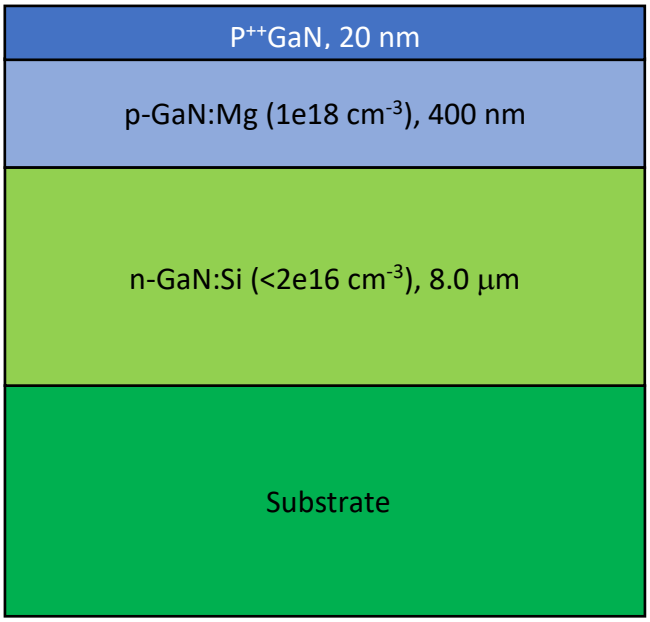

Figure 3.2. Layer of GaN wafer with p-n structure. 400 nm Mg-doped p-GaN and 8 μm Si doped n-GaN drift layer on a wafer substrate, capped with a 20 nm p^{++} layer for ohmic contact purpose.

3.3 Photolithography: The fabrication starts with spin coating of AZ® nLOFTM 2020 on the GaN wafer at 6000 rpm for 1 minute and a soft bake. AZ nLOF 2000 series requires exposure energy at the 365 nm wavelength, therefore, both the ABM Contact Aligner and i-line (365 nm) stepper are suitable. Photomask layout is shown in Figure 3.3. The designed striped patterns are ranging from 0.5 to 20.0 μm, which arrayed along the $<1\bar{2}10>$ and $<10\bar{1}0>$ directions. A post expose bake (PEB) is required to crosslink the exposed resist for proper imaging. PEB is maintained at 115 °C for 1 minute. Afterwards, photoresist is developed in aqueous alkaline developer (AZ® 726 MIF) for 70 seconds for dissolution of expose resist area, resulting in reverse patterns. After development, oxygen plasma treatment (descum) is performed to remove the photoresist residue from the surface. Then GaN wafer is ready for metal evaporation.

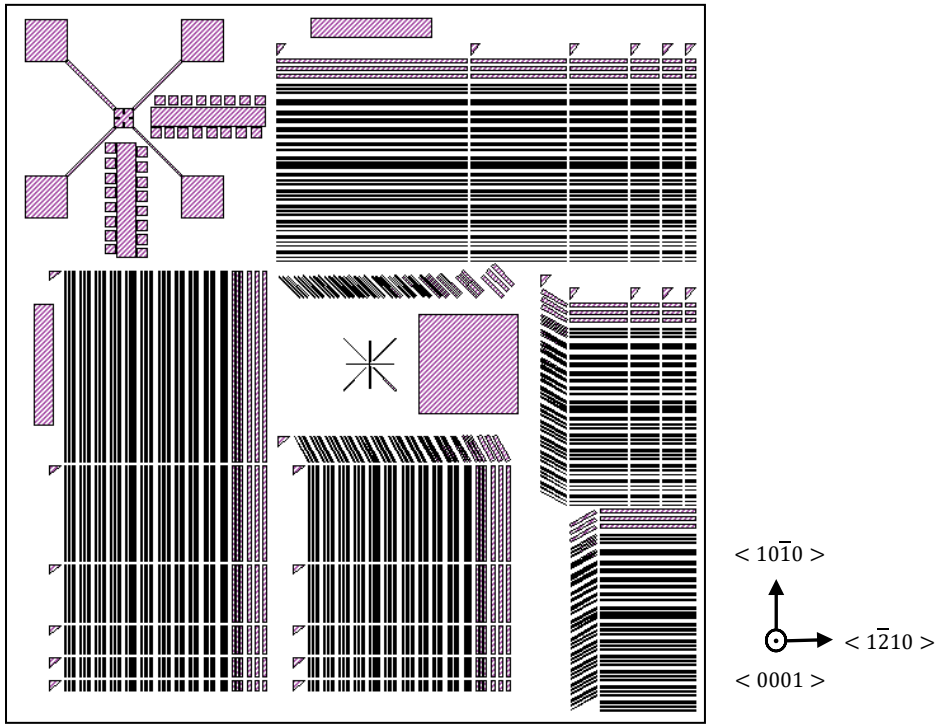

Figure 3.3. Mask Layout of the etching pattern. The designed striped patterns are ranging from 0.5 to 20.0 μm, which arrayed along the $<1\bar{2}10>$ and $<10\bar{1}0>$ directions.

3.4 Metal hard mask: Ni/Cr based hard mask is used for GaN RIE etching. 80 nm Ni is evaporated on GaN wafers using CVC SC4500 Thermal Evaporation System at a working pressure of $1.4x10^{-6}$ Torr. 50 nm Cr is a buffer layer to increase the adhesion between Ni hard mask and GaN substrate. The metals are covered the whole area of the wafer, including on the top of the photoresist and the parts of the wafer that were cleaned of the photoresist in the previous developing step. After evaporation, the photoresist is stripped by MICROPOSIT Remover 1165, thus Ni/Cr film remained only in the region where it had a direct contact with the p-GaN. After lift-off, the descum is performed to remove the photoresist residue. (O_2=42 sccm, 20 mTorr; RIE=500w, 2 mins)

3.5 Dry etching: An extensive chamber cleaning (seasoning) is carried out before the etching process in order to exclude any influence on the final pattern from possible chamber contamination. The first etching with an etch rate of 80 nm/min is performed using Cl_2/BCl_3/Ar combination plasma at a flow rate of 20/10/10 sccm, vapor pressure of 6 mtorr, and RIE/ICP power of 22/250 W using Plasma-Therm770 ICP-RIE system. Figure 3.4 shows the schematic of ICP system. Two independent RF sources are used to generate a high-density plasma (ICP) and direct the reactive ions to the GaN wafers (RIE). For generation of high density inductively coupled plasma (ion density generally $>10^{11}$ cm^3), radio frequency (RF) power is applied to a coil outside an insulating tube. RIE bias power is applied to the wafer electrode to provide independent control of the ion energy at the substrate. The helium backside cooling is applied to allow for good thermal conductance between the electrode and the wafer.[2,3] The etch depth is maintained to be about 750 nm, etched down to n-GaN. The second etching with an etch rate of 5 nm/min is performed using BCl_3 plasma at a flow rate of 30 sccm, vapor pressure of 4 mtorr, and RIE/ICP power of 6/300 W to smooth the etched surface sidewall. The etching total depth was maintained at about 800 nm (measured by profilometer).

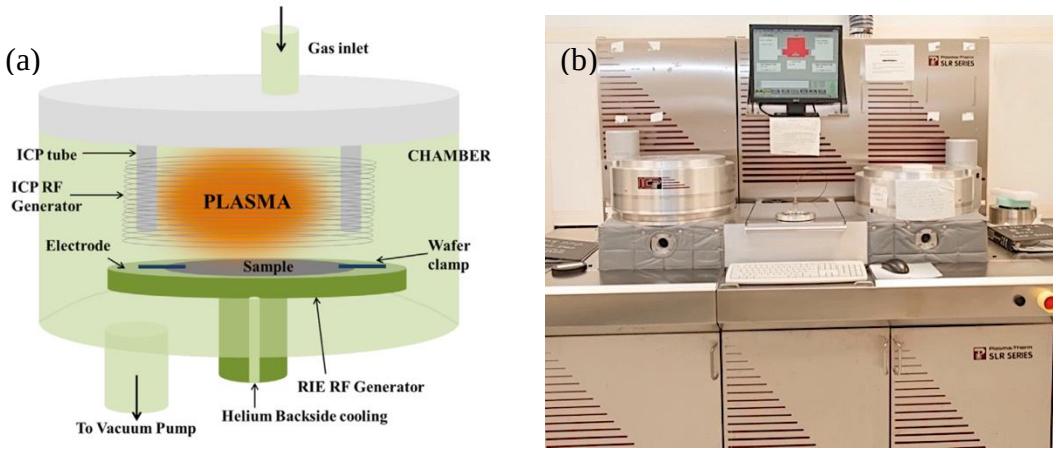

Figure 3.4 (a) Schematic ICP system and (b) photos of dual chamber ICP system in CNF at Cornell.[2] Two independent RF sources are used to generate a high-density plasma and direct the reactive ions to the GaN wafers.

3.6 Tetramethylammonium hydroxide (TMAH) wet etching: After the pattern is transferred onto the substrate, the GaN is then dipped in 25% Tetramethylammonium hydroxide (TMAH) at 85 °C with constant 200 RPM magnetic stirring in order to form smooth and vertical sidewalls, as shown in Figure 3.5.

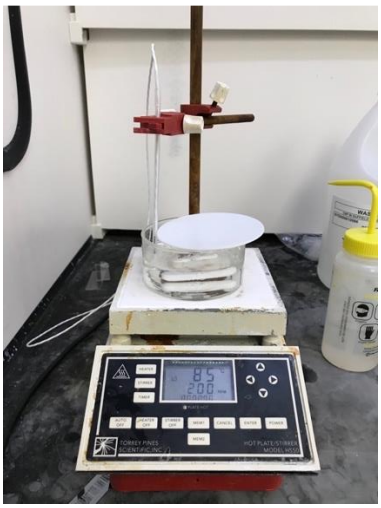

Figure 3.5. Setup for TMAH wet etching. The beaker is covered by a lid to prevent TMAH from evaporating into its surrounding air.

3.7 UV-assisted TMAH etching: The GaN wafer is immersed in 25% TMAH at 85 °C. A 6 W handheld lamp with the wavelength of 254 nm is used to provide the ultraviolet (UV) illumination during the wet etching. The lamp is directly placed on the top of beaker to illuminate the GaN wafer. The intensity of the UV light during wet etching was 0.52 mW/cm^2. Electron-hole pairs were generated through excitation by optical energy because the illumination energy (4.8 eV) was larger than the band gap of GaN (3.4 eV). The generated holes in the valence band may participate the reaction with the oxidant at the GaN/TMAH interface to speed up the etch rate.[4]

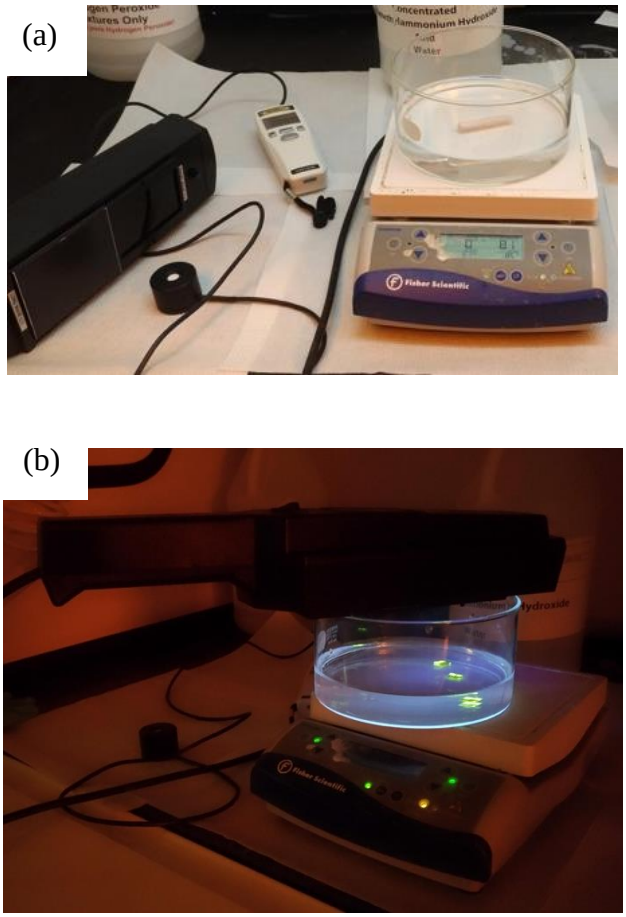

Figure 3.6. (a) Preparation of UV-assisted TMAH etching. The handheld lamp and intensity detector are shown. (b) TMAH etching with UV illumination. The lamp is directly placed on the top of beaker to illuminate the GaN wafer.

3.8 Hydrogen-passivation-assisted wet etching: Before fabrication of etching pattern, thermal annealing is performed on unpattern GaN wafer for hydrogen passivation. Our speculation is that the wet etch rate of p-GaN may increase owing to the hole compensation. Two different annealing tools/conditions are conducted in this work, the annealing furnaces are shown in Figure 3.7: (a) Carbon Nanotube/Graphene Furnace in CNF at Cornell: 100% hydrogen at 800 ˚C for 40 minutes. (b) Commercial MOCVD system (Aixtron 200/4 RF) at Yale: NH_3-N_2 environment at 800 ˚C and the pressure of 200 mbar for 40 minutes. The flow rates of NH_3 and N_2 are 2 and 4 slm, respectively. After wet etching, the GaN wafer is reactivated by N_2-ambient annealing at 750 ˚C to effectively break the Mg-H bond and release hydrogen.[6,7]

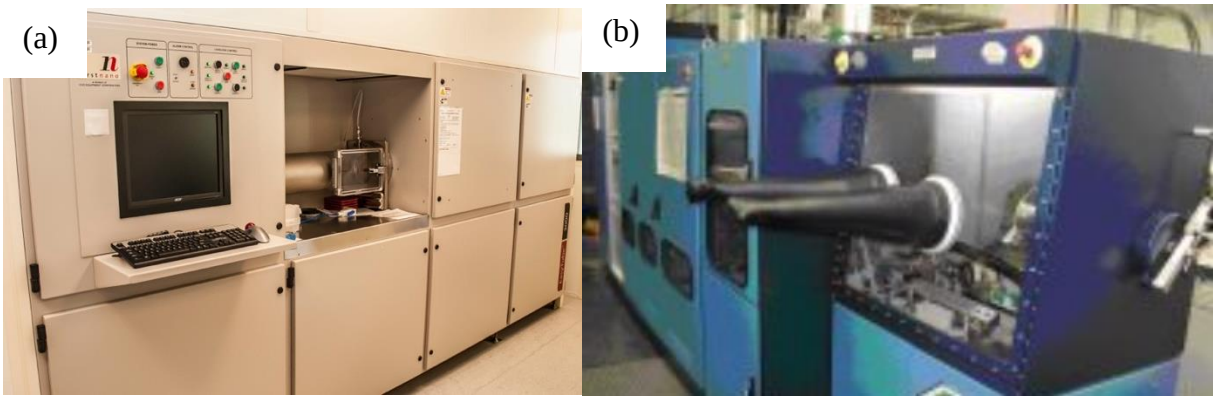

Figure. 3.7 (a) Carbon Nanotube/Graphene furnace in CNF at Cornell, (b) Commercial MOCVD system (Aixtron 200/4 RF) at Yale University.[5]

BIBLIOGRAPHY

[1]Hu, Zongyang, et al. "Near unity ideality factor and Shockley-Read-Hall lifetime in GaN-on-GaN pn diodes with avalanche breakdown." *Applied Physics Letters* 107.24 (2015): 243501.

[2]Ng, Doris Keh-Ting, et al. "Sub-Micron Anisotropic InP-based III–V Semiconductor Material Deep Etching for On-Chip Laser Photonics Devices." *Advanced Engineering Materials* 20.2 (2018): 1700465.

[3]Pearton, S. J., R. J. Shul, and Fan Ren. "A review of dry etching of GaN and related materials." *Materials Research Society Internet Journal of Nitride Semiconductor Research*5.1 (2000).

[4]Minsky, M. S., M. White, and E. L. Hu. "Room-temperature photoenhanced wet etching of GaN." *Applied Physics Letters*68.11 (1996): 1531-1533.

[5]https://www.eng.yale.edu/hanlab/Facilities.html

[6]Nakamura, Shuji, et al. "Hole compensation mechanism of p-type GaN films." *Japanese Journal of Applied Physics* 31.5R (1992): 1258.

[7]Nakamura, Shuji, et al. "Thermal annealing effects on p-type Mg-doped GaN films." *Japanese Journal of Applied Physics*31.2B (1992): L139.

CHAPTER 4

Results and Discussion

4.1 Conventional TMAH etching (Sample ID: JH-GaN on Sapphire-Control01)

4.1.1 Chlorine-based dry etching:

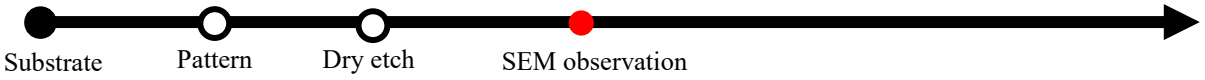

The GaN wafer used in this work consists of top 420 nm p-GaN base layer and underneath 8 μm n-GaN drift layer on sapphire substrate. Ni was served as an etching hard mask due to its lack of oxide erosion effect during the high energy plasma. After mask patterning, the etching experiment was performed on the GaN wafer by ICP-RIE. The anisotropic etching was performed in two steps: (1) Fins were first obtained at the etch rate of about 79 nm/min with an etch chemistry of $BCl_3/Cl_2/Ar$. (2) A second etch step with Bl_3 plasma was introduced at the etch rate of about 5 nm/min to smooth the sidewall. The etched depth of fins was controlled to be 780 nm, measured by ellipsometer. Several typical results were found in plasma etching such as uneven etched surfaces and sidewall damages.[1] The etching of GaN samples with Ni hard mask resulted in uneven etching. This may due to the sputtering and redeposition of the nickel during high energy plasma. The considerable amount of metal residue, acted as micro-mask, caused the formation of pillars on the GaN surface, as shown in Figure 4.1 (a). Besides, the high energy plasma led to the ion bombardments on etched surface, resulting in damages on sidewalls, as shown in Figure 4.1 (b). Thus, even though the anisotropic dry etching process was capable to form a deep fin structure, the dry etched profile such as slanted rough sidewalls and pillars on the GaN surface was not desired for a gate channel of trench GaN MOSFETs. Therefore, post-treatment by wet etching was then considered to reduce the surface roughness, remove the damages, and form vertical sidewalls for a gate channel.

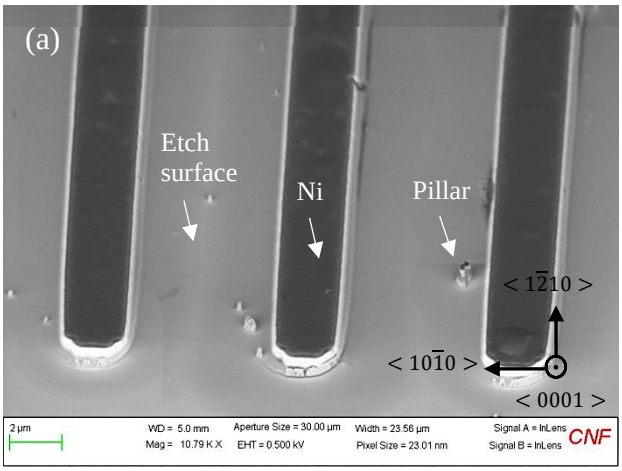

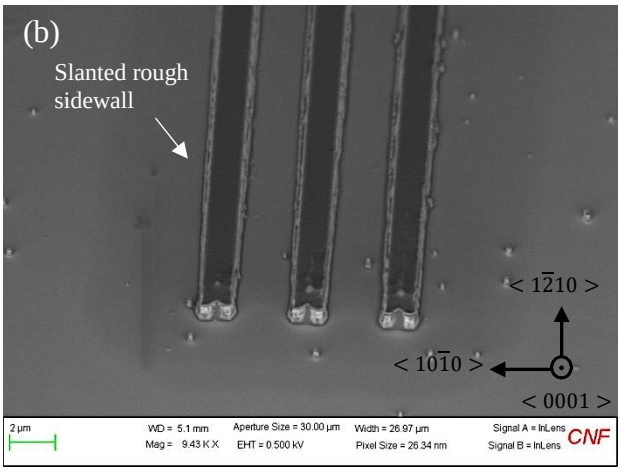

Figure 4.1. Sample ID: JH-GaN on Sapphire-Control01. Scanning electron microscope (SEM) images of the Mg-activated dry-etched fins along <1$\bar{2}$10> direction after Cl_2-based dry etching. Slanted rough sidewalls and uneven etched surface due to ion bombardments and redeposition of nickel under high energy plasma. Widths of fins were (a) 2 µm and (b) 1.6 µm.

4.1.2 TMAH chemical wet etching (30 minutes):

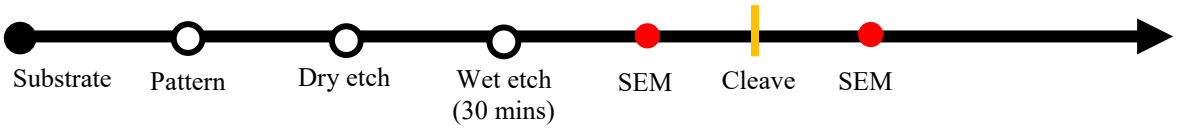

TMAH wet etching has been reported to be a suitable post-treatment to remove the damages and form a non-polar plane sidewall on UID and n-GaN after dry etch process.[2-8] Therefore, TMAH etching was performed to remove the pillars and smooth the fins in this work. Figure 4.2 shows the SEM images of the Mg-activated dry-etched-then-wet-etched fins after etching in hot TMAH at 85 ^{o}C for 30 mins. In our wet etching results, the pillars formed in plasma etching were totally removed by TMAH treatment due to the oxidation of the GaN pillars and subsequent dissolution, as shown in Figure 4.2 (a). In addition, strong anisotropic etching profile was found. After wet etching for 30 minutes, sidewalls of the fins along <10$\bar{1}$0> direction were hierarchical nano-prism structures formed by adjacent m-planes due to the surface bonding configuration, as shown in Figure 4.2 (d). It is well known that the hydroxide ions (OH^-) based etching are quite sensitive to the electrical polarity of the GaN surface.[9-13] For a-plane surface, Ga back bonds were more stable and the repelling forces between OH^- ions and N dangling bonds were larger than that of m-plane surface. Therefore, a smaller number of OH^- ions can react with the Ga back bonds as well as Ga dangling bonds in the a-plane. As a result, the m-plane sidewall was exposed and can be observed in SEM images. Besides, for the fins along <1$\bar{2}$10> direction, staircase-shaped m-plane sidewalls and semi-polar planes at the base of the fins can be observed after wet etching, as shown in Figure 4.2 (b) and (c). The GaN crystallographic m-plane and semi-polar surfaces were formed due to the lower repulsion forces on the little negatively charged surfaces can make the OH^- easily access the GaN to perform etching. In contrast, for the c-plane etched surface, the etch depth was remained the same before and after wet etch because the strong repelling force by electrically negative

charge. Even though crystallographic etching occurred on fin sidewalls and successfully removed the pillars on GaN surface, some damages were found on the sidewalls of the fin along <11$\bar{2}$0> direction. In addition, the sidewalls were not vertical but slanted, measured to be about 100^{o}, as shown in Figure 4.2 (c). An ideal non-polar plane was not formed by the TMAH wet etching for 30 minutes. Therefore, a longer wet etching time was then considered.

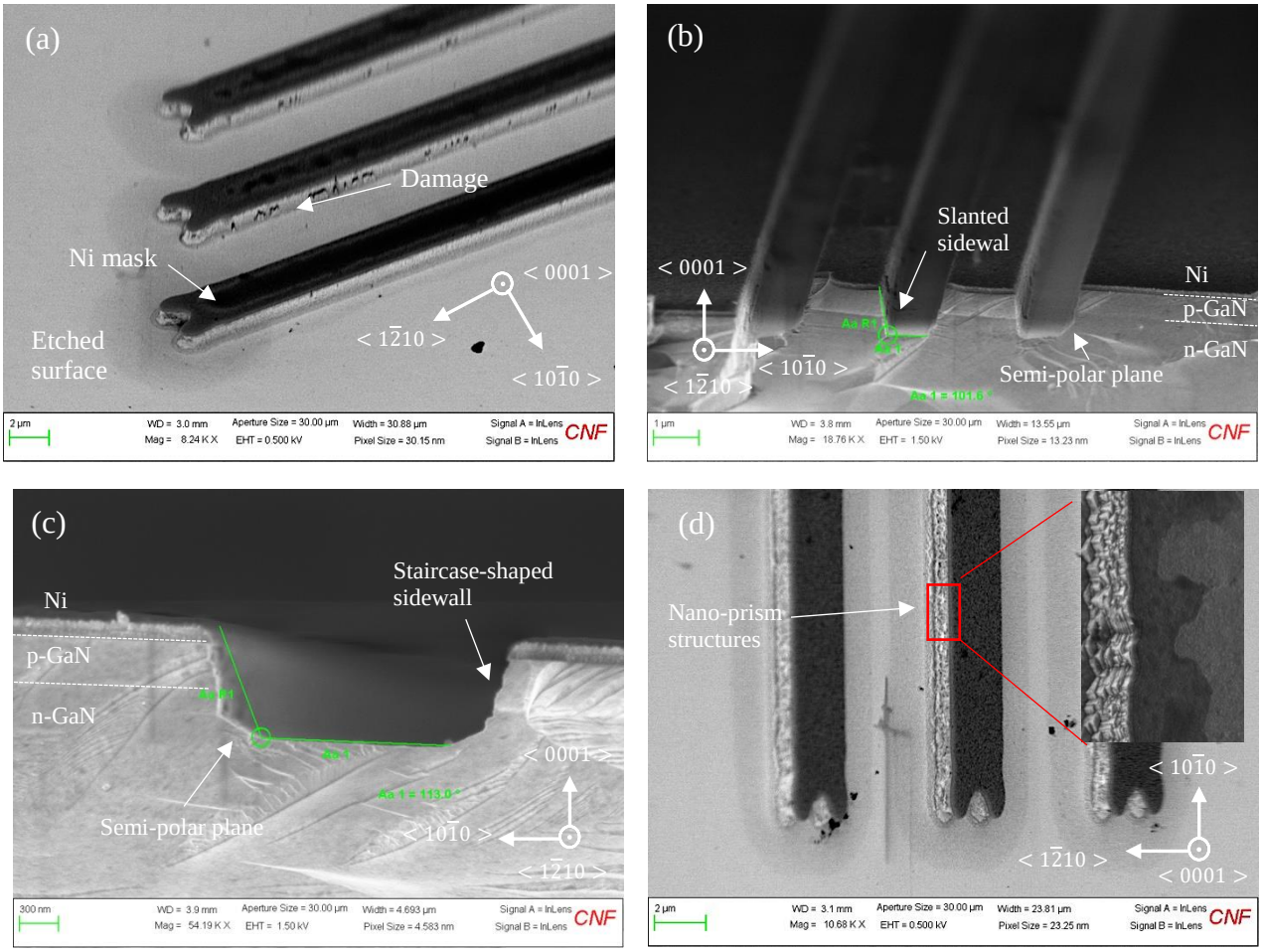

Figure 4.2. Sample ID: JH-GaN on Sapphire-Control01. SEM images of the Mg-activated dry-etched-then-wet-etched fins with p-n structure after etching in hot TMAH at 85 ^{o}C for 30 mins. (a), (b), and (c): The fins along <1$\bar{2}$10> direction. Pillars were removed after TMAH treatment. Besides, staircase-shaped m-plane sidewalls and semi-polar planes were formed. (d): The fins along <10$\bar{1}$0> direction with the formation nano-prism structures due to the surface bonding configuration.

TMAH chemical wet etching (cleave then etch):

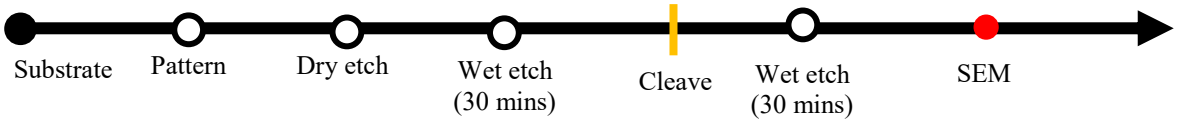

Based on the previously result, we found that the crystallographic etching has occurred on GaN in TMAH solution. However, the sidewall of the fins along <1$\bar{2}$10> was still slanted and has some damages induced by dry etch, which is not ideal for the gate channel. Therefore, the wet etching was performed at 85 °C with 25% TMAH on the same GaN wafer again for 30 minutes. Figure 4.3 (a) and (b) show the cross-sectional SEM images of the cleaved-then-TMAH-etched fins along <1$\bar{2}$10> direction. The m-plane facets can be observed on the cleavage plane. In addition, the m-plane sidewalls were formed after TMAH wet etching near the fin edges. The sidewall was entirely vertical in the region of p-GaN. However, they were not vertical toward to the bottom of sidewalls, which was clearly revealed in the cross-sectional SEM images. Unetched n-GaN at the base of the fins with semi-polar plane was observed.

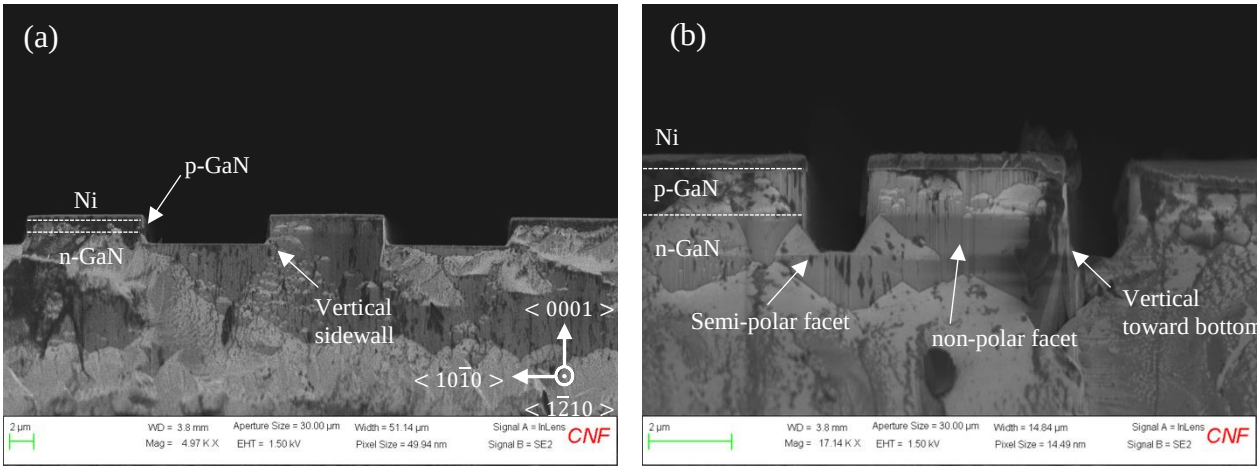

Figure 4.3. Sample ID: JH-GaN on Sapphire-Control01. Cross-sectional SEM images of the cleaved-then-TMAH-etched fins along <1$\bar{2}$10> direction after etching in hot TMAH at 85 ºC for 30 mins. (a) Vertical sidewalls achieved. (b) Semi-polar and non-polar facet exposed on the surface. M-plane sidewalls were formed near the fin edges but not toward to the bottom of sidewalls.

TMAH chemical wet etching (etch then cleave):

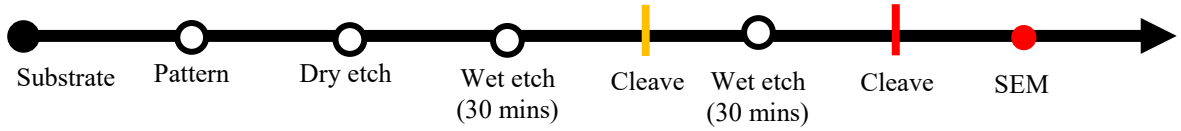

After total of 1 hr TMAH etching, we have already proved that TMAH can etch p-GaN to form vertical sidewalls near the fin edge. However, this result doesn't mean the entire p-GaN sidewalls of the fins were vertical. Therefore, a second cleave was performed to observe sidewall profile of the interior fins. Figure 4.4 shows the fin pattern on the GaN wafer and the cleavage plane. The sidewalls of the interior fins, tens of micrometer away from the fin edge, were observed by SEM.

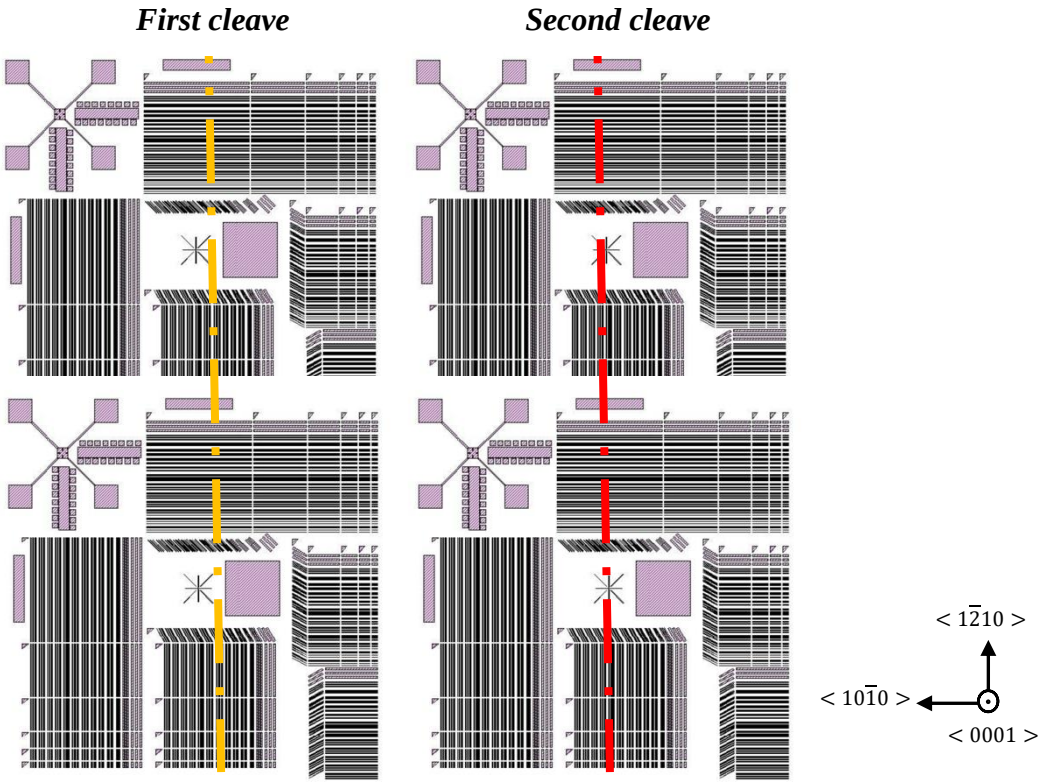

Figure 4.4. (Top view) Schematic of fin pattern and cleavage plane. The designed striped patterns are ranging from 0.5 to 20.0 μm, which arrayed along the <1$\bar{2}$10> and <10$\bar{1}$0> directions.

Instead of staircase-shaped or vertical sidewalls, a slanted sidewall with three-stage slope was found at the interior Mg-activated dry/wet etched-then-cleaved fins along <1$\bar{2}$10> direction after etching in hot TMAH at 85 ºC for 1 hr , as shown in Figure 4.5 (a) and (b). The results indicate that the wet etching has a higher etch rate at the fin edge compared to the interior position.

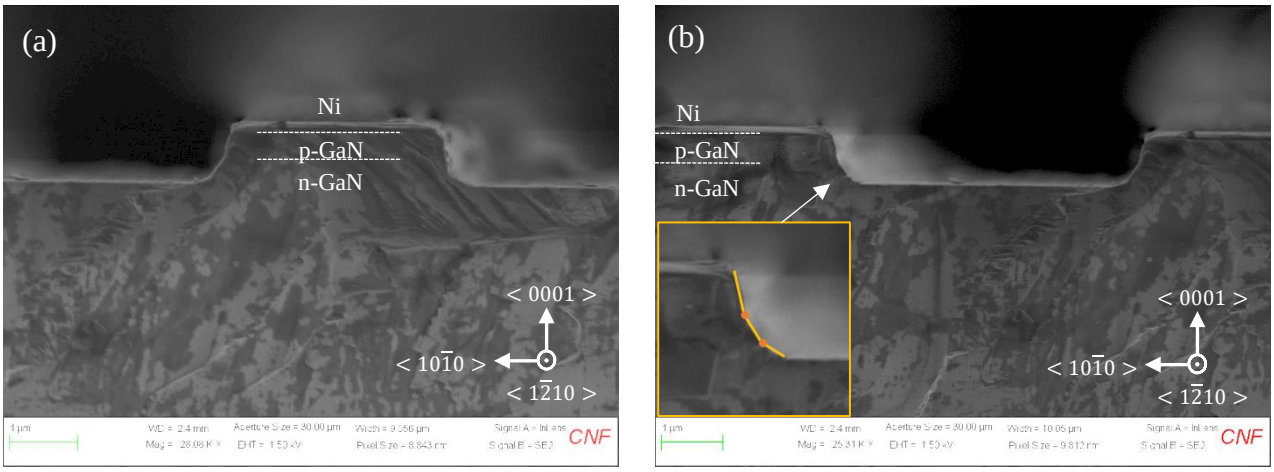

Figure 4.5. Sample ID: JH-GaN on Sapphire-Control01. SEM images of the Mg-activated dry/wet etched-then-cleaved fins along <1$\bar{2}$10> direction after etching in hot TMAH at 85 ºC for 1 hr. A slanted sidewall with three-stage slope were formed at the interior fin.

TMAH chemical wet etching (cleave then etch):

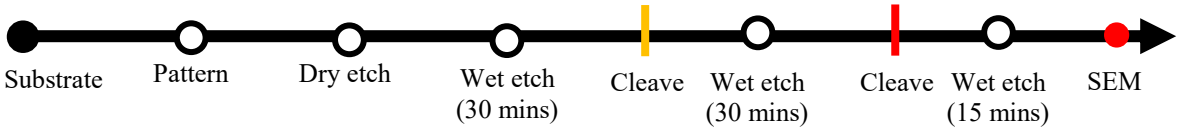

To further demonstrate high-etch rate of p-GaN sidewall near the fin edge, the wet etching was again performed again at 85 °C with 25% TMAH on the same GaN wafer. As a result, the vertical p-GaN sidewalls were formed near the fin edge and aligned with m-plane after etching in hot TMAH at 85 ^{o}C for simply 15 minutes, as shown in Figure 4.6 (a) and (b). The non-dry-etched GaN exposed by cleaving was found at the base of the fins with semi-polar planes exposed as a result of the wet etch. Besides, the hexagonal prism-like features can be observed on the cleavage plane. These angles are all 120°, indicating that these Zig-zag features are formed by the two adjacent m-planes.

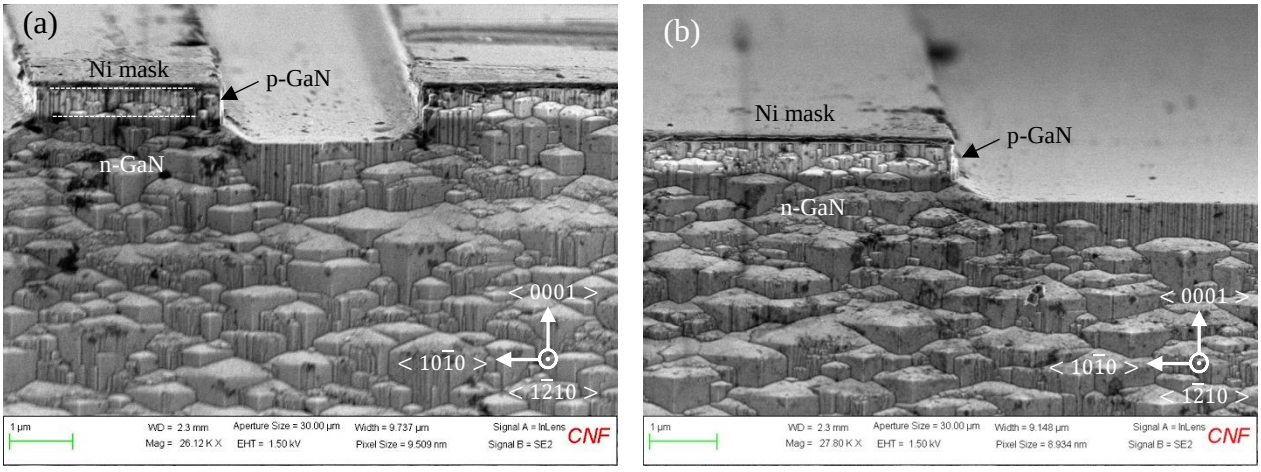

Figure 4.6. Sample ID: JH-GaN on Sapphire-Control01. SEM images of the Mg-activated cleaved-then-wet-etched fins along <11$\bar{2}$0> direction after etching in hot TMAH at 85 ^{o}C for 15 mins. Vertical sidewall of p-Gan was formed near the fin edge by TMAH etching for 15 mins. Hexagonal prism-like features were exposed on the cleavage plane after wet etching.

4.1.3 Diffusion-limited mechanism: The etched sidewalls have different profiles at near the fin edge and interior position, indicating the etch process started from the fin edge but difficult to proceed to interior sidewalls. Here, a diffusion-limited mechanism of TMAH etching was proposed.[14-17] During the wet etching process, the etchant was constantly moving across the area of GaN to be etched, and there was a field of velocity (gradient) at every point of the materials. In fluid dynamics, the entrance length is the distance a flow travels after entering a pipe before the flow profile becomes fully developed. In our case, TMAH entered the confined region between two sidewalls/fins also experienced from hydrodynamic entrance region with uniform velocity to fully developed region due to the confining of fin sidewalls. When TMAH entered the region between two fins, TMAH was easy to reach the sidewalls of the fins due to the thin boundary layer, therefore, the hydroxide ions can react with Ga-dangling bonds to form a Ga-OH complex by electrostatic attraction. In contrast, the velocity at the surface of interior sidewalls is near zero owing to the thick boundary layer. It was thus relatively difficult for the etchant to approach the sidewall to react with Ga and it is also hard for the gallium oxide dissolved in the solution to diffuse out from the thick boundary layer. Therefore, the interior sidewalls between the fins were much harder to be wet etched compared to the location near the fin edge.

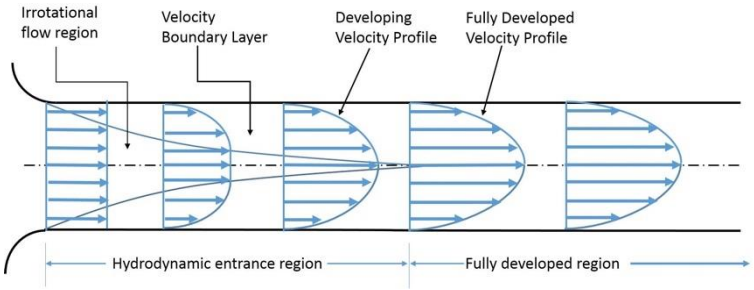

Figure 4.7. (Top view) The developing velocity profile of a TMAH fluid entering fins during the wet etching process, experiencing from hydrodynamic entrance region to full developed region between the fins. Interior sidewalls between the fins were difficult to be wet etched due boundary layer increases as the distance from fin edge increases.[15]

4.1.4 Description of etch sequence: The above-discussed results indicate that the vertical m-plane sidewalls were chemically stable, while the inclined sidewalls could be etched away by TMAH solution. The experimental observations are largely in agreement with the results from nanowire fabrication in hydroxide solutions published by Chen et al, as shown in Figure 4.8 (a-d).[2] Sandia National Lab also reported that the wet etching tends to occur faster at convex point compared to that of concave point, as shown in Figure 4.8 (e).[34] Based on my own observations, a proposed chemical etching process of a slanted sidewall toward a vertical sidewall in TMAH solution is illustrated in Figure 4.9. First of all, the staircase-shaped sidewall was formed after 30 mins of TMAH etching. Then the three-stage slope was formed after 1 hr of TMAH etching on the interior sidewalls. Compare to m-plane facets, it is easy for hydroxide ions to react with GaN on the inclined surfaces because N-atom on the (1101) N-polar facet only has a single electronegative dangling bond. Therefore, OH ions can react with GaN continually and form gallium oxide for the dissolution. In contrast, the vertical m-plane facets are chemically stable.[9-13] Another mechanism is needed to explain the chemical stability of the non-polar sidewalls. It is known that the chemical stability of the GaN crystal plane is related to its surface energy, which is a function of the dangling bonds density. The m-plane facets are more chemically stable in compared with the semi-polar facets due to the dangling bands density of (1100) facets (12.1 per nm^2) is smaller than that of (1101) facets (16.0 per nm^2).[2] Thus, the m-plane sidewalls would not be etched away in TMAH solution. With increasing wet-etching duration in TMAH solution, the semi-polar facets of the GaN were removed gradually accompanied with the exposure of the m-plane facets. However, the smooth vertical sidewall only formed near the fin edge due to the diffusion-limited etching mechanism.

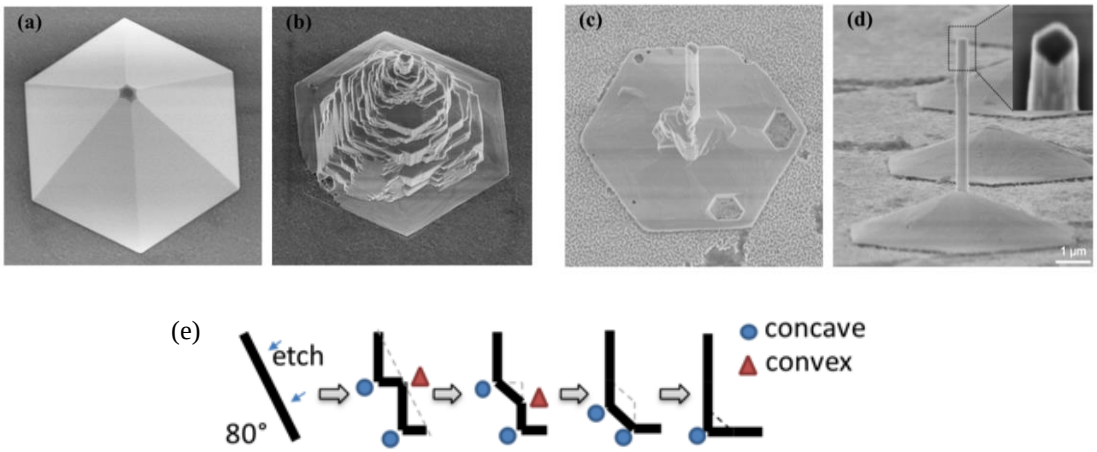

Figure 4.8. SEM images of GaN micro truncated-pyramids immerged into KOH solution for (a) 0 min, (b) 10 min, (c) 30 min and (d) 40 min, respectively (reported by Chen et al.).[2] (e) shows the schematic of etch process (reported by Sandia National Lab). High etch rate at convex point.[34]

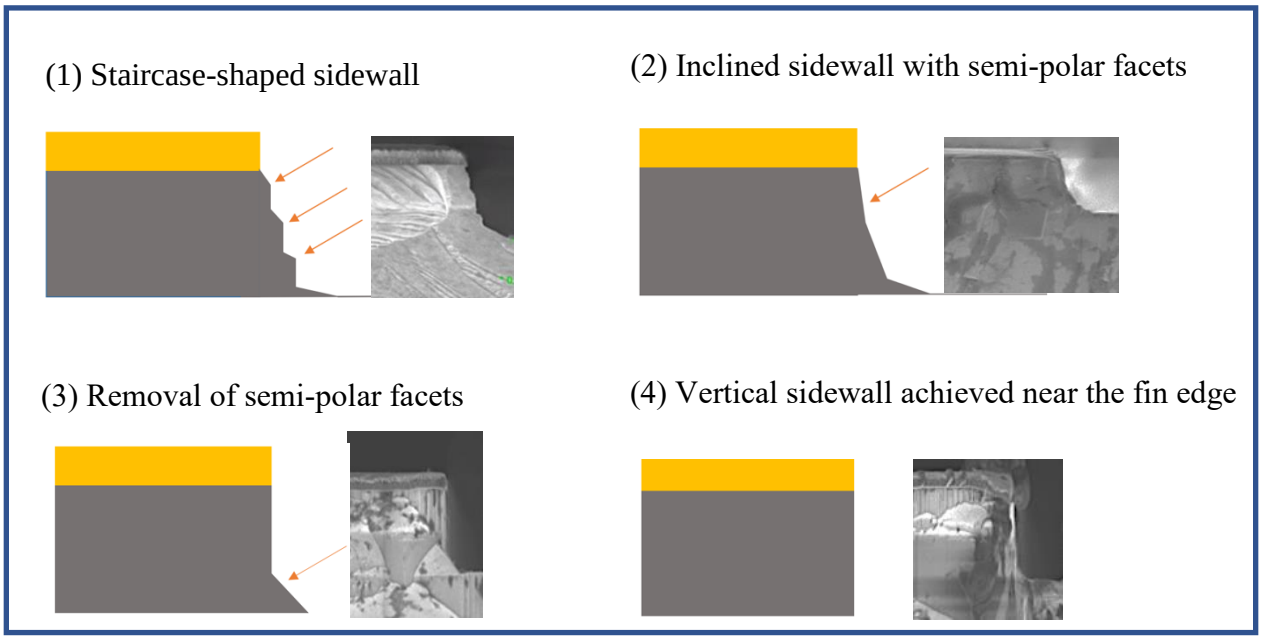

Figure 4.9. Schematic and cross-sectional SEM images illustrating the etch sequence of a slanted sidewall toward a vertical sidewall in TMAH. (1) Staircase-shaped sidewall first appeared after TMAH etching for 30 mins. (2) Slanted sidewall with semi-polar facets then formed with increased etching time of 60 mins. (3) and (4) vertical sidewalls were achieved near the fin edge. The semi-polar facets of the GaN were removed gradually accompanied with the exposure of the m-plane facets.

4.2 UV-assisted TMAH etching

Motivation: The vertical sidewall was only achieved near the fin edge by conventional TMAH etching. Photo-enhanced wet etching was thus considered to increase the etch rate of GaN. To wet etch GaN, the first step is to oxidize the materials. Oxidation of the semiconductor is due to reaction between holes in the valence band and oxidants in the chemicals. Here, the idea is to generate electron-hole pairs through excitation by UV energy.[18-23] The photogenerated holes can assist in the oxidation of Ga and subsequently dissolve in TMAH solution. Figure 4.10 shows the mechanisms of UV-assisted TMAH etching of n-GaN. For n-GaN, the photogenerated holes are accumulated at the GaN/TMAH interface due to the potential gradient in the depleted layer. Then holes (essentially broken bond) at the GaN surface react with the oxidant in an atomic proximity to release Ga into the solution resulting in etching. On the other hand, for p-GaN, the photogenerated holes are swept into bulk materials. However, generated holes may participate the etching process before being swept into the GaN. In this work, UV lamp and etching time were our two variables. Three samples have been prepared: (1) JH-GaN on Sapphire-UV01 (2) JH-GaN on Sapphire-UV02, (3) JH-GaN on Sapphire-Control02.

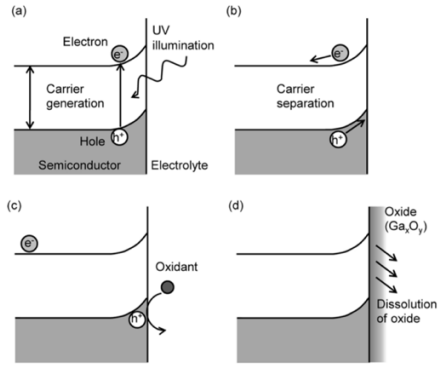

Figure 4.10. Process of UV-assisted TMAH etching: (a) Electron-hole pairs are generated by UV energy. (b) Carriers are separated along the potential gradient in the depleted layer. (c) Holes react with the oxidant at the semiconductor/chemicals interface. (d) An oxide film is formed on the semiconductor surface, and the surface is etched if this oxide is soluble in the chemicals.[22]

4.2.1 UV-assisted TMAH etching for 30 mins

Etching results on JH-GaN on Sapphire-UV01:

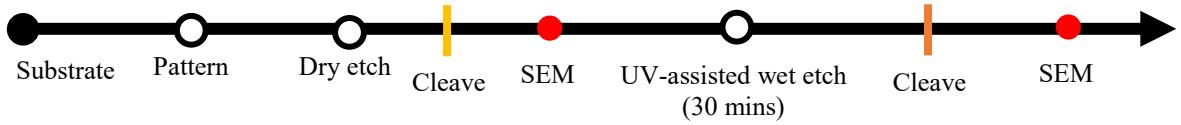

Figure 4.11 (a) and (b) show the SEM images of the Mg-activated fins along <1$\bar{2}$10> direction after dry etch. During the dry etching process, the high energy plasma eroded the Ni mask owing to the sputtering. The taper in the masking layer was then transferred to the pattern, leading to slanted sidewalls. Fig. 4.11 (c) and (d) show the SEM images of the fins along <1$\bar{2}$10> direction after UV-assisted wet etching for 30 minutes. The GaN sidewalls were found to be slanted and the sidewall angles were similar to the one with treatment of conventional TMAH etching. The possible reason was that the power density was only 0.35 mW/cm^2, which was not generated sufficient holes for the assistance of wet etching on p-GaN. Assuming 100% absorption and each absorbed photon generates one electron-hole pair (EHP). Number of EHP generated per second per area equal to number of incident photons per second per area= P/hv = (0.35x10^{-3}) Wcm^{-2}/ (7.82x10^{-19}) J= 4.5x10^{14} s^{-1} cm^{-2}. The absorption coefficient (α) at the illumination wavelength (4.88 eV)= 39360 cm^{-1}. According to the Lambert-Beer law, it means ~(1-1/e) amount of photons are absorbed in a depth of GaN: 1/α = 1/39360 cm = 254 nm. Assuming all generated electron-hole pairs are uniformly distributed within this slab of GaN near the surface, we can calculate the volume density per second to be 4.5x10^{14} s^{-1} cm^{-2}/254 nm ~10^{19} cm^{-3}/s. Whenever carriers are generated $np > n_0p_0$, they will recombine. Assuming a carrier lifetime of 1 nanosecond, we can calculate the steady state volume density of carriers under optical illumination. 10^{19} cm^{-3}/s*10^{-9}s = 10^{10} cm^{-3}, which is low and barely bend the GaN energy bands at all near the surface. As a result, photogenerated holes were swept away from the depletion region near the surface into the bulk,

thus, photo-assisted etching is not effectively working on p-GaN due to lack of the holes. The accumulation of electrons near the surface could strengthen the Ga-O bonding of surface Ga oxides and results in chemical resistance to the etching solutions.[18-23] However, instead of staircase-shaped sidewalls formed by conventional TMAH etching, the smooth sidewalls with two-step slope were formed by UV-assisted wet etching, as shown in Figure 4.12 (a) and (b). In addition, there was no unetched GaN at the base of the fins. This was possible due to the photogenerated holes were accumulated in the interface of n-GaN and TMAH, which assisted the etching of n-GaN.

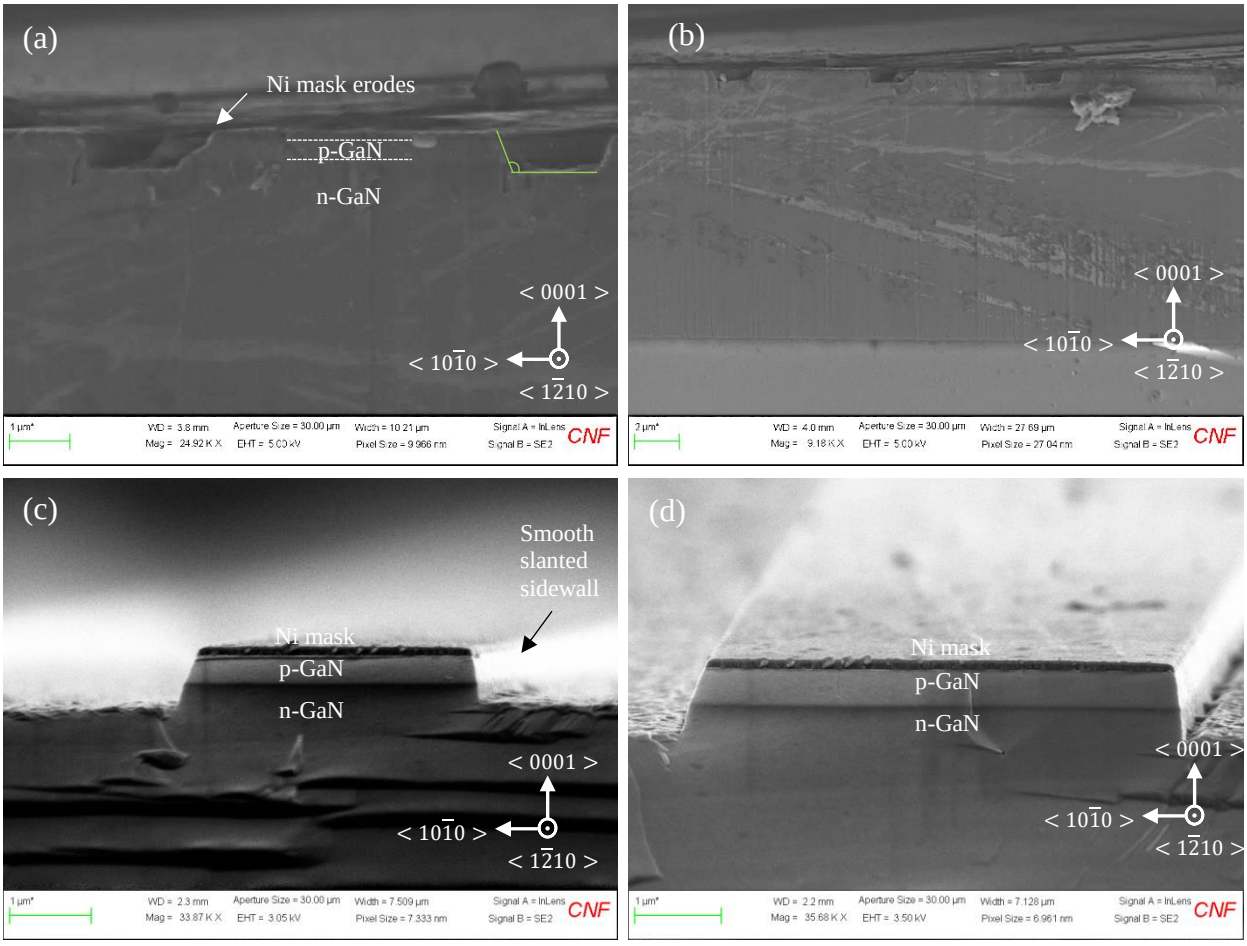

Figure 4.11. Sample ID: JH-GaN on Sapphire-UV01. SEM images of the Mg-activated fins along <1$\bar{2}$10> direction. (a) and (b): rough slanted sidewalls after dry etch. (c) and (d): after UV-assisted

wet etching for 30 mins. Smooth semi-polar sidewalls without staircases was formed by UV-assisted wet etching.

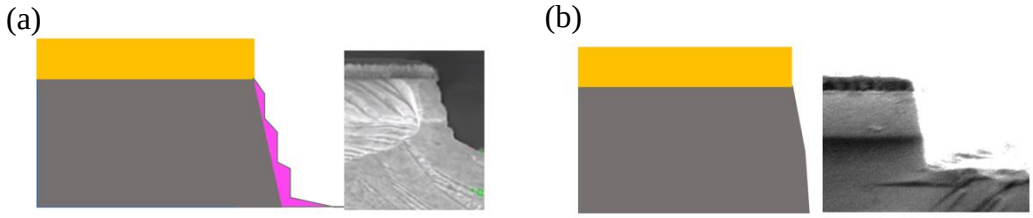

Figure 4.12. Schematic of sidewalls of the fins along <11$\bar{2}$0> direction after etching in hot TMAH at 85 ^{o}C for 30 mins. (a) Staircase-shaped sidewall after conventional wet etching and (b) smooth sidewalls with two-step slope sidewall after UV-assisted wet etching for 30 mins.

4.2.2 UV-assisted TMAH etching for 1 hr

Etching results on JH-GaN on Sapphire-UV02 and JH-GaN on Sapphire-Control02:

JH-GaN on Sapphire-UV02

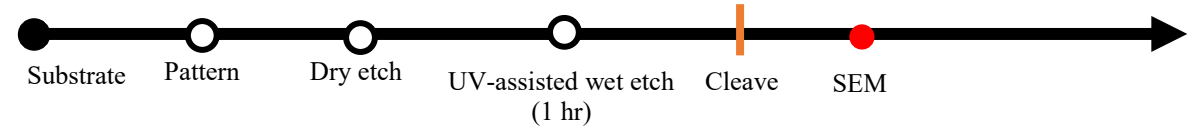

JH-GaN on Sapphire-Control02

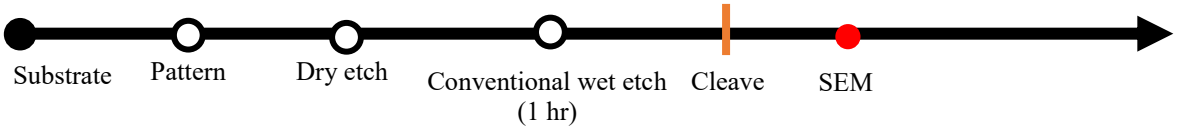

To make a fair comparison between conventional etching and UV-assisted wet etching, two samples were fabricated from the same batch under same cleaning process and dry etch environment. The only variation was whether applying UV-source during TMAH etching for 1 hr. Figure 4.13 (d) shows the SEM image of fin sidewalls along <1$\bar{2}$10> direction after conventional TMAH etching. Similar to the previous results, staircase-shaped sidewalls were formed after conventional TMAH etching. On the other hand, semi-polar planes sidewalls were exposed and smoothed after UV-assisted TMAH etching, as shown in Figure 4.13 (a), (b), and (c). These

etching results indicate UV light enhance the etch rate of GaN to a certain degree but not sufficient to form a vertical sidewall in the interior fin with 1 hr wet etching.

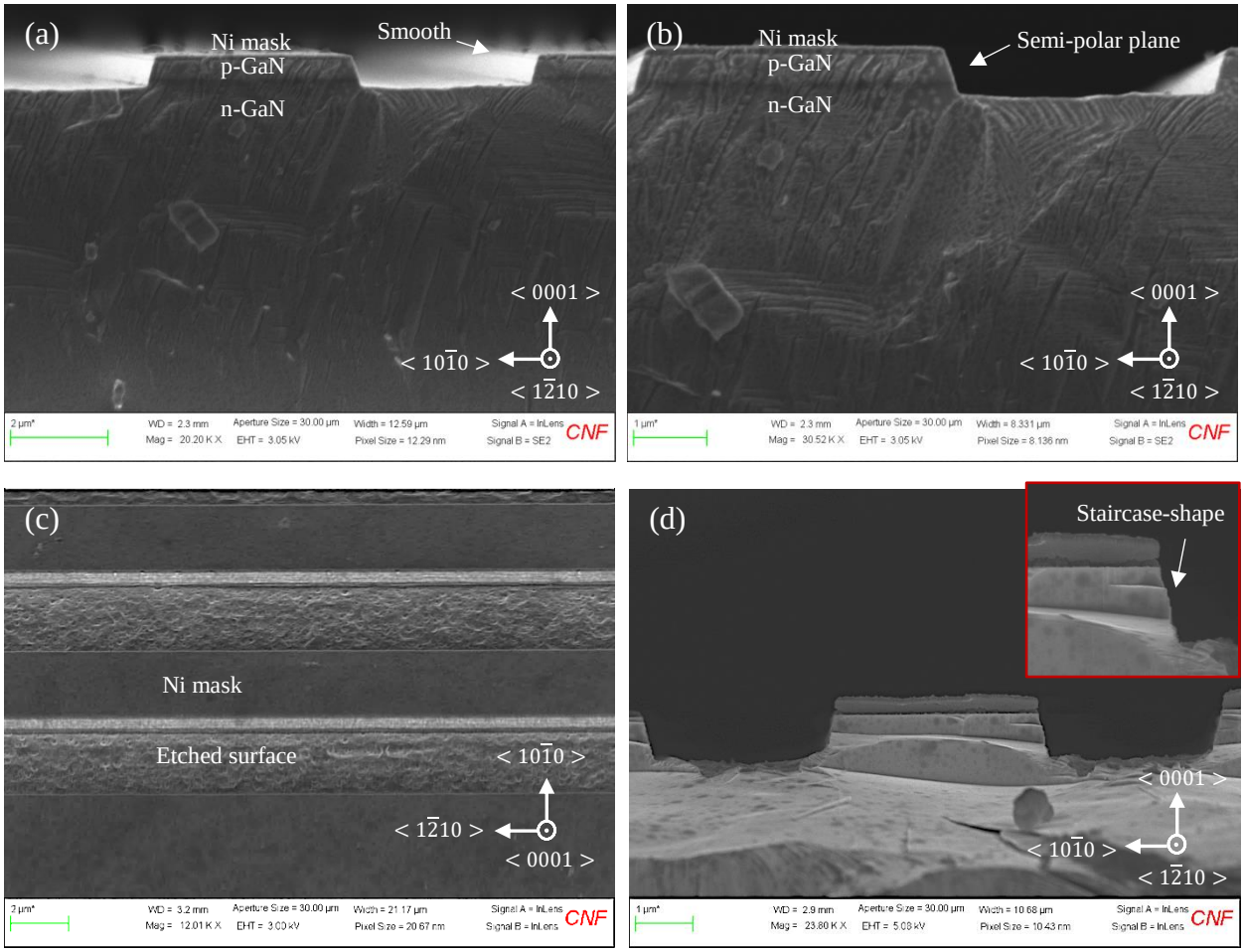

Figure 4.13. SEM images of the Mg-activated dry-etched-then-wet-etched fins along <11$\bar{2}$0> direction after etching in hot TMAH at 85 ^{o}C for 1 hr. (a), (b), and (c): Sample ID: JH-GaN on Sapphire-UV02. Smooth semi-polar planes sidewalls were exposed after UV-assisted TMAH etching (d) Sample ID: JH-GaN on Sapphire-C02. Without applying UV source after an hour TMAH etching. Staircase-shaped sidewalls were formed after conventional TMAH etching, while smooth semi-polar planes sidewalls were exposed after UV-assisted TMAH etching.

Formation of hexagonal GaN cavity: Figure 4.14 (a) and (b) show the SEM images of the fins along <10$\bar{1}$0> direction after dry etch and hot TMAH etch, respectively. Different from the "*JH-GaN on Sapphire-Control01"* sample with even dry-etched surface, the etched surface of "*JH-GaN on Sapphire-Control02"* sample was non-uniform and extremely rough. A slower etch rate was found in the latter etch process. This phenomenon was possible because the etched surface was contaminated by photoresist residue before dry etch. Since the photoresist covered the GaN surface, reactive ions were thus required to stripped it off in order to reach the GaN target surface. Therefore, a non-uniform distribution of photoresist resulted in uneven surface after dry etch. After TMAH etching, prism-like structures were formed on the sidewall of the fins along <10$\bar{1}$0> direction. Besides, the formation of hexagonal GaN cavity (hexagonal-shaped holes) with smooth vertical sidewalls was found. The wet etching of c-plane surface was initialized by the defective dry-etched surface. Although Ga-face GaN is inert to the OH^-, it is well known that etching prefer to start with the weak point in materials such as dislocation pit. Therefore, hexagonal-shaped holes were formed due to the hexagonal crystal structure of wurtzite GaN. The facets that were revealed by the etch were the m-planes of GaN.

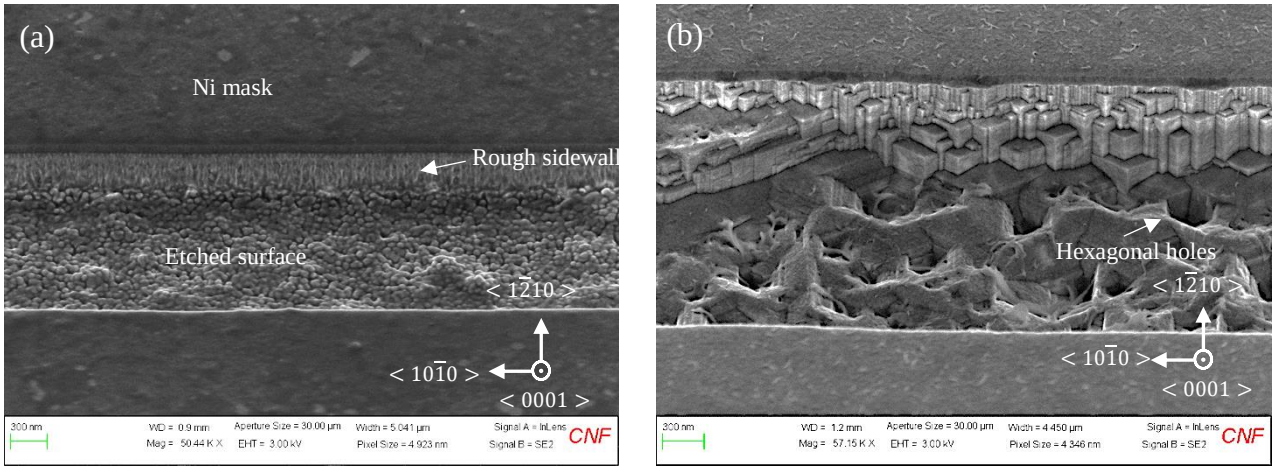

Figure 4.14. Sample ID: JH-GaN on Sapphire-Control02. SEM images of the fins along <10$\bar{1}$0> direction after etching in hot TMAH at 85 ^oC for 1 hr. (a) Rough sidewalls after dry etching due

to non-uniform distribution of photoresist cover the surface before dry etching; (b) Formation of hexagonal holes after TMAH etch initialize by defective dry-etched surface.

4.3 H-passivation-assisted TMAH etching (H-annealing)

Motivation: To date, several groups have reported that TMAH can smooth the n-GaN or UID GaN etched surface to align with m-plane, while negligible etching occurs on p-GaN.[2-8] Thermal annealing in hydrogen environment was considered to increase the etch rate of p-GaN, mitigating the dopant selectivity. In this work, hydrogen atoms were used to purposely passivate the Mg-acceptors by H-annealing at 800 $^{\circ}$C for 40 minutes. In the H-annealing process, dissociated hydrogen atoms are adsorbed at the surface of GaN films because dangling bonds exist mainly at the surface. Then the small hydrogen atoms can diffuse into the GaN film. It has been shown that the hydrogen atom is able to passivate the electrical activity of the material when diffused into p-GaN due to the formation of Mg-H complexes.[24-25] Our speculation is that the etch rate of H-passivated p-GaN could have a comparable etch rate to n-GaN because the hole compensation could bring the fermi levels of p-GaN toward the position close to the mid-gap of GaN and the surface band bending might be the smallest, i.e. a charge neutral condition where the band bending at surface is zero. Since we not only need to demonstrate the fast etch rate of H-passivated GaN but also have to re-activate Mg after etching process for the device operation. Here, we compared two samples: “JH-GaN on sapphire-H01” and “JH-GaN on sapphire-H02”. They were both H-passivated GaN wafer. The only variation of the two samples was that the nitrogen annealing was performed on “JH-GaN on sapphire-H02” for the Mg activation before pattering.

4.3.1 H-passivation-assisted TMAH etching for 1 hr

JH-GaN on sapphire-H01:

Instead of staircase-shaped or inclined sidewalls, "smooth vertical p-n structure m-plane sidewall" was formed on H-passivated GaN wafer after 1 hour of TMAH wet etching, as shown in Figure 4.15. This result confirmed our speculation that the etch rate of p-GaN can be accelerated by essentially adjusting the electrical property. A faster etch rate also can be observed from a-plane sidewalls of the H-passivated wafer than that of Mg-activated wafer. For Mg-activated wafer, staircase-shaped sidewall was found. On the other hand, the sidewalls of H-passivated wafer were straight from the top toward etched surface, as shown in Figure 4.16. This H passivation pre-treatment help to overcome the p-GaN etching resistance, thus forming a vertical non-polar sidewall. The smooth and vertical termination is ideal for U-trench GaN MOSFETs, which is favorable not only for normally-off operation but also for low R_{on} by high integration. In high-power switching devices, it is desirable to achieve low on-resistance (R_{on}) and high breakdown voltage (BV). A good interface quality between the semiconductor channel and the dielectric material could minimize the trap states and suppress the leakage current. This smooth vertical non-polar sidewall provides carries a higher mobility due to the minimum broken bonds.[26-29]

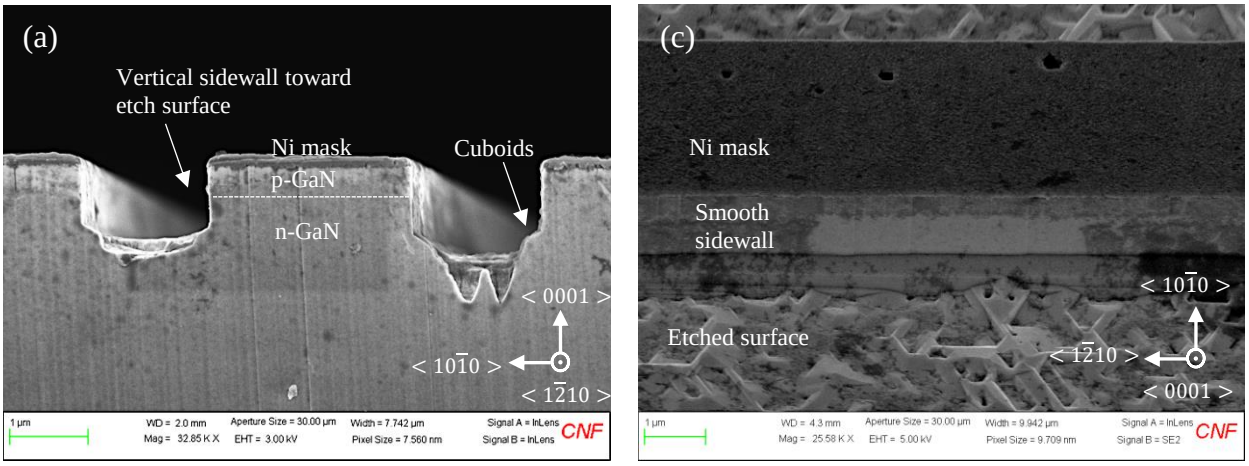

Figure 4.15. Sample ID: JH-GaN on sapphire-H01. SEM images of the H-passivated dry-etched-then-wet-etched fins along <1$\bar{2}$10> direction after etching in hot TMAH at 85 ^{o}C for 1 hr. Vertical and smooth sidewalls achieved. (a) Cross-sectional and (b) 45° view.

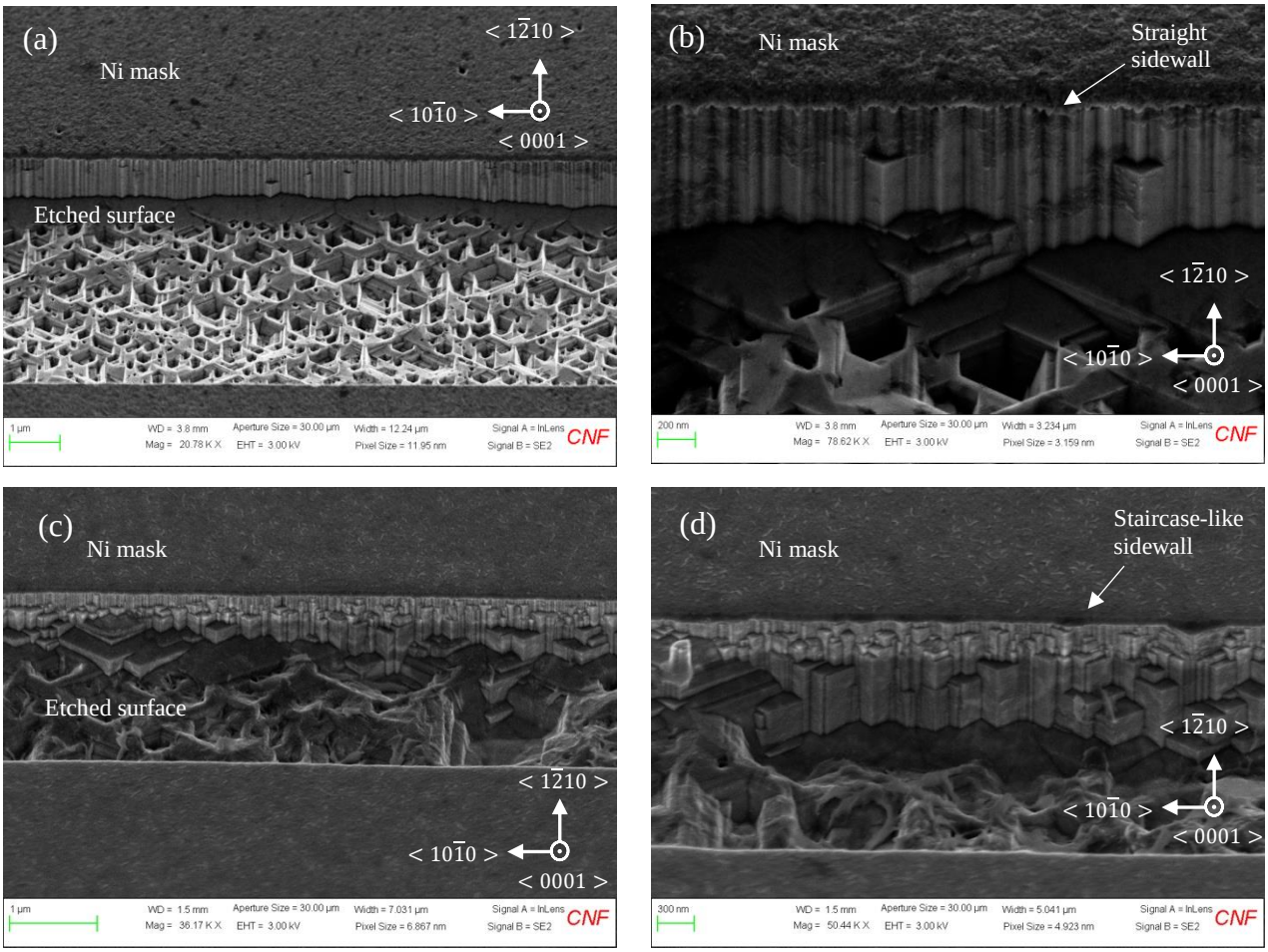

Figure 4.16. SEM images of the dry-etched-then-wet-etched fins along <10$\bar{1}$0> direction after etching in hot TMAH at 85 ^{o}C for 1 hr. (a) and (b): Sample ID: JH-GaN on sapphire-H01. Straight

sidewalls on H-passivated GaN wafer. (c) and (d): Sample ID: JH-GaN on Sapphire-Control02. Staircase-shaped sidewalls on Mg-activation wafer.

Problems: Even though p-GaN sidewalls of the H-passivated fins along <1$\bar{2}$10> direction became completely vertical after 1 hr of hot TMAH wet etching. Two problems were found in this sample: The formation of (a) cuboid-shape GaN at the base of the fins and (b) hexagonal-shape holes (nanoscale etching holes with m-plane), as shown in Figure 4.17. The latter one has been discussed in the previous section. This phenomenon is definitely not preferable to the device. However, this problem can be prevented by simply optimizing the descum process or applying acid cleaning for the photoresist removal. For the former one, He al. also reported the similar results on 3-μm-thick crack-free high-quality GaN film.[6] Some small cuboids were found at the bottom of the sidewall after TMAH etching for 1 hr, as shown in Figure 4.18. These unetched GaN at the base of the fin can be removed as the etching time was prolonged to 2.5 hrs. Therefore, the above-mentioned problems are both resolvable.

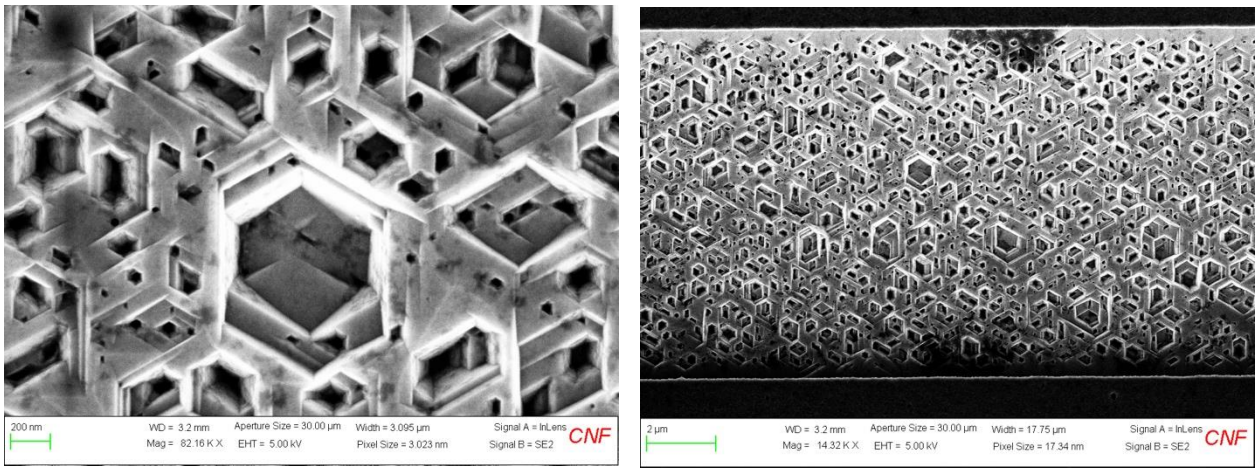

Figure 4.17. Sample ID: JH-GaN on sapphire-H01. (Top view) SEM images of the H-passivated dry-etched-then-wet-etched samples after etching in hot TMAH at 85 oC for 1 hr. Hexagonal-shape holes were appeared on the etched c-plane with m-plane sidewalls. The left image is a zoom-in view of the right.

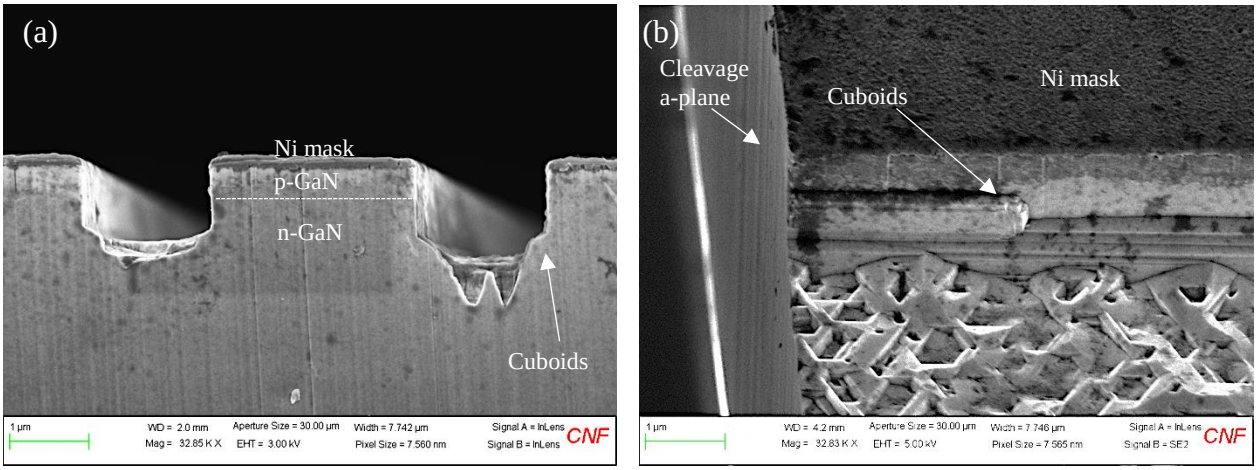

Figure 4.18. Sample ID: JH-GaN on sapphire-H01. SEM images of the H-passivated dry-etched-then-wet-etched fins along <1$\bar{2}$10> direction after etching in hot TMAH at 85 ^{o}C for 1 hr. Cuboids on the m-plane sidewalls viewed at (a) a-plane cross-section and (b) 45° from the cleavage plane (i.e. a-plane).

The Hall effect measurement was conducted to obtain the electrical properties of p-GaN layers (note: indium dots placed by tweezers were used as contacts here). Sheet concentration and hole mobility of Mg-activated GaN wafer (JH-GaN on Sapphire-Control02) were +1.2x10^{13}/cm^2 and 17.1 cm^2/V-s, respectively. These values are typical in Mg-doped GaN and the positive sheet concentration represents the positively charged holes. On the other hand, sheet concentration and mobility of H-passivated GaN wafer (JH-GaN on sapphire-H01) were -7.3x10^{13}/cm^2 and 368 cm^2/V-S, respectively. The negative value of sheet concentration and a much higher mobility indicate electrons were the dominant carriers of current flow. The possible reason for this result might due to the p-GaN layer may become insulating or highly resistivity after thermal annealing in hydrogen. Thus, it is possible for current to flow to the n-GaN layer through some leakage paths in p-GaN over a large area (possibly through dislocations but this needs further understanding).

4.3.2 **Reactivation of H-passivated GaN (*Sample ID: JH-GaN on sapphire-H02*)**

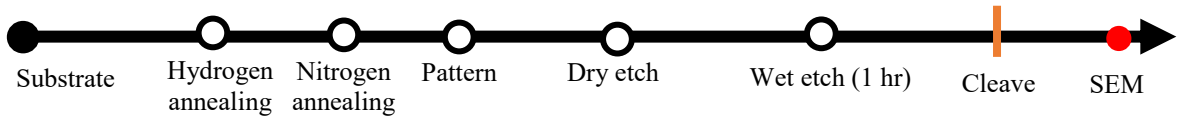

The activation annealing of p-GaN layer is necessary after wet etching of GaN. Successful activation of p-GaN required two steps: (1) break Mg-H bonds and (2) drive the hydrogen out of the GaN[24,25,30]. Nakamura et al. reported that the hydrogen can diffuse out from exposed p-GaN surfaces at the temperature above 700 °C in nitrogen environment.[25] Therefore, we prepared a sample with the treatment of H annealing-then-N annealing in order to see whether we are able to reactivate H-passivated GaN wafer in N_2-ambient gas at 800 °C for 30 minutes. However, under this condition, the sheet concentration and mobility were similar to the one before annealing process of -7.29x10^{13}/cm^2 and 221.1 cm^2/V-S, respectively. This hall measurement results were not what we expected because ideally H atoms can be released at this condition to reactivate the Mg acceptor. In addition, the vertical sidewalls were found on this wafer after the combination of plasma and TMAH etching, as shown in Figure 4.19. This result indicate that the Mg acceptors were not activated based on our previous results that the vertical sidewalls were only achieved on H-passivated wafer, while the slanted sidewalls were found on Mg-activated wafer.

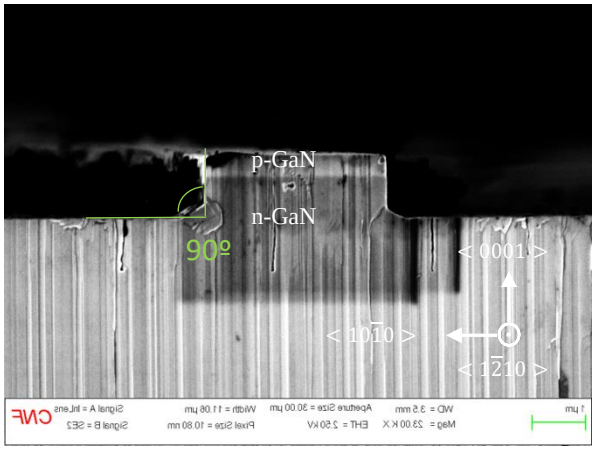

Figure 4.19. Sample ID: JH-GaN on sapphire-H02. SEM images of the H-passivated dry-etched-then-wet-etched fins along <1$\bar{2}$10> direction after etching in hot TMAH at 85 ºC for 1 hr. Mg acceptors were not successfully activated by N thermal annealing, therefore, the vertical sidewall was formed after TMAH etching.

To further study the reactivation condition, another sample was prepared in H-annealing. However, a black layer was found to cover the sample after thermal annealing (shown in Figure 4.20 (a)), which was not happened to the previous H-passivated samples. Since this annealing furnace was also for the growth of graphene, the particles on the sample may be diffused copper molecules. Graphene is usually grown on copper foil at around 1000 °C which can act as a self-limiting catalytic growth template.[31,32] Therefore, the quartz tube inside the graphene furnace was easily contaminated by copper molecules, as shown in Figure 4.20 (b). As a result, copper atoms were easily sublimed and diffused to the sample during the H-annealing. Therefore, another tool needs to be considered for H-annealing.

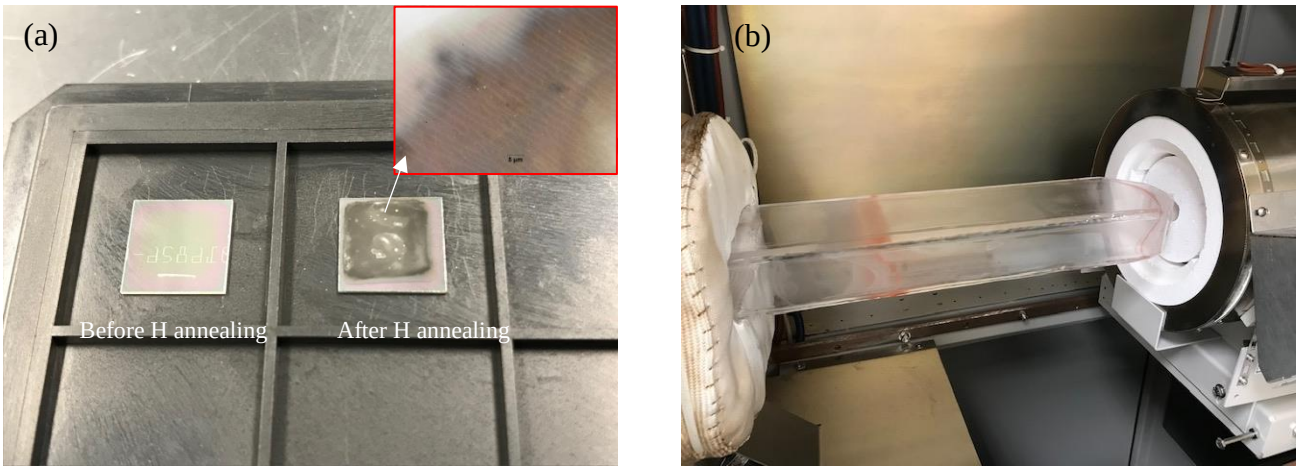

Figure 4.20. Pictures of (a) GaN wafer before and after H annealing and (b) Copper residue in the tube of annealing furnace. This annealing furnace was typical for the growth of graphene, the particles on the sample may be diffused copper molecules.

4.4 H-passivation-assisted TMAH etching (NH_3 annealing)

Motivation: The smooth vertical sidewall was successfully demonstrated on H-passivated GaN wafer. However, the reactivation condition still needed to be figured out. Besides, the hydrogen annealing furnace used in previous study was not suitable anymore for the GaN device fabrication because the copper contaminations could strongly affect the device performance. Therefore, NH_3-N_2 annealing (2slm NH_3 and 4 slm N_2) at 800 ˚C in MOCVD was then considered. Figure 4.21 (a) and (b) show the schematic of hole compensation and acceptors activation process. Hydrogen atoms dissociated from NH_3 can diffuse into the GaN to passivate the Mg-acceptors by forming the Mg-H complexes.[24,25] In this work, we would like to demonstrate the formation of smooth vertical sidewalls is repeatable on H-passivated GaN wafer and H atoms can be released from GaN after wet etching process. Control and experimental samples were named as "*JH-GaN on GaN-C01"* and "JH-GaN on GaN-NH301".

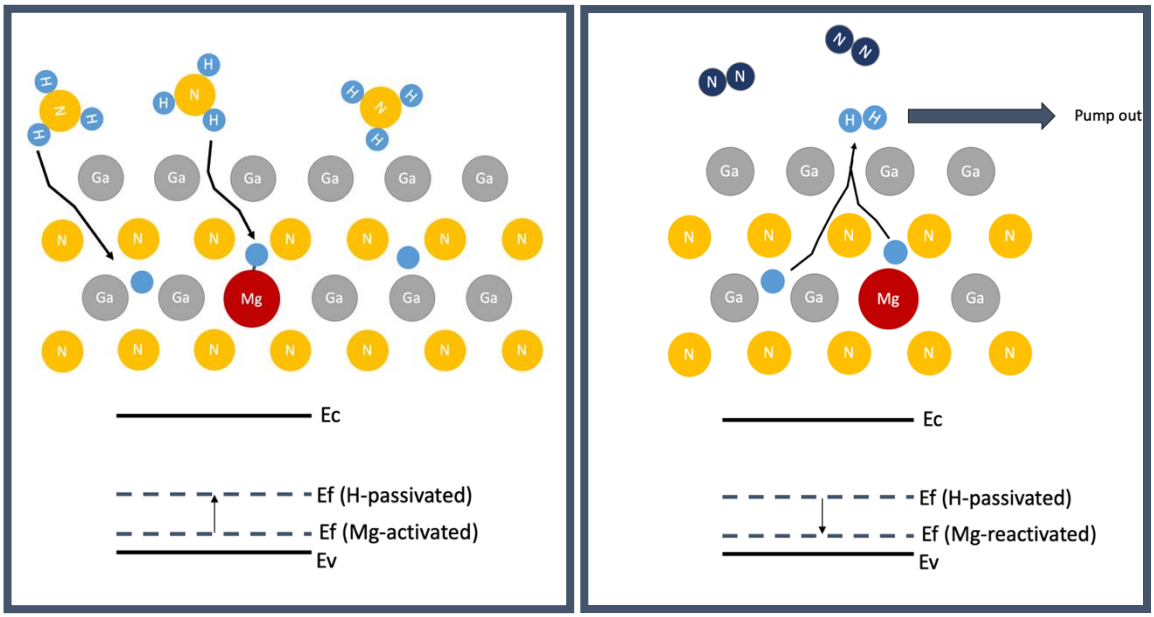

Figure 4.21. Schematic of hole compensation and Mg activation. (a) Hydrogen atoms diffuse into GaN to form Mg-H bonds. The fermi level is raised due to the hole compensation. (b) Hydrogen atoms are driven out from GaN. The fermi level is lowered due to the Mg activation.

4.4.1 Mg-activated sample (JH-GaN on GaN-C01)

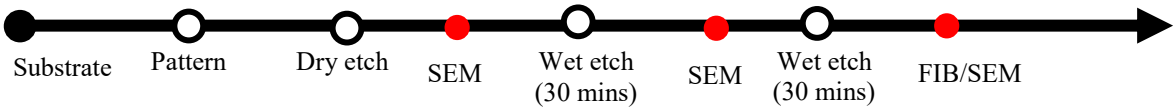

Cl-based dry etch: Similar to the results on sapphire substrate. The sidewalls of the fins along <1$\bar{2}$10> direction was slanted and rough after dry etch, as shown in Figure 4.22. The morphology of the as-etched sidewall of the fins along <10$\bar{1}$0> direction was nearly same as that of m-plane thus not shown here. Even though an ideal etch profile can achieve a perfect 90° sidewall angle. However, there is a certain degree of lateral etch which produces tapered structures. The two main reasons of lateral etch were mask erosion (sputtering of Ni mask) and wider ion angular distribution function.

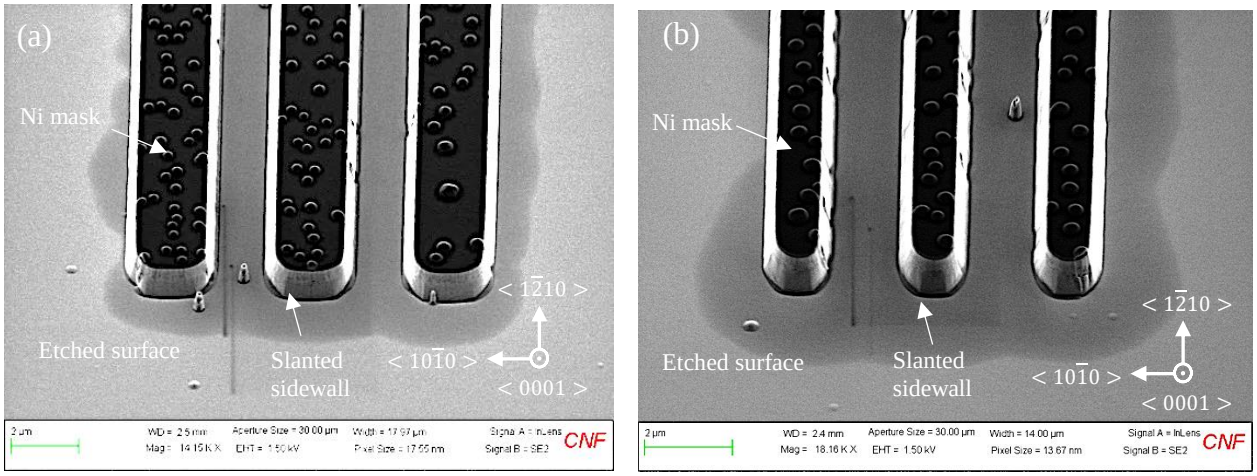

Figure 4.22. Sample ID: JH-GaN on GaN-C01. SEM images of Mg-activated dry-etched samples. (a) and (b): slanted sidewalls.

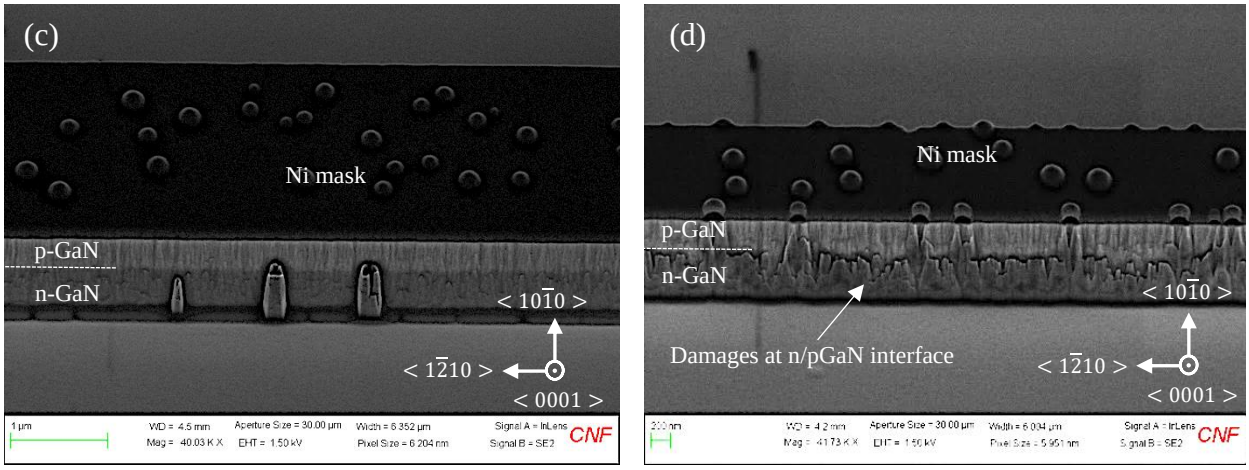

Figure 4.22. Sample ID: JH-GaN on GaN-C01. SEM images of Mg-activated dry-etched samples. (c) and (d): rough defective sidewall.

Uneven etched surfaces were observed due to the sputtering and redeposition of the nickel under high energy plasma. These metal residues acted as micro-mask caused the formation of cones on the etched surface. Figure 4.23 clearly shows the nickel on top of the cones. From the top view, GaN hexagonal cones with well-defined six-fold sidewalls (hexagonal truncated cones) were found after dry etching, as shown in Figure 4.24. The etch selectivity on specific planes was due to wurtzite GaN is hexagonal close-packed lattice of six-fold symmetry. The sidewalls with semi-polar planes were etched preferentially in the chemical etching process. The formation of these hexagonal truncated cones, indicating the combination of chemical reaction and the radical-assisted bond breaking was dominant in this etching process. In the etching process, BCl_2^+, $SiCl_2^+$, Ar^+, Cl^+, and $Cl2^+$ were present in the plasma. The bombardment by heavy radicals contributes to GaN etching in two ways: (1) physical sputtering (etch is isotropic to crystal) and (2) break the bonds between GaN and N (speeds up the chemical etching process). In our dry etching process, Cl radicals promote the chemical etch, and heavy radicals help break the bond between Ga and N to speed up the chemical etching process.[1,33]

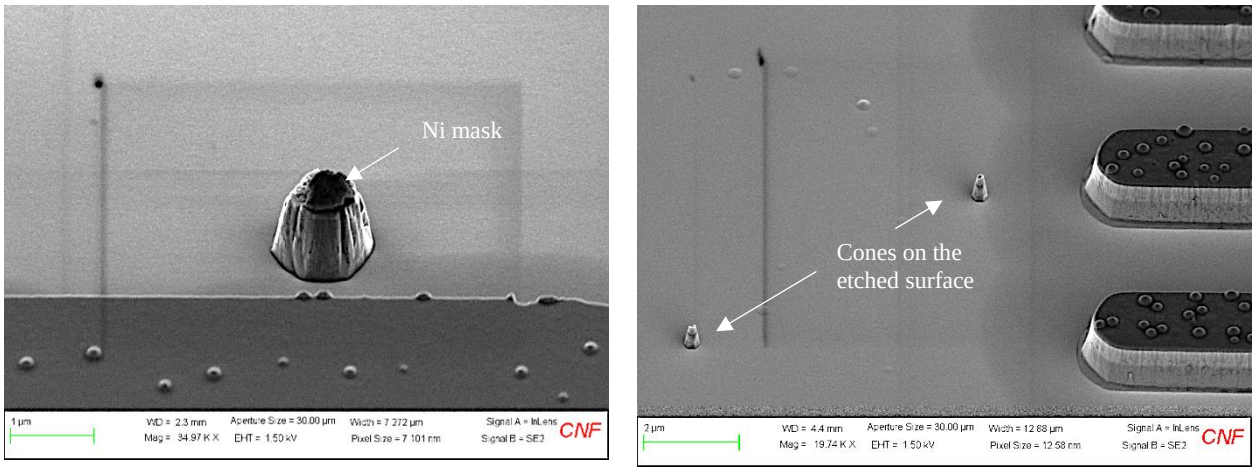

Figure 4.23. Sample ID: JH-GaN on GaN-C01. SEM images of the Mg-activated dry-etched samples, showing the cones caused by micro-masking effect due to the Ni residue.

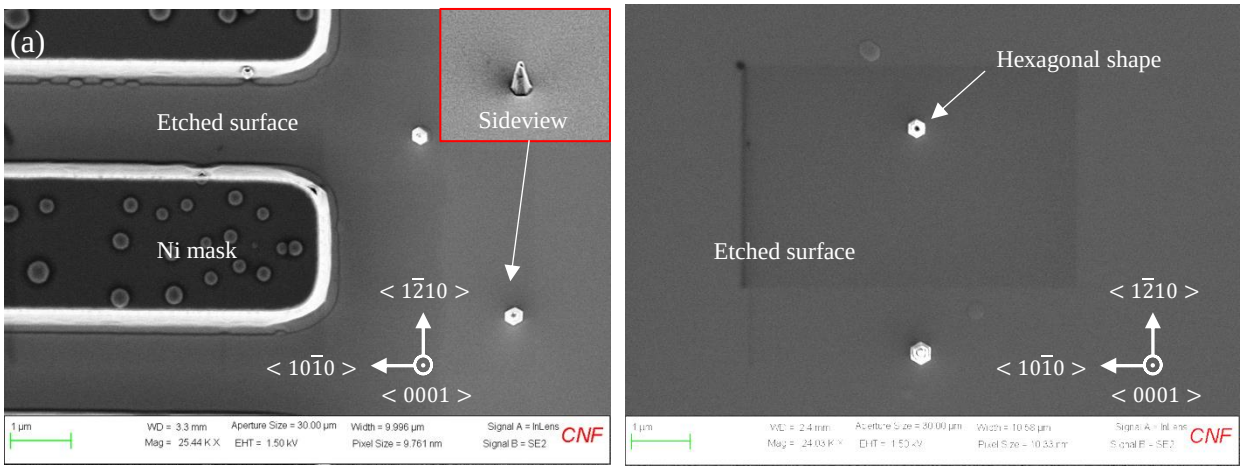

Figure 4.24. Sample ID: JH-GaN on GaN-C01. SEM images of the Mg-activated dry-etched samples, showing hexagonal truncated cones with well-defined six-fold sidewalls after dry etch due to the combination of chemical reaction and the radical-assisted bond breaking.

TMAH wet etching for 30 mins: The SEM images of the fins after wet etching for 30 minutes are shown in Figures 4.24. Similar to the results on sapphire samples, TMAH removed the hexagonal truncated cones formed by micro-masking effect from GaN surface. Besides, the morphology of the wet etched fin sidewall was related with the fin orientation. Sidewalls of the fins along <10$\bar{1}$0> direction were hierarchical nano-prism structures due to the surface bonding configuration. These angles are all 120°, indicating these zig-zag features were formed by the two adjacent m-planes, as shown in Figure 4.25 (a) and (b). In contrast, the sidewalls of the fin along <1$\bar{2}$10> direction were smoothed by TMAH and the texture on the sidewall turned to lateral, as shown Figure 4.25 (c) and (d). Although the smooth m-plane planes were exposed, the sidewalls were still slanted with staircase-shaped after TMAH for 30 minutes, as shown in Figure 4.25 (e) and (f).

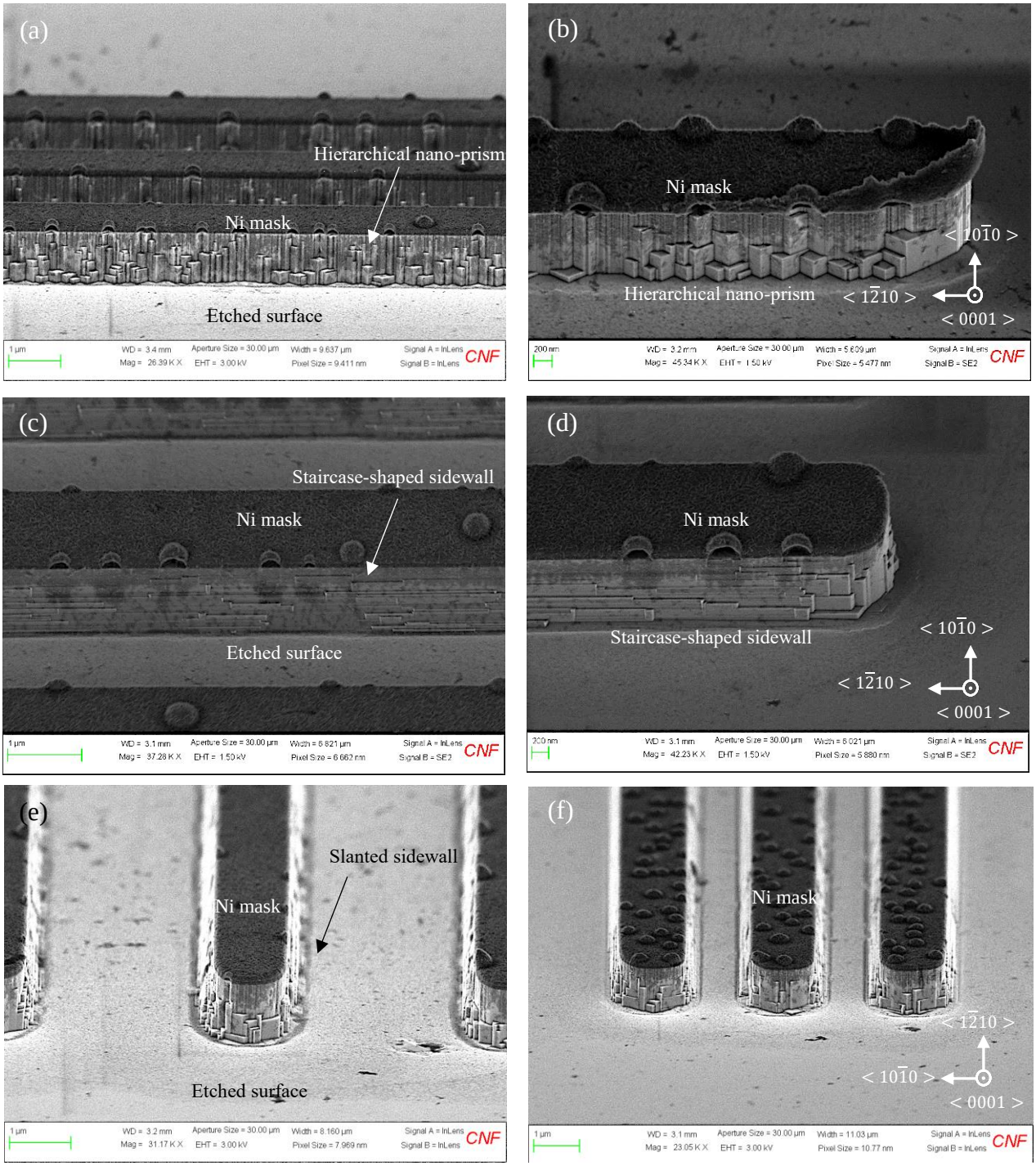

Figure 4.25. Sample ID: JH-GaN on GaN-C01. SEM images of the Mg-activated dry-etched-then-wet-etched fins along <1$\bar{2}$10> direction (a, b, c, and, d figures) and along <10$\bar{1}$0> direction (e and f figures) after etching in hot TMAH at 85 ºC for 30 mins. Hexagonal nano-prism on a-plane sidewalls, while lateral texture on m-plane sidewalls.

TMAH wet etching for 1 hr: The sidewalls of the fins along <1$\bar{2}$10> direction near the fin edge were nearly vertical and smooth after TMAH etching for 1 hr, as shown in Figure 4.26 (a), (b) and (c). However, the cuboids at base of the fins were appeared at the location few micrometers away from the fin edge, as shown in Figure 4.26 (d). The staircase-shaped sidewalls were observed at the middle of the fins. This phenomenon basically confirmed the diffusion-limited mechanisms we proposed in the previous section that etching is easy to occur at the sidewalls near the fin edge due to the thin boundary layer, while it's difficult to etch interior sidewalls because of the thick boundary layer.

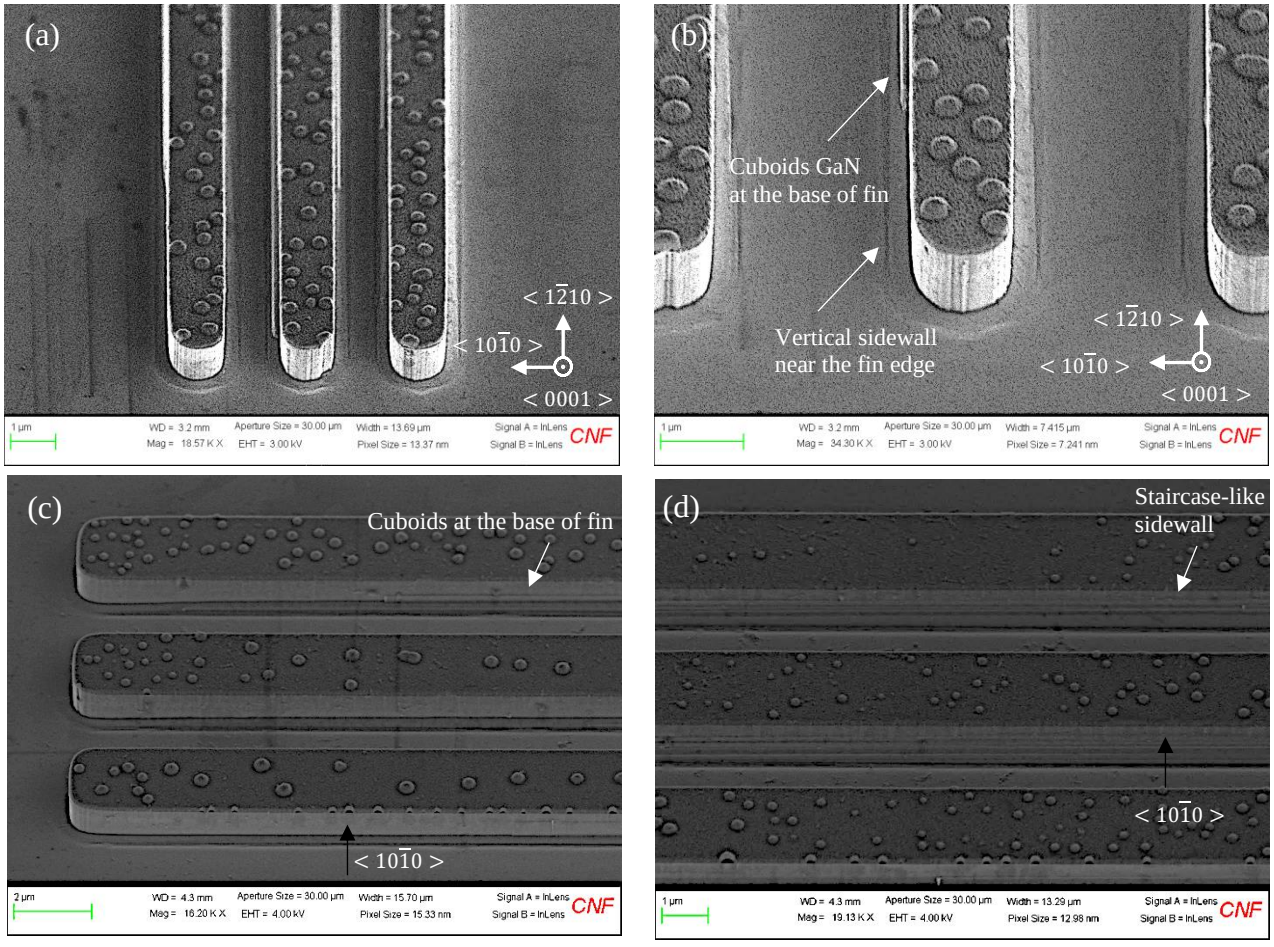

Figure 4.26. Sample ID: JH-GaN on GaN-C01. SEM images of the Mg-activated dry-etched-then-wet-etched fins along <1$\bar{2}$10> direction after etching in hot TMAH at 85 ^{o}C for 1 hr. Smooth vertical sidewall near the fin edge, staircase-shaped sidewall at interior.

In addition, we found a perfect smooth plane at the outer sidewalls of 50-μm-long fins (the shortest one), while staircase-shaped sidewalls were observed at the interior sidewalls between two fins, as shown in Figure 4.27. This was also due to the etching process was primarily determined by diffusion in TMAH solution. For the outer sidewalls, hydroxide ions were not limited by the thick boundary layer between two fins. Therefore, the etch rate was much faster at the outer sidewalls than the one between two fins. In addition, since the length of the fins was only 50 μm, p-GaN was entirely smoothed by TMAH on 50-μm-long fins. Only cuboids were left at the base of the fins.

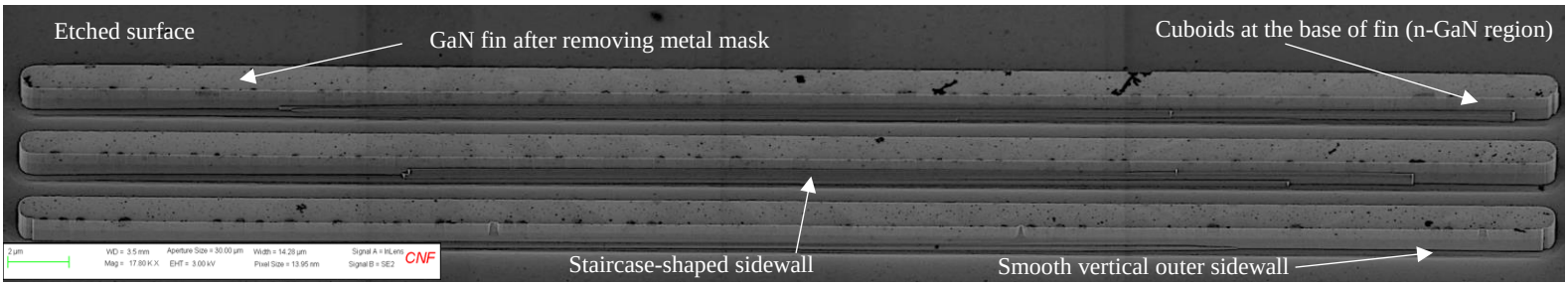

Figure 4.27. Sample ID: JH-GaN on GaN-C01. SEM images of the Mg-activated dry-etched-then-wet-etched fins along $<1\bar{2}10>$ direction after etching in hot TMAH at 85 ^{o}C for 1 hr (after removing Ni mask). Smooth vertical outer sidewalls, while staircase-shaped interior sidewalls.

To make a fair comparison between Mg-activated and H-passivated wafer, we chose the middle part of the 800-μm-long fins to observe their sidewall angles. For accuracy, FIB was used instead of cleaving by diamond scriber. Figure 4.28 shows the cross-sectional SEM images of the fins along <1$\bar{2}$10> direction. The Pt film around the fin was deposited to protect the fin surface from incurring FIB induced damage. As a result, the sidewall angles were slanted after TMAH etching for 1 hr for the interior sidewalls of 800-μm-long fins.

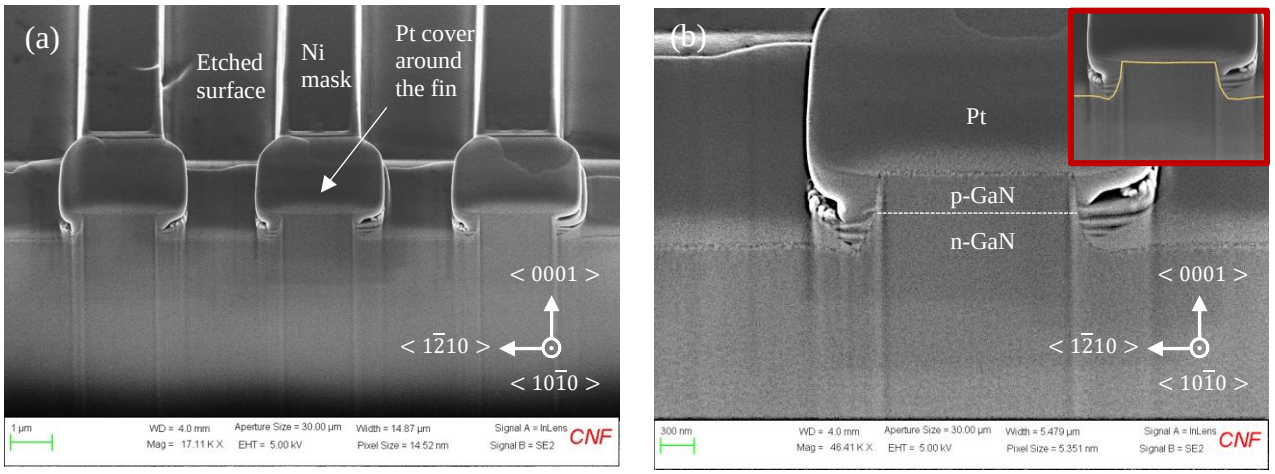

Figure 4.28. Sample ID: JH-GaN on GaN-C01. SEM images of the Mg-activated dry-etched-then-wet-etched fins along <1$\bar{2}$10> direction after etching in hot TMAH at 85 ^{o}C for 1 hr, FIB-ed from the middle section of a 800 um fin. The Pt film around the fin was deposited to protect the fin surface from incurring FIB induced damage. The slanted sidewalls indicate even the n-GaN was not smoothened in the hot TMAH etch due to limited diffusion of etchants and dissolution of the etch reaction by-product.

4.4.2 H-passivated sample (JH-GaN on GaN-NH301)

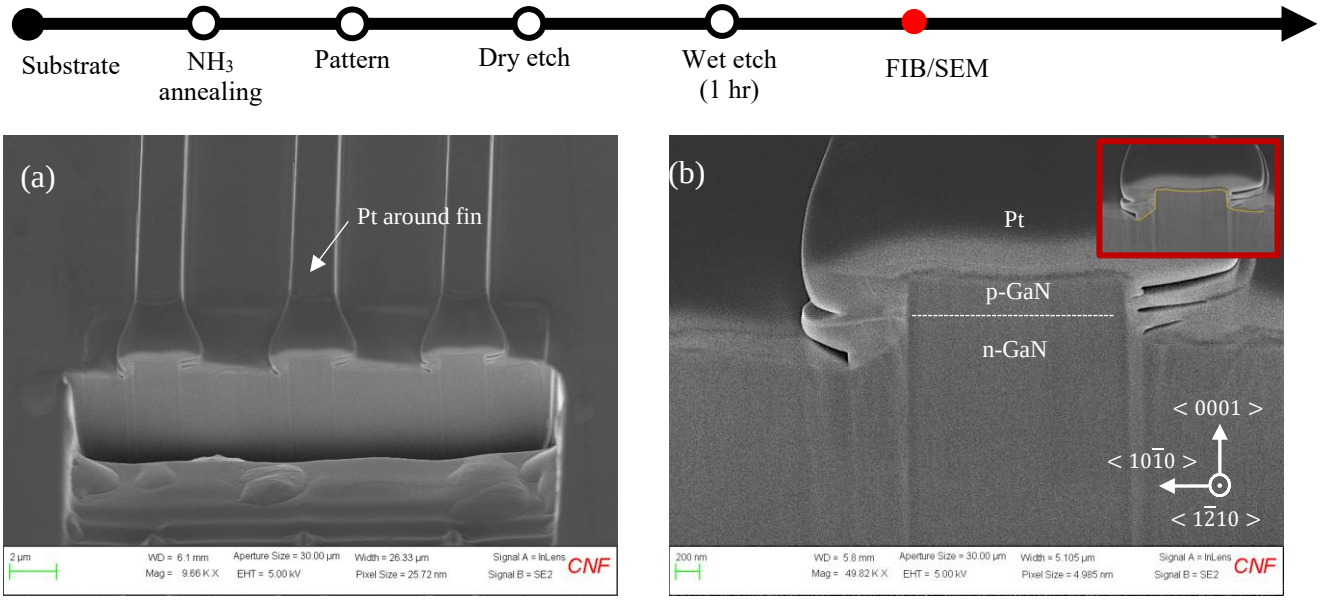

Figure 4.29. Sample ID: JH-GaN on GaN-NH301. SEM images of the H-passivated dry-etched-then-wet-etched fins along <1$\bar{2}$10> direction after etching in hot TMAH at 85 ^{o}C for 1 hr, FIB-ed from the middle section of a 800 um fin. The Pt film around the fin was deposited to protect the fin surface from incurring FIB induced damage. The vertical sidewalls indicate the etch rate of p-GaN was increased due to the hole compensation.

TMAH wet etching for 1 hr: On the other hand, the sidewalls of the H-passivated fins along <1$\bar{\mathbf{2}}$10> direction were vertical after TMAH etching for 1 hr, as show in Figure 4.29 (a) and (b). In addition, ultra-smooth non-polar planes were exposed on the sidewalls, which is ideal for the gate/channel interface, as shown in Figure 4.30 (a) and (b). A fast etch rate of H-passivated GaN can be observed from the fins along <10$\bar{\mathbf{1}}$0> as well, the sidewalls were very straight from top toward bottom without any staircase-shaped profile. These results again confirmed our speculation that wet etching rate can be increased by H-passivation-assisted wet etching.

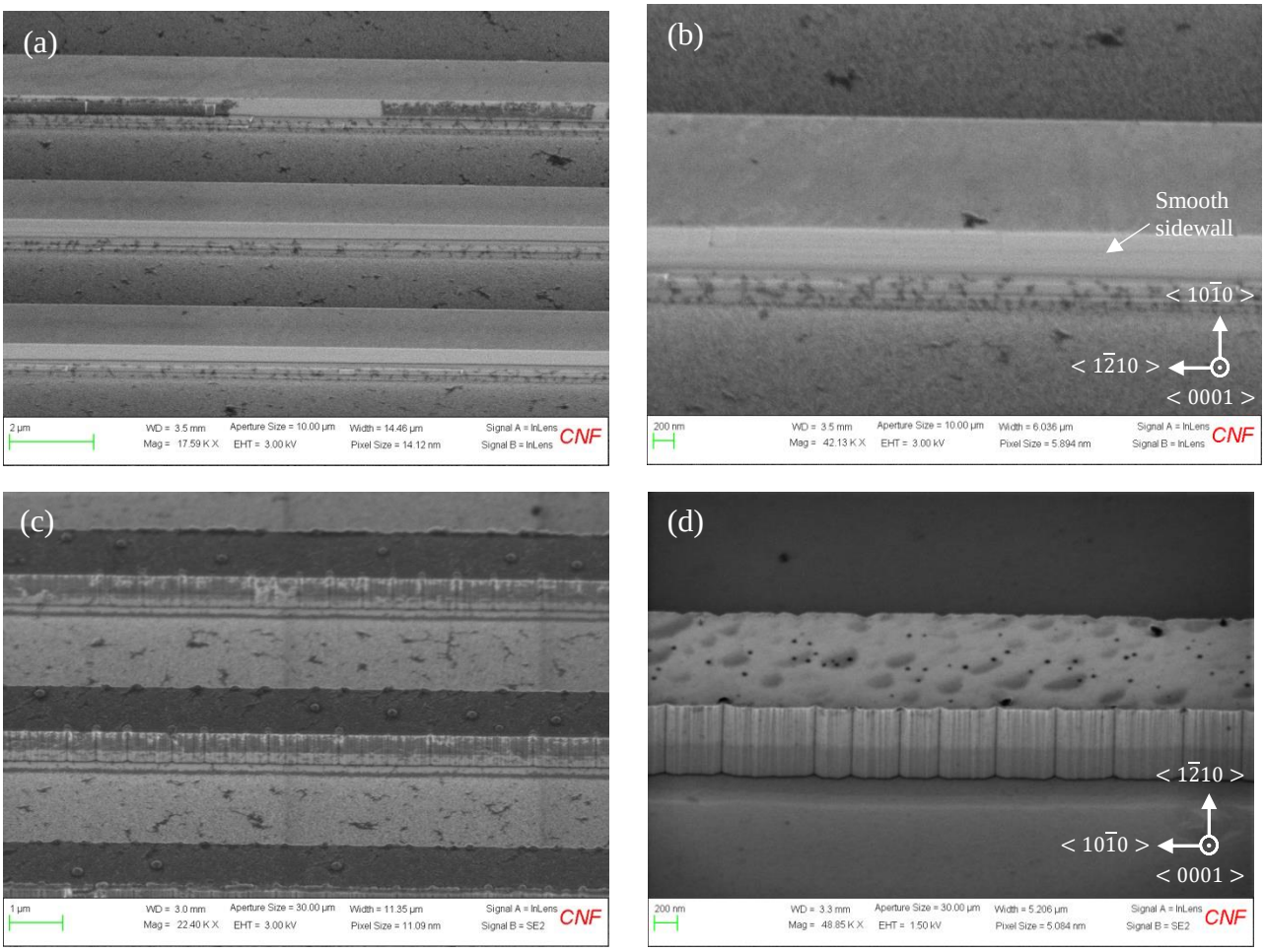

Figure 4.30. Sample ID: JH-GaN on GaN-NH301. SEM images of the H-passivated dry-etched-then-wet-etched fins after etching in hot TMAH at 85 ºC for 1 hr. (a) and (b): formation of Ultra-smooth m-plane sidewalls. (c) and (d): a-plane straight sidewalls textured by adjacent m-planes.

Reactivation: Hall measurements were conducted to obtain the electrical properties of p-GaN layer (note: Pd/Pt deposited by e-beam evaporation and a liftoff process were used as contacts here). Before NH_3-N_2 annealing, sheet concentration and hole mobility of p-type GaN with Mg doping layer (*JH-GaN on GaN-C01*) were $+4.8x10^{12}/cm^2$ and 24.8 cm^2/V-s, respectively. Assuming the thickness of p-GaN layer is 400 nm, the calculated doping concentration of p-GaN is $1.2x10^{17}/cm^3$ was as-expected. After hydrogen passivation (*JH-GaN on GaN-NH301*), sheet concentration and mobility that we measured on p-GaN were $-6.6x10^{13}/cm^2$ and 402 cm^2/V-S, respectively. Similar to the previous results on sapphire sample, the negative value of sheet concentration and a much higher mobility were measured, indicating that electrons are the dominant carriers of current flow. An ultra-smooth and vertical m-plane sidewall was formed on the fin along $<1\bar{2}10>$ direction. Afterwards, we then recovered the p-GaN by sidewall activation via N_2-ambient thermal annealing for 40 mins. Sheet concentration and mobility were recovered to $+9.76x10^{13}/cm^2$ and 19.2cm^2/V-S, respectively, showing that the Mg-acceptors could be reactivated after wet etching purpose.

	Sheet Concentration ($/cm^2$)	Mobility (cm^2/V-s)	Resistivity (ohm/sq)
Mg-activation	$4.7x10^{12} \pm 7.7x10^{11}$	25.8 ± 4.9	$5.3x10^4 \pm 1.2x10^3$
H-passivation	$-6.9x10^{13} \pm 2.7x10^{12}$	386.7 ± 13.43	234.2 ± 2.17
Mg-reactivation	$1.1x10^{13} \pm 8.0x10^{11}$	18.4 ± 1.7	$3.2x10^4 \pm 1.9x10^3$

Table 4.1. Electrical properties of Mg-activated, H-passivated, and Mg-reactivated p-GaN films.

BIBLIOGRAPHY

[1]Pearton, S. J., R. J. Shul, and Fan Ren. "A review of dry etching of GaN and related materials." *Materials Research Society Internet Journal of Nitride Semiconductor Research*5.1 (2000).

[2]Chen, Weijie, et al. "GaN nanowire fabricated by selective wet-etching of gan micro truncated-pyramid." *Journal of Crystal Growth* 426 (2015): 168-172.

[3]Uesugi, Tsutomu, and Tetsu Kachi. "GaN power switching devices for automotive applications." *Proc. Int. Conf. CS Matech*. 2009.

[4]Kodama, Masahito, et al. "GaN-based trench gate metal oxide semiconductor field-effect transistor fabricated with novel wet etching." *Applied physics express* 1.2 (2008): 021104.

[5]Im, Ki-Sik, et al. "Lateral GaN nanowire prepared by using two-step TMAH wet etching and HfO2 sidewall spacer." *Journal of Crystal Growth* 441 (2016): 41-45.

[6]He, Junlei, et al. "On-wafer fabrication of cavity mirrors for InGaN-based laser diode grown on Si." *Scientific reports* 8.1 (2018): 7922.

[7]Zhang, Yuhao, et al. "Trench formation and corner rounding in vertical GaN power devices." *Applied Physics Letters* 110.19 (2017): 193506.

[8]Zhang, Yuhao, et al. "Origin and control of OFF-state leakage current in GaN-on-Si vertical diodes." *IEEE Transactions on Electron Devices* 62.7 (2015): 2155-2161.

[9]Tautz, Markus, and David Diaz Diaz. "Wet-Chemical Etching of GaN: Underlying Mechanism of a Key Step in Blue and White LED Production." *ChemistrySelect* 3.5 (2018): 1480-1494.

[10]Li, Dongsheng, et al. "Selective etching of GaN polar surface in potassium hydroxide solution studied by x-ray photoelectron spectroscopy." *Journal of Applied Physics* 90.8 (2001): 4219-4223.

[11]Itoh, Morimichi, et al. "Straight and smooth etching of GaN (1100) plane by combination of reactive ion etching and KOH wet etching techniques." *Japanese journal of applied physics*45.5R (2006): 3988.

[12]Ng, Hock M., Nils G. Weimann, and Aref Chowdhury. "GaN nanotip pyramids formed by anisotropic etching." *Journal of applied physics* 94.1 (2003): 650-653.

[13]Ng, Hock M., et al. "Patterning GaN microstructures by polarity-selective chemical etching." *Japanese Journal of Applied Physics* 42.12A (2003): L1405.

[14]Zhuang, D., and J. H. Edgar. "Wet etching of GaN, AlN, and SiC: a review." *Materials Science and Engineering: R: Reports*48.1 (2005): 1-46.

[15] https://en.wikipedia.org/wiki/Entrance_length

[16]Anderson, John David, and J. Wendt. *Computational fluid dynamics*. Vol. 206. New York: McGraw-Hill, 1995.

[17]Schlichting, Hermann, and Klaus Gersten. *Boundary-layer theory*. Springer, 2016.

[18] Zhang, Yu, et al. "A conductivity-based selective etching for next generation GaN devices." *physica status solidi (b)* 247.7 (2010): 1713-1716.

[19]Hwang, J. M., et al. "Efficient wet etching of GaN and p-GaN assisted with chopped UV source." *Superlattices and Microstructures* 35.1-2 (2004): 45-57.

[20]Yue, Yuanzheng, et al. "Faceted sidewall etching of n-GaN on sapphire by photoelectrochemical wet processing." *Journal of Vacuum Science & Technology B, Nanotechnology and Microelectronics: Materials, Processing, Measurement, and Phenomena* 32.6 (2014): 061201.

[21]Youtsey, C., I. Adesida, and G. Bulman. "Highly anisotropic photoenhanced wet etching of n-type GaN." *Applied physics letters* 71.15 (1997): 2151-2153.

[22]Photo-electrochemical etching of free-standing GaN wafer surfaces grown by hydride vapor phase epitaxy

[23]Youtsey, C., G. Bulman, and I. Adesida. "Dopant-selective photoenhanced wet etching of GaN." *Journal of electronic materials* 27.4 (1998): 282-287.

[24]Nakamura, Shuji, et al. "Hole compensation mechanism of p-type GaN films." *Japanese Journal of Applied Physics* 31.5R (1992): 1258.

[25]Nakamura, Shuji, et al. "Thermal annealing effects on p-type Mg-doped GaN films." *Japanese Journal of Applied Physics*31.2B (1992): L139.

[26]Li, Ray, et al. "600 V/$1.7~\Omega $ Normally-Off GaN Vertical Trench Metal–Oxide–Semiconductor Field-Effect Transistor." *IEEE Electron Device Letters* 37.11 (2016): 1466-1469.
[27] Fukushima, Hayata, et al. "Vertical GaN pn diode with deeply etched mesa and capability of avalanche breakdown." *Applied Physics Express* (2019).
[28]Amano, H., et al. "The 2018 GaN power electronics roadmap." *Journal of Physics D: Applied Physics* 51.16 (2018): 163001.

[29]Oka, Tohru, et al. "1.8 mΩ· cm2 vertical GaN-based trench metal–oxide–semiconductor field-effect transistors on a free-standing GaN substrate for 1.2-kV-class operation." *Applied Physics Express* 8.5 (2015): 054101.

[30]Li, Wenshen, et al. "Activation of buried p-GaN in MOCVD-regrown vertical structures." *Applied Physics Letters* 113.6 (2018): 062105.

[31]Cai, Weiwei, et al. "Thermal transport in suspended and supported monolayer graphene grown by chemical vapor deposition." *Nano letters* 10.5 (2010): 1645-1651.

[32]Yu, Qingkai, et al. "Control and characterization of individual grains and grain boundaries in graphene grown by chemical vapour deposition." *Nature materials* 10.6 (2011): 443.

[33]Liu, Zhe, et al. "Fabrication of GaN hexagonal cones by inductively coupled plasma reactive ion etching." *Journal of Vacuum Science & Technology B, Nanotechnology and Microelectronics: Materials, Processing, Measurement, and Phenomena* 34.4 (2016): 041226.

[34]Leung, Benjamin, et al. *Controlled top-down fabrication of GaN nanostructures and mechanism*. No. SAND2016-5919C. Sandia National Lab.(SNL-NM), Albuquerque, NM (United States), 2016.

CHAPTER 5
Summary

GaN vertical power devices are still under development due to the unsatisfactory termination structures. We demonstrated the fabrication of "smooth and vertical p-n GaN sidewalls" by H-passivation-assisted TMAH etching. A vertical cleavage plane, with the fewest broken bonds, promises a higher mobility and better material quality of the channel. This trench gate structure with non-polar m-plane is favorable not only for normally-off operation but also for low R_{on} of trench GaN MOSFETs. In addition, etching of GaN in TMAH was found to be limited by diffusion (mass transport). In the past, p-GaN has been known to be more resistant to base etch solution compared to n-GaN. Two strategies were implemented to enhance the etch rate of p-GaN: (1) UV-assisted and (2) hydrogen-passivation-assisted wet etching. A smooth semi-polar sidewall without staircases was formed by UV-assisted wet etching. The cuboids at the base of the fin were removed likely as a result of enhanced etch rate of n-GaN due to the photogenerated holes. This finding potentially provides a solution to generate smooth sidewalls for GaN waveguides with trapezoid cross-sections. However, the sidewalls were still slanted after etching in hot TMAH for 1 hr. The low power of the UV source, 0.35 mW/cm^2, failed to generate sufficient holes to effectively increase the etch rate of p-GaN because photo generated holes were still swept away from the depletion region near the surface into the bulk due to the strong band bending. On the other hand, smooth vertical sidewalls were achieved by the H-passivation-assisted wet etching. Mg dopants were passivated by H through a treatment of either H- or NH3- thermal annealing. H-passivation moves the Fermi level to the midgap of GaN and consequentially lowering the surface band bending that prevents holes from reaching the GaN surface, therefore, the etch rate of H-passivated p-GaN increases in hot TMAH. I am able to achieve smooth vertical sidewalls in p-GaN in H-passivation-assisted wet etch and recover the mobile hole conduction in p-GaN after nitrogen thermal annealing. Thus, this novel etching technique is useful for realizing damage-free high mobility normally-off channel for GaN U-trench MOSFETs.

Summary of all experiments

#1 Conventional TMAH etching on sapphire substrate sample

- Goal of the research
  - Study the effects of chlorine-based dry etching and TMAH chemical wet etching on the GaN with the p-n structure.

Sample ID: JH-GaN on Sapphire-Control01

- Key observation:
  - Cl-based dry etch: Uneven etched surface and sidewall damages.
  - Hot TMAH for 1 hr: Strong anisotropic etching profile was found.
    a. Sidewalls of the fins along <10$\bar{1}$0> direction were hierarchical nano-prism structures.
    b. Sidewalls of the fins along <1$\bar{2}$10> direction were staircase-shaped m-plane sidewalls and semi-polar planes were observed at the base of the fins. The sidewalls are slanted even after 1 hr TMAH etching.
    c. The pillars formed in plasma etching were totally removed
  - Cleaved-then-TMAH-etched fins: p-GaN sidewall became entirely vertical near the fin edge, while the inner sidewalls were still slanted. The wet etching process was limited by diffusion.
  - Description of etch sequence: with increasing etching duration in TMAH solution, the semi-polar facets of the GaN were removed gradually accompanied with the exposure of the m-plane facets.

Conclusions: 1 hr TMAH wet etching is a suitable post-treatment to remove the damages after dry etch. However, it can only form the vertical sidewalls near the fin edge due to the limitation of mass transport. Therefore, other methods need to be considered to increase the etch rate of p-GaN.

#2 UV-assisted TMAH etching on sapphire substrate sample

- Goal of the research
  - Implement the UV source into wet etching process in order to increase the etch rate of GaN.

Sample ID: JH-GaN on Sapphire-UV01 (30 mins UV-assisted TMAH etching)

- Key observation:
  - The GaN sidewalls of the fins along <1$\bar{2}$10> direction were found to be slanted after UV-assisted TMAH etching under the power density of 0.35 mW/cm^2 for 30 minutes. The smooth sidewalls with two-step slope were formed, instead of staircase-shaped sidewalls formed by conventional TMAH etching. In addition, there was no unetched GaN at the base of the fins.

Sample ID: JH-GaN on Sapphire-UV02 (1 hr UV-assisted TMAH etching)

- Key observation:
  - Photonic waveguides with very smooth sidewalls can be formed on GaN after UV-assisted wet etching for 1 hr.

Sample ID: JH- GaN on Sapphire-Control02 (1 hr conventional TMAH etching)

- Key observation:
  - The photoresist residue before dry etch caused uneven surface after dry etch, leading to the formation of hexagonal GaN cavity after TMAH etching. This phenomenon was observed in UV-assisted samples as well.

Conclusions: A smooth semi-polar sidewall without staircases was formed by UV-assisted wet etching. The cuboids at the base of the fin were removed likely as a result of enhanced etch rate of n-GaN due to the photogenerated holes. This finding potentially provides a solution to generate smooth sidewalls for GaN waveguides with trapezoid cross-sections.

#3 H-passivation-assisted TMAH etching on sapphire substrate sample

- Goal of the research: Thermal annealing in hydrogen environment was considered to increase the etch rate of p-GaN, mitigating the dopant selectivity.

Sample ID: JH-GaN on Sapphire-H01 (H-passivation-assisted TMAH etching for 1 hr)

- Key observation: Smooth vertical p-n structure m-plane sidewalls were formed for entirely fins along <$1\bar{2}10$> direction.

Sample ID: JH-GaN on Sapphire-H02 (H passivated-then-reactivated sample)

- Key observation: The vertical sidewalls were still formed on this wafer, indicating the Mg acceptors were not activated successfully.

Conclusions: We demonstrated the fabrication of "smooth and vertical p-n GaN sidewalls" by H-passivation-assisted TMAH etching. However, the reactivation condition still needed to be figure out.

#4 Conventional vs. H-passivation-assisted etching (by NH_3 annealing) on n-GaN substrate sample

- Goal of the research:
  - Compare the difference of etching profiles between conventional and H-passivation-assisted etching
  - Demonstrate the formation of smooth vertical sidewalls is repeatable on H-passivated GaN wafer and Mg acceptors in p-GaN can be re-activated after wet etching process.

Sample ID: JH-GaN on GaN-CO1

- Key observation:
  - Cl-based dry etch: Similar to the results on sapphire substrate sample, the sidewalls of the fins were slanted and rough. In addition, GaN hexagonal cones with well-defined six-fold sidewalls were found after dry etching due to the chemical reaction.
  - TMAH wet etching for 1 hr: the sidewalls of the fins along <1$\bar{2}$10> direction near the fin edge were nearly vertical and smooth, while the staircase-shaped slanted sidewalls were observed at the middle of the fins.

Sample ID: JH-GaN on GaN-NH301

- Key observation:
  - The sidewalls of the H-passivated fins along <1$\bar{2}$10> direction became ultra-smooth and vertical after TMAH etching for 1 hr.
  - The sidewalls of the H-passivated fins along <10$\bar{1}$0> were very straight from top toward bottom without any staircase-shaped profile.
  - Successfully recover the p-GaN by sidewall activation via N_2 -ambient thermal annealing.

  Conclusions: We are able to achieve smooth vertical sidewalls in p-GaN in H-passivation-assisted wet etch and recover the mobile hole conduction in p-GaN after nitrogen thermal annealing. This novel etching technique is useful for realizing damage-free high mobility normally0off channel for GaN U-trench MOSFETs.

Appendix: detailed process flow

#	Process	Process	Conditions
1	Substrate & Photomask Cleaning	Solvent cleaning	Cleaning: 1:1 DHF (5 min) and rinse in DI+N2 blow Cleaning: 1:1 HCl (5 min) and rinse in DI+N2 blow Cleaning1: Acetone and methanol with sonication (each 3 mins), DI rinse (3 times)+ N2 blow
2		Check profile (OM)	
3	PECVD (back side)	Deposition	500 nm
4		Cleaning1	Acetone and methanol with sonication (each 3 mins), DI rinse (3 times)+ N2 blow
5	Lithography for isolation mask (Stepper) Diode ver. 3 Layout: Device isolation (+PR)	Spin resist (SPR2020)	6000 rpm, 5000 ramp, 60 s
6		Pre baking	115 °C, 60 sec
7		Exposure	Exposure time: 0.22 s
8		PEB	115 °C, 60 sec
9		Development	AZ-726 MIF: 100 sec@RT
10		Rinse	DI rinse 30 sec+N_2 blow
11		**Check Patterns (OM)**	
12		Baking	115C, 5 mins
13		BOE 30:1	1 min
14		1:1 HCl	1min
15		Solvent cleaning	
16	Evaporation (Odd hour)	Cr (50 nm)	Density: 7.2; Z-Ratio:0.305; Tool Factor:72, Thickness: 50nm, Rate: _____ nm/min
17		Ni (80 nm)	Density: 8.91; Z-Ratio:0.331; Tool Factor:66, Thickness: 80nm, Rate: _____ nm/min
18		Lift off (1)	1165 rinse 20 mins, sonicate 5mins
19		Lift off (2)	Hot 1165, 80 deg. C, 20 mins
20		Cleaning1	Acetone and methanol with sonication (each 3 mins), DI rinse (3 times)+ N2 blow
21		Descum	O_2=42 sccm, 20mTorr, RIE = 500W, 2 mins (mode 3)
22		**Check Patterns (OM)**	Nomarski mode
23		Film thickness (P-10)	_____ nm
24	Dry etch (PT-770 right chamber)	ICP-RIE etching: Xing1	GaN _____nm, $BCl_3/Ar/Cl_2$=10/10/20 sccm, 6 mTorr, RIE/ICP = 22/250 W, DC: ____V, rate: ___nm/min, Time: ___mins
25		Step (P-10)	Etched height: _____**nm** *Rate: (Etched height-Film thickness)/ Etch time*
26		ICP-RIE etching: Xing2	GaN ____nm, BCl_3=30 sccm, 4 mTorr, RIE/ICP = 6/300 W, DC: _____V, rate: ____nm/min, Time: ___mins
27		Step (P-10)	Etched height: **nm**.
28	SEM (sidewall observation)	SEM	Sidewall morphology, sidewall angle
29	Wet etching	25 % TMAH	85 deg. C, 1 hr (Hot plate+stir bar)
30		Cleaning1	Acetone and methanol with sonication (each 3 mins), DI rinse (3 times)+ N2 blow
31		Remove SiO2	HF 10 mins
32		OM	Observation
33		Cleaning1	Acetone and methanol with sonication (each 3 mins), DI rinse (3 times)+ N2 blow
34	SEM (sidewall observation)	SEM	Sidewall morphology, sidewall angle
35	Remove etching Mask	Remove Ni	Ni etchant
36		Remove Cr	Cr etchant
37		Surface cleaning 1	1:6 BHF 2 min, DI rinse, N2 blow
38		Surface cleaning 2	1:1 HCl 1 min, DI rinse, N2 blow
39		**Check Patterns (OM)**	
40		Cleaning1	Acetone and methanol with sonication (each 3 mins), DI rinse (3 times)+ N2 blow
41	Reverse I-V measurement of the circular diodes w/o metal contacts	Probe & Chuck	leakage current
42	Lithography for ohmic mask (Stepper) Diode ver. 3 Layout: Anode contact (-PR)	Spin resist (SPR2020)	6000 rpm, 5000 ramp, 60 s
43		Pre baking	115 °C, 60 sec
44		Exposure	Exposure time: 0.22 s, Alignment
45		PEB	115 °C, 60 sec
46		Development	AZ-726 MIF: 100 sec@RT
47		Rinse	DI rinse 30 sec+N_2 blow
48		**Check Patterns (OM)**	Nomarski mode;
49		Post baking	115 oC, 5 mins
50		Surface cleaning 3	1:30 BHF 1 min, DI rinse, N2 blow
51		Surface cleaning 2	HCl:DI=1:1, 1 min, DI rinse, N2 blow
52	Evaporation (Odd hour) Anode ohmic contact	Pd (< 1e-6 Torr)	Density: ; Z-Ratio: ; Tool Factor: , Thickness: 50nm, Rate: _____ nm/min
53		Pt (< 1e-6 Torr)	Density: ; Z-Ratio: ; Tool Factor: , Thickness: 100nm, Rate: _____ nm/min
54		Lift off (1)	1165 rinse 20 mins, sonicate 5mins
55		Lift off (2)	Hot 1165, 80 deg. C, 20 mins
56		Cleaning1	Acetone and methanol with sonication (each 3 mins), DI rinse (3 times)+ N2 blow
57		descum	O_2=42 sccm, 20mTorr, RIE = 500W, 2 mins (mode 3)
58		**Check Patterns (OM)**	
59	Dry etch (PT-770 right chamber) Etch P+ GaN	ICP-RIE etching: Xing2	GaN __**50**__nm, BCl_3=30 sccm, 4 mTorr, RIE/ICP = 6/300 W, DC: _____V, rate: ____nm/min, Time: ___mins
60		Step (P-10)	Etched height: ____**nm**.
61	Hall Measurement	Hall bar	Sheet concentration: _____**/cm2**

62	Evaporation (Odd hour) Cathode ohmic contact	Resist coating(1813)	4000 rpm 45 s --> 1.8 µm
63		Pre baking	115 oC, 5 mins
64		Surface cleaning 1	1:6 BHF 2 min, DI rinse, N2 blow
65		Surface cleaning 2	1:1 HCl 1 min, DI rinse, N2 blow
66		Ti (< 1e-6 Torr)	Density: ; Z-Ratio: ; Tool Factor: , Thickness: 50 nm, Rate: _____ nm/min
67		Pt (< 1e-6 Torr)	Density: ; Z-Ratio: ; Tool Factor: , Thickness: 100 nm, Rate: _____ nm/min
68		PR removal	Acetone and methanol w/ sonication, IPA rinse
69	Reverse and forward I-V characteristics		Breakdown V
70	FIB/SEM	Spin resist (1813)	6000 rpm, 5000 ramp, 60 s
71		Baking	110 deg. C, 60 sec
72		Cleaving	Diamond scriber cleave from back side
73		Cleaning1	Acetone and methanol with sonication (each 3 mins), DI rinse (3 times)+ N2 blow
74		SEM	Xsection image, sidewall angle: _____ deg